

UNIVERSITY OF WEST BOHEMIA IN PILSEN  
**FACULTY OF MECHANICAL ENGINEERING**

Study Program: N 2301 Mechanical Engineering  
Field of Study: Design of Power Machines and Equipment

# **MASTER'S THESIS**

Optimization of an industrial heat exchanger by the minimalization of  
entropy

Author: **Bc. Richard PISINGER**  
Supervisor: **Doc. Ing. Petr ERET, Ph.D.**

Academic year 2017/2018

ZÁPADOČESKÁ UNIVERZITA V PLZNI

Fakulta strojní

Akademický rok: 2017/2018

## ZADÁNÍ DIPLOMOVÉ PRÁCE

(PROJEKTU, UMĚLECKÉHO DÍLA, UMĚLECKÉHO VÝKONU)

Jméno a příjmení: **Bc. Richard PISINGER**

Osobní číslo: **S15N0027P**

Studijní program: **N2301 Strojní inženýrství**

Studijní obor: **Stavba energetických strojů a zařízení**

Název tématu: **Optimization of an industrial heat exchanger  
by the minimalization of entropy**

Zadávající katedra: **Katedra energetických strojů a zařízení**

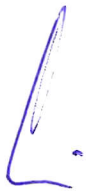
### Z á s a d y p r o v y p r a c o v á n í :

1. Prepare an overview of the types of heat exchangers and their application in the industrial sphere.
2. Define entropy and its significance in the process of designing a heat exchanger.
3. Devise a mathematical model and perform a sensitivity analysis.
4. Specify the guidelines for an optimized design of a heat exchanger.

Rozsah grafických prací: **dle potřeby**  
Rozsah kvalifikační práce: **50 - 70 stran**  
Forma zpracování diplomové práce: **tištěná/elektronická**  
Jazyk zpracování diplomové práce: **Angličtina**  
Seznam odborné literatury:

- **Koorts J. M., 2014: Entropy Minimisation and Structural Design for Industrial Heat Exchanger Optimisation, University of Pretoria, MSc thesis**
- **P. P. P. M. Lerou, T. T. Veenstra, J. F. Burger, H. J. M. ter Brake, H. Rogalla, 2005: Optimization of counterflow heat exchanger geometry through minimization of entropy generation, Cryogenics 45, 659-669**
- **Jiangfeng Guo, Lin Cheng, Mingtian Xu, 2009: Optimization design of shell-and-tube heat exchanger by entropy generation minimization and genetic algorithm, Applied Thermal Engineering 29, 2954-2960**

Vedoucí diplomové práce: **Doc. Ing. Petr Eret, Ph.D.**  
Katedra energetických strojů a zařízení  
Konzultant diplomové práce: **Doc. Ing. Petr Eret, Ph.D.**  
Katedra energetických strojů a zařízení  
Datum zadání diplomové práce: **30. října 2017**  
Termín odevzdání diplomové práce: **21. května 2018**



Doc. Ing. Milan Edl, Ph.D.  
děkan



Dr. Ing. Jaroslav Synáč  
vedoucí katedry

V Plzni dne 20. října 2017

## **Declaration of authorship**

I hereby present my master's thesis for assessment and defense, the completion of which is to close off my master's studies at the Faculty of Mechanical Engineering (FST) at the University of West Bohemia (ZČU) in Pilsen, Czech Republic.

I hereby declare that this master's thesis is entirely my own work and that I only used the cited sources.

Pilsen, May 15, 2018

---

Bc. Richard Pisinger

## **Acknowledgments**

I would like to express my thanks to all who have positively supported me in my endeavors related to my master's thesis.

I would also like to express my thanks to my supervisor and consultant, Doc. Ing. Petr Eret, Ph.D. for his help with my master's thesis.

I would likewise like to thank my family for their extended support during the writing of this thesis. Lastly, I would like to thank my friends for providing their support to the very end.

## ANOTAČNÍ LIST DIPLOMOVÉ PRÁCE

|                      |   |                         |
|----------------------|---|-------------------------|
| <b>AUTOR</b>         | <b>Příjmení</b><br>Bc. Pisinger   | <b>Jméno</b><br>Richard |
| <b>STUDIJNÍ OBOR</b> | N2301 Strojní inženýrství   |                         |
| <b>VEDOUCÍ PRÁCE</b> | <b>Příjmení (včetně titulů)</b><br>Doc. Ing. Eret, Ph.D.                    | <b>Jméno</b><br>Petr    |
| <b>PRACOVIŠTĚ</b>    | ZČU – FST – KKE   |                         |
| <b>DRUH PRÁCE</b>    | <b>DIPLOMOVÁ</b>  |                         |
| <b>NÁZEV PRÁCE</b>   | Optimalizace industriálního tepelného výměníku pomocí minimalizace entropie |                         |

|                |         |                |     |                    |      |
|----------------|---------|----------------|-----|--------------------|------|
| <b>FAKULTA</b> | strojní | <b>KATEDRA</b> | KKE | <b>ROK ODEVZD.</b> | 2018 |
|----------------|---------|----------------|-----|--------------------|------|

### POČET STRAN (A4 a ekvivalentů A4)

|               |    |                     |    |                      |   |
|---------------|----|---------------------|----|----------------------|---|
| <b>CELKEM</b> | 81 | <b>TEXTOVÁ ČÁST</b> | 58 | <b>GRAFICKÁ ČÁST</b> | 0 |
|---------------|----|---------------------|----|----------------------|---|

|                      |   |
|----------------------|---|
| <b>STRUČNÝ POPIS</b> | Práce pojednává o analýze tří různých druhů tepelných výměníků pomocí druhého termodynamického zákona. Generace entropie, jako kvantitativní míra nevratnosti (nedokonalosti) vztažené k přenosu tepla a tekutinového tření při provozu, slouží jako přímá míra ztracené schopnosti přenést teplo. Dále byl vytvořen matematický model, který využívá metodu efektivnosti-NTU společně s citlivostní analýzou a minimalizace čísla generace entropie, které je funkcí optimální proudové cesty a bezrozměrové hmotnostní rychlosti. |
| <b>KLÍČOVÁ SLOVA</b> | tepelný výměník, generace entropie, nevratnost, souproud, protiproud, křížový proud, přenos tepla, tekutinové tření, optimální proudová cesta, bezrozměrná hmotnostní rychlost, efektivnost, NTU, citlivostní analýza, konstrukční návrh  |

## SUMMARY OF DIPLOMA SHEET

|                          |   |                 |
|--------------------------|---|-----------------|
| <b>AUTHOR</b>            | Surname<br>Bc. Pisinger   | Name<br>Richard |
| <b>FIELD OF STUDY</b>    | Design of Power Machines and Equipment  |                 |
| <b>SUPERVISOR</b>        | Surname (Inclusive of Degrees)<br>Doc. Ing. Eret, Ph.D.                       | Name<br>Petr    |
| <b>INSTITUTION</b>       | ZČU – FST – KKE   |                 |
| <b>TYPE OF WORK</b>      | <b>DIPLOMA</b>  |                 |
| <b>TITLE OF THE WORK</b> | Optimization of an industrial heat exchanger by the minimalization of entropy |                 |

|                |                        |                   |     |                     |      |
|----------------|------------------------|-------------------|-----|---------------------|------|
| <b>FACULTY</b> | Mechanical Engineering | <b>DEPARTMENT</b> | KKE | <b>SUBMITTED IN</b> | 2018 |
|----------------|------------------------|-------------------|-----|---------------------|------|

**NUMBER OF PAGES (A4 and eq. A4)**

|              |    |                  |    |                       |   |
|--------------|----|------------------|----|-----------------------|---|
| <b>TOTAL</b> | 81 | <b>TEXT PART</b> | 58 | <b>GRAPHICAL PART</b> | 0 |
|--------------|----|------------------|----|-----------------------|---|

|                          |  |
|--------------------------|--|
| <b>BRIEF DESCRIPTION</b> | A second law of thermodynamics analysis of three different types of heat exchangers is the subject of this thesis. Entropy generation is introduced as a quantitative measure of the irreversibility (imperfectness) related to heat transfer and fluid friction during operation and serves as a direct measure of the lost ability to transfer heat. Furthermore, a mathematical model was developed, utilizing the effectiveness-NTU method, along with a sensitivity analysis, and the minimization of the entropy generation number as a function of the optimum flow path and dimensionless mass velocity. |
| <b>KEY WORDS</b>         | heat exchanger, entropy generation, irreversibility, parallel-flow, counter-flow, cross-flow, heat transfer, fluid friction, optimum flow path, dimensionless mass velocity, effectiveness, NTU, sensitivity analysis, constructal design  |

## Table of Contents

|  |    |
|--|----|
| Introduction.....  | 17 |
| 1 Overview of Heat Exchangers.....   | 18 |
| 1.1 Classification of heat exchangers according to fluid flow direction..... | 18 |
| 1.1.1 Parallel and counter-flow.....   | 18 |
| 1.1.2 Cross-flow heat exchangers.....  | 22 |
| 1.1.3 Shell-and-tube heat exchangers.....                                    | 24 |
| 1.1.4 Plate heat exchangers.....   | 27 |
| 2 Entropy and its significance.....  | 30 |
| 2.1 Entropy balance.....   | 31 |
| 2.2 Entropy generation.....  | 33 |
| 2.3 Entropy Generation Minimization.....                                     | 36 |
| 3 Developing the mathematical model.....                                     | 37 |
| 3.1 Effectiveness-NTU Method.....  | 37 |
| 3.2 Sensitivity analysis of the mathematical model.....                      | 51 |
| 3.3 Graphs and results.....  | 57 |
| 4 Guidelines for an optimized design of a heat exchanger.....                | 64 |
| 4.1 Empirical equations.....   | 64 |
| 4.2 Design constraints.....  | 67 |
| 4.2.1 Heat transfer area design constraint.....                              | 68 |
| 4.2.2 Practical application of the heat transfer area design constraint..... | 68 |
| 5 Conclusion.....  | 72 |
| References.....  | 74 |
| A Charts.....  | 75 |
| A.1 Effectiveness-NTU charts.....  | 78 |
| B Equations for the optimum flow path.....                                   | 81 |



## Table of Figures

|  |    |
|--|----|
| Figure 1: A parallel-flow heat exchanger [2].....  | 18 |
| Figure 2: A counter-flow heat exchanger [2].....   | 19 |
| Figure 3: Overall heat transfer through a plane wall [4].....  | 20 |
| Figure 4: Schematic of a double-pipe heat exchanger [4].....   | 20 |
| Figure 5: Thermal-resistance network for overall heat transfer for a double-pipe heat exchanger [4].....   | 20 |
| Figure 6: A detailed diagram of the parallel and counter-flow heat exchangers [5].....   | 21 |
| Figure 7: A detailed diagram of the cross-flow heat exchanger [5].....   | 22 |
| Figure 8: Cross-flow heat exchanger – unmixed and mixed flow [2].....  | 22 |
| Figure 9: Cross-flow heat exchanger pg 521 [4].....  | 23 |
| Figure 10: Correction factor for a single-pass cross-flow heat exchanger with both fluids unmixed [4].....   | 24 |
| Figure 11: Correction factor for a single-pass cross-flow heat exchanger with one fluid mixed and the other unmixed [4].....   | 24 |
| Figure 12: Schematic of a shell-and-tube heat exchanger (one-shell pass and one-tube pass) [2].....  | 24 |
| Figure 13: Multi-pass flow arrangements in shell-and-tube heat exchangers [2].....   | 25 |
| Figure 14: Types of baffles used in shell-and-tube exchangers [7].....   | 26 |
| Figure 15: Correction-factor plot for exchanger with one shell pass and two, four, or any multiple of tube passes [4].....   | 27 |
| Figure 16: Correction-factor plot for exchanger with two shell passes and four, eight, or any multiple of tube passes [4].....   | 27 |
| Figure 17: Gasketed plate-and-frame heat exchanger [8].....  | 28 |
| Figure 18: Plates showing gaskets around the ports [8].....  | 28 |
| Figure 19: Plate patterns: (a) washboard; (b) zigzag; (c) chevron or herringbone; (d) protrusions and depressions; (e) washboard with secondary corrugations; (f) oblique washboard [8]..... | 29 |
| Figure 20: Number of micro-states for each macro-state.....  | 31 |
| Figure 21: Energy and entropy balances of a system.....  | 32 |
| Figure 22: Mechanism of entropy transfer for a general system.....   | 34 |
| Figure 23: Entropy, heat, and mass transfer for a control volume (CV).....   | 35 |
| Figure 24: Outlet and inlet points of a heat exchanger.....  | 37 |
| Figure 25: A case where the hot fluid has the minimum heat capacity rate (L) and a case where the cold fluid has the minimum heat capacity rate (R).....                                     | 38 |
| Figure 26: Effectiveness for heat exchangers.....  | 41 |
| Figure 27: Comparison of the effectiveness of three heat exchangers for two different capacity ratios.....   | 42 |
| Figure 28: Comparison of the effectiveness of three heat exchangers for two different  |    |

|  |    |
|--|----|
| capacity ratios and small NTU numbers.....   | 42 |
| Figure 29: Effectiveness as a relation of NTU for $c = 0$ for all heat exchangers.....   | 43 |
| Figure 30: Relative-sensitivity analysis for the entropy generation function.....  | 56 |
| Figure 31: Variation between the optimum flow path length and the dimensionless mass velocity for all of the heat exchangers with $c = 0.595238095238095$ .....  | 57 |
| Figure 32: Variation between the minimum entropy generation number and the optimum flow path length for all of the heat exchangers with $c = 0.595238095238095$ .....  | 58 |
| Figure 33: Variation between the optimum flow path length and the dimensionless mass velocity for all of the heat exchangers with $c = 1$ .....  | 58 |
| Figure 34: Variation between the minimum entropy generation number and the optimum flow path length for all of the heat exchangers with $c = 1$ .....  | 59 |
| Figure 35: Optimum flow path comparison of parallel-flow heat exchangers.....  | 59 |
| Figure 36: Minimum entropy generation number comparison of parallel-flow heat exchangers.....  | 60 |
| Figure 37: Optimum flow path comparison of counter-flow heat exchangers.....   | 60 |
| Figure 38: Minimum entropy generation number comparison of counter-flow heat exchangers.....   | 61 |
| Figure 39: Optimum flow path comparison of cross-flow heat exchangers.....   | 61 |
| Figure 40: Minimum entropy generation number comparison of cross-flow heat exchangers.....   | 62 |
| Figure 41: Plots of the comparison between the original $\varepsilon$ -NTU relation (blue) and the empirically-derived approximations (red).....   | 65 |
| Figure 42: Number of entropy generation units per side, as a function of $(L/rh)$ , $g$ , and $NRe$ [17].....  | 68 |
| Figure 43: Dependence of the heat transfer area on $(4L/D)$ for a given $Re$ and fixed $Ns$ for the various types of heat exchangers.....  | 72 |
| Figure 44: Variation between the optimum flow path length and the dimensionless mass velocity ( $L$ ) and variation between the minimum entropy generation number and the optimum flow path length ( $R$ ) for a parallel-flow heat exchanger ( $c = 0.595238095238095$ )..... | 75 |
| Figure 45: Variation between the optimum flow path length and the dimensionless mass velocity ( $L$ ) and variation between the minimum entropy generation number and the optimum flow path length ( $R$ ) for a parallel-flow heat exchanger ( $c = 1$ ).....                 | 75 |
| Figure 46: Variation between the optimum flow path length and the dimensionless mass velocity ( $L$ ) and variation between the minimum entropy generation number and the optimum flow path length ( $R$ ) for a counter-flow heat exchanger ( $c = 0.595238095238095$ ).....  | 76 |
| Figure 47: Variation between the optimum flow path length and the dimensionless mass velocity ( $L$ ) and variation between the minimum entropy generation number and the optimum flow path length ( $R$ ) for a counter-flow heat exchanger ( $c = 1$ ).....                  | 76 |
| Figure 48: Variation between the optimum flow path length and the dimensionless mass velocity ( $L$ ) and variation between the minimum entropy generation number and the optimum flow path length ( $R$ ) for a cross-flow heat exchanger ( $c = 0.595238095238095$ ).....    | 77 |

Figure 49: Variation between the optimum flow path length and the dimensionless mass velocity (L) and variation between the minimum entropy generation number and the optimum flow path length (R) for a cross-flow heat exchanger ( $c = 1$ ).....77

Figure 50: Variation between the effectiveness and the number of transfer units for a parallel-flow heat exchanger.....78

Figure 51: Variation between the effectiveness and the number of transfer units for a counter-flow heat exchanger.....78

Figure 52: Variation between the effectiveness and the number of transfer units for a cross-flow heat exchanger.....79

Figure 53: Variation between the effectiveness and the number of transfer units for all of the heat exchangers with  $c = 0.595238095238095$ .....79

Figure 54: Variation between the effectiveness and the number of transfer units for all of the heat exchangers with  $c = 1$ .....80

## Table of Tables

|  |    |
|--|----|
| Table 1: Effectiveness relations for heat exchangers [13].....                                     | 40 |
| Table 2: NTU relations for heat exchangers [13].....   | 44 |
| Table 3: Modified entropy generation equations.....  | 49 |
| Table 4: Modified entropy generation equations.....  | 50 |
| Table 5: Table of derivatives for the sensitivity analysis.....                                    | 54 |
| Table 6: Normal Operating Point (NOP).....   | 55 |
| Table 7: X and Y coefficients of the empirically-derived equations.....                            | 64 |
| Table 8: Entropy generation equations for the empirically-derived equations.....                   | 66 |
| Table 9: Optimum flow path equations for the empirically-derived equations.....                    | 67 |
| Table 10: Optimum flow path equations for the empirically-derived equations.....                   | 69 |
| Table 11: Minimum heat transfer area equations for the empirically-derived equations.....          | 70 |
| Table 12: Optimum dimensionless mass velocity equations for the empirically-derived equations..... | 71 |

## List of Abbreviations

- $\varepsilon$ -NTU – effectiveness-NTU method
- EGM – entropy generation minimization
- LMTD – logarithmic mean temperature difference
- NTU – number of transfer units

## List of Frequently Used Symbols

| Symbol    | Unit  | Property  |
|-----------|---|---|
| $A$       | $[\text{m}^2]$                                    | Surface area through which convection heat transfer takes place                   |
| $A_i$     | $[\text{m}^2]$                                    | Surface area of the inner wall through which convection heat transfer takes place |
| $A_o$     | $[\text{m}^2]$                                    | Surface area of the outer wall through which convection heat transfer takes place |
| $A_s$     | $[\text{m}^2]$                                    | Heat transfer surface area of the heat exchanger                                  |
| $c$       | $[-]$   | Heat capacity ratio   |
| $C_c$     | $[\text{J}\cdot\text{kg}^{-1}\cdot\text{K}^{-1}]$ | Heat capacity rate of the “cold” fluid  |
| $C_h$     | $[\text{J}\cdot\text{kg}^{-1}\cdot\text{K}^{-1}]$ | Heat capacity rate of the “hot” fluid   |
| $C_{max}$ | $[\text{J}\cdot\text{kg}^{-1}\cdot\text{K}^{-1}]$ | The larger of the two heat capacities of a heat exchanger                         |
| $C_{min}$ | $[\text{J}\cdot\text{kg}^{-1}\cdot\text{K}^{-1}]$ | The smaller of the two heat capacities of a heat exchanger                        |
| $C_p$     | $[\text{J}\cdot\text{kg}^{-1}\cdot\text{K}^{-1}]$ | Heat capacity   |
| $D$       | $[\text{m}]$                                      | Diameter  |
| $F$       | $[-]$   | Correction factor   |
| $f$       | $[-]$   | Friction  |
| $G$       | $[\text{kg}\cdot\text{m}^{-2}\cdot\text{s}^{-1}]$ | Mass velocity   |
| $G^*$     | $[-]$   | Dimensionless mass velocity   |
| $h_1$     | $[\text{W}\cdot\text{m}^{-2}\cdot\text{K}^{-1}]$  | Convection heat transfer coefficient of fluid 1                                   |
| $h_2$     | $[\text{W}\cdot\text{m}^{-2}\cdot\text{K}^{-1}]$  | Convection heat transfer coefficient of fluid 2                                   |
| $k$       | $[\text{W}\cdot\text{m}^{-2}\cdot\text{K}^{-1}]$  | Thermal conductivity of a material  |
| $k$       | $\text{J}\cdot\text{K}^{-1}$                      | Boltzmann constant  |
| $L$       | $[\text{m}]$                                      | Length  |
| $m$       | $[\text{kg}]$                                     | Mass  |
| $\dot{m}$ | $[\text{kg}\cdot\text{s}^{-1}]$                   | Mass transfer rate  |
| $m_e$     | $[\text{kg}]$                                     | Exit mass   |

| Symbol          | Unit                                   | Property                            |
|-----------------|--|-------------------------------------|
| $m_i$           | [kg]                                   | Inlet mass                          |
| NTU             | [-]                                    | Number of heat transfer units       |
| Nu              | [-]                                    | Nusselt number                      |
| $P$             | [-]                                    | Temperature Ratio                   |
| $P_{1,in}$      | [Pa]                                   | Inlet pressure of fluid 1           |
| $P_{1,out}$     | [Pa]                                   | Outlet pressure of fluid 1          |
| $P_{2,in}$      | [Pa]                                   | Inlet pressure of fluid 2           |
| $P_{2,out}$     | [Pa]                                   | Outlet pressure of fluid 2          |
| $p_{c,in}$      | [Pa]                                   | Inlet pressure of the “cold” fluid  |
| $p_{c,out}$     | [Pa]                                   | Outlet pressure of the “cold” fluid |
| $p_{h,in}$      | [Pa]                                   | Inlet pressure of the “hot” fluid   |
| $p_{h,out}$     | [Pa]                                   | Outlet pressure of the “hot” fluid  |
| Pr              | [-]                                    | Prandtl number                      |
| $q$             | [J]                                    | Heat transfer                       |
| $Q$             | [J]                                    | Heat transfer                       |
| $\dot{Q}$       | [J·s <sup>-1</sup> ]                   | Heat transfer rate                  |
| $\dot{Q}_{max}$ | [J·s <sup>-1</sup> ]                   | Max heat transfer rate              |
| $R_1$           | [J·kg <sup>-1</sup> ·K <sup>-1</sup> ] | Ideal gas constant                  |
| $R_2$           | [J·kg <sup>-1</sup> ·K <sup>-1</sup> ] | Ideal gas constant                  |
| Re              | [-]                                    | Reynolds number                     |
| $r_i$           | [m]                                    | Radius of inner wall                |
| $r_o$           | [m]                                    | Radius of outer wall                |
| $S$             | [m <sup>2</sup> ]                      | Surface area                        |
| $S$             | [J·K <sup>-1</sup> ]                   | Entropy                             |
| $s$             | [J·K <sup>-1</sup> ]                   | Entropy                             |
| $s_e$           | [J·K <sup>-1</sup> ]                   | Exit entropy                        |
| $S_{gen}$       | [J·K <sup>-1</sup> ]                   | Entropy generation                  |
| $s_i$           | [J·K <sup>-1</sup> ]                   | Inlet entropy                       |
| St              | [-]                                    | Stanton number                      |
| $T_{1,in}$      | [K]                                    | Inlet temperature of fluid 1        |
| $T_{1,out}$     | [K]                                    | Outlet temperature of fluid 1       |
| $T_{2,in}$      | [K]                                    | Inlet temperature of fluid 2        |

| <b>Symbol</b>      | <b>Unit</b>                           | <b>Property</b>  |
|--------------------|---------------------------------------|--|
| $T_{2,out}$        | [K]                                   | Outlet temperature of fluid 2  |
| $T_{c,in}$         | [K]                                   | Inlet temperature of the “cold” fluid                                    |
| $T_{c,out}$        | [K]                                   | Outlet temperature of the “cold” fluid                                   |
| $T_{h,in}$         | [K]                                   | Inlet temperature of the “hot” fluid                                     |
| $T_{h,out}$        | [K]                                   | Outlet temperature of the “hot” fluid                                    |
| $U$                | [W·m <sup>-2</sup> ·K <sup>-1</sup> ] | Overall heat transfer coefficient  |
| $V$                | [m <sup>3</sup> ]                     | Volume of the system   |
| $W$                | [-]                                   | Number of micro-states   |
| $\alpha_1$         | [m <sup>2</sup> ·s <sup>-1</sup> ]    | Thermal diffusivity of fluid 1   |
| $\alpha_2$         | [m <sup>2</sup> ·s <sup>-1</sup> ]    | Thermal diffusivity of fluid 2   |
| $\delta$           | [m]                                   | Wall thickness   |
| $\Delta S_{CV}$    | [J·K <sup>-1</sup> ]                  | Entropy for a control volume   |
| $\Delta T_{lm}$    | [K]                                   | Logarithmic mean temperature difference                                  |
| $\Delta T_{lm,CF}$ | [K]                                   | Logarithmic mean temperature difference of a counter-flow heat exchanger |
| $\varepsilon$      | [-]                                   | Effectiveness  |
| $\lambda$          | [W·m <sup>-1</sup> ·K <sup>-1</sup> ] | Thermal conductivity   |
| $\rho$             | [kg·m <sup>-3</sup> ]                 | Density  |



## Introduction

A heat exchanger can be thought of as any device, the primary purpose of which is to transfer heat from a fluid with a higher amount of thermal energy (enthalpy) to a second fluid, which has a lower amount of thermal energy. These two fluids are prevented from mixing by a solid wall, which is one of the primary components of the heat exchanger. Examples of heat exchangers are quite commonplace in the everyday life of the individual. An elementary example of a heat exchanger is a kettle, which is used to transfer heat from a heating element into the water, the continuing transferring of which eventually results in the boiling of said water. Another common example is a refrigerator, the basic principle of which involves transferring heat from the stored victuals and expelling the heat into the surrounding area, with the aid of electrical energy to power the fridge.

A more refined example of where heat exchangers can be used is in power plants that generate electricity using steam turbines. At the end of a turbine, when the steam has expanded such and expended most of its usable energy to the generator (for generating electricity), it still has enough enthalpy to be useful for heat regeneration. This process is done via heat exchangers, where some of the heat from the steam (before it reaches the condenser) is taken and used to heat the condensate in a process called “regeneration”, which ultimately increases the thermal efficiency of the power plant. With regard to power plants, a visible example of a heat exchanger is a cooling tower, notably a wet cooling tower, where sprinklers in the cooling tower release liquid water onto hot tubes containing water, which is holding the disposable thermal energy of the power plant. The water then evaporates off of the outside of the tubes and into the atmosphere, resulting in a usually visible cloud stemming from the tower.

In a heat exchanger, there are usually two different kinds of heat transfer – *convection* in each fluid and *conduction* through the wall, which is keeping the two fluids from mixing. However, when working with heat exchangers, these processes are usually combined into an overall heat transfer coefficient. The value of this coefficient can vary depending on the position along the wall separating the two fluids.

# 1 Overview of Heat Exchangers

The classification of heat exchangers can be either based on how the mediums flow with respect to one another or according to how they are built. An example of the former includes heat exchangers with counter-current flow, where the two fluids flow in opposite directions to each other, but in a parallel manner. Another example is a heat exchanger with cocurrent or parallel flow, which is the same as the previous example but the two fluids now flow in the same direction. Cross-flow heat exchangers have the media flow perpendicular to one another. A cross-flow/counter-flow heat exchanger is a hybrid of the previously mentioned heat exchangers. The first two types of heat exchangers can be seen in figures 1 and 2.

As mentioned, heat exchangers can be classified according to how they are constructed. From here they can be further classified into the following categories – recuperative and regenerative heat exchangers. Recuperative heat exchangers have a wall separating the fluids flowing through the heat exchanger, which have different flow paths and exchange their heat through this separating barrier. Regenerative heat exchangers on the other hand involves a single flow path, through which the hot and cold mediums alternatively flow. [1]

## 1.1 Classification of heat exchangers according to fluid flow direction

### 1.1.1 Parallel and counter-flow

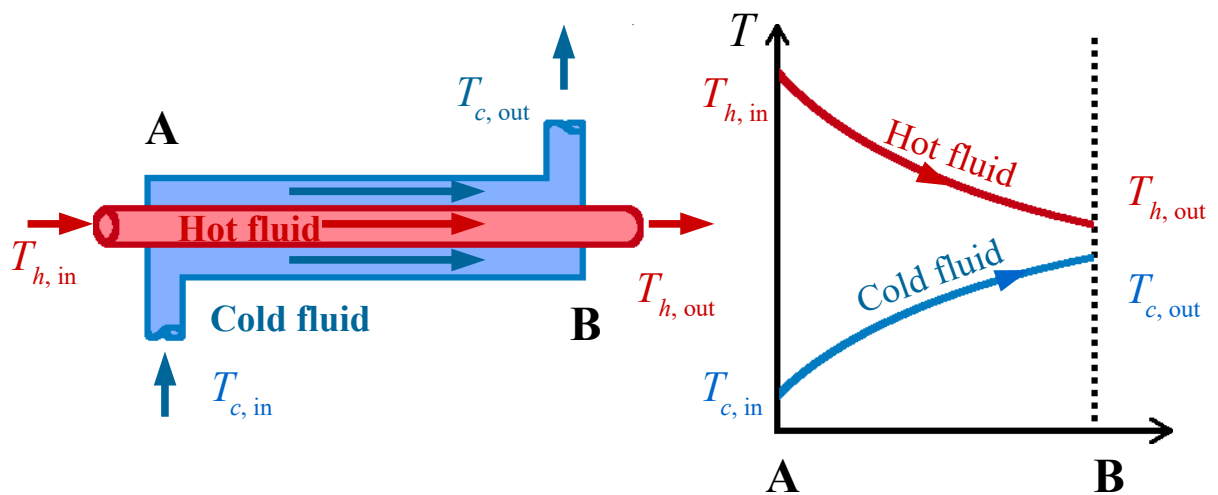


Figure 1: A parallel-flow heat exchanger [2]

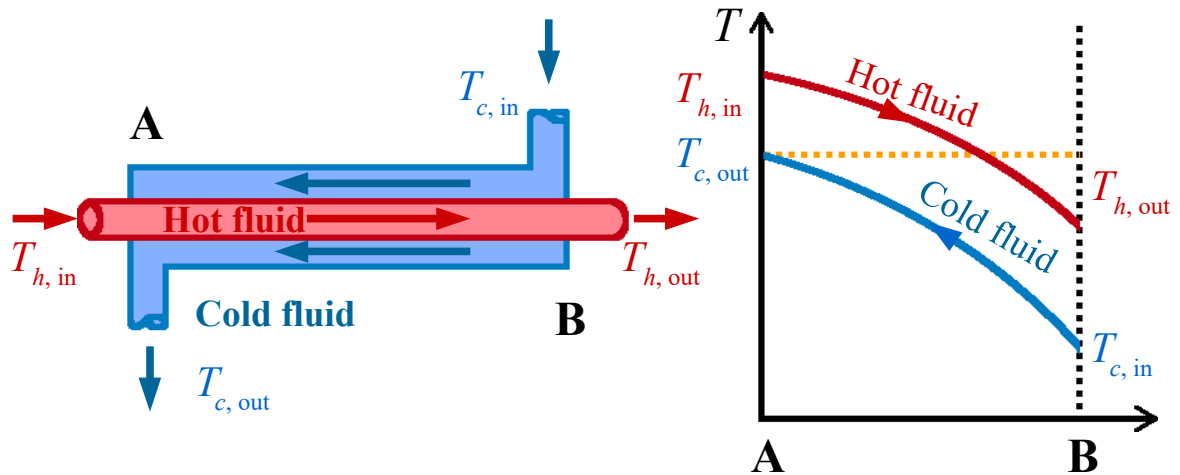


Figure 2: A counter-flow heat exchanger [2]

The prevailing types of fluid flow arrangement within heat exchangers are those with parallel or counter-flow. Regarding how the heat transfer process works pertaining to both of these arrangements, both conduction and convection are involved. The heat transfer process starts with the hot fluid, where the fluid starts to transfer its heat by convection to the tubular wall, whereby the heat is conducted through the wall to the side of the wall, which is in contact with the second, colder fluid. The heat is then transferred by the process of convection to this second fluid. Nevertheless, this process of heat transfer is not constant along the entire length of the tube within the heat exchanger, for the temperature difference between the two fluids varies along this length, thereby affecting the rate of heat transfer. Figure 3 shows an example of how this works.

A counter-flow heat exchanger is generally preferred to that of a heat exchanger with parallel-flow due to some of the advantages of the former to that of the latter. One of the advantages lies in the fact that the outlet temperature of the cold fluid can come close to, or be lower than, that of the inlet temperature of the hot fluid. Another advantage is that the more uniform temperature difference between the two fluids provides for a more uniform rate of heat transfer along the length of the tubular contact between the two fluids within the heat exchanger, which has the added advantage of mitigating the thermal stresses of the heat exchanger. These advantages yield greater heat recovery and to a more compact heat exchanger, regarding the counter-flow design.

Adding to the advantages of the counter-flow heat exchanger, there are two significant disadvantages of the parallel-flow design. One of the disadvantages is evidenced in the considerable temperature difference between the starting and ending points of the heat exchanger. This can lead to unwarranted large thermal stresses, contributing to possible material failure. A second point to make is that at the end of the heat exchanger, the outlet temperature of the cold fluid can never be lesser than that of the inlet temperature of the hot fluid, which however, can be considered an advantage if the goal is to have both of the outlet temperatures to be at around the same temperature [3].

Notwithstanding, there can be cases where a parallel-flow design can be advantageous. Besides cases where one would require the outlet temperatures of the fluids to be similar, should one require fast heat transfer, then the parallel-flow design should be suitable, as at the start of the heat exchanger, there is an enormous temperature difference, which is more easily achieved with this kind of design, contrary to the counter-flow type. Another case arises when one of the fluids is undergoing a phase change, during which the

temperature for this fluid does not change during its phase change, which means that either of the two designs, the parallel or counter-flow, can be utilized to no disadvantage [1].

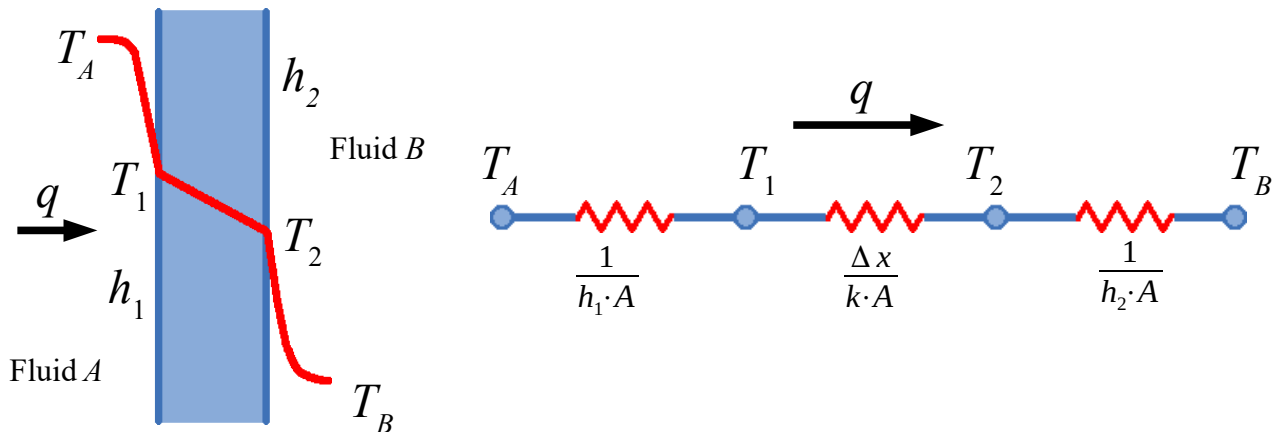


Figure 3: Overall heat transfer through a plane wall [4]

When it comes to calculating the heat transfer through a planar surface, the following calculations apply (eqs. (1) and (2)):

$$Q = k \cdot S \cdot \Delta T_s = \frac{1}{\frac{1}{\alpha_1} + \frac{\delta}{\lambda} + \frac{1}{\alpha_2}} \cdot S \cdot \Delta T_s \quad (1)$$

$$k = \left( \frac{1}{\alpha_1} + \frac{\delta}{\lambda} + \frac{1}{\alpha_2} \right)^{-1} \quad (2)$$

where  $S$  is the area,  $\delta$  is the thickness,  $\lambda$ ,  $\alpha_1$ ,  $\alpha_2$ ,  $k$  is the heat transfer coefficient, and  $\Delta T_s$  is the mean temperature difference. Figure 4 shows an example of the heat transfer process in a double-pipe (parallel-flow) heat exchanger.

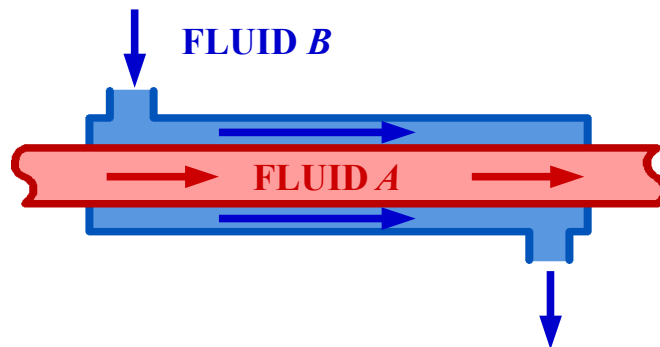


Figure 4: Schematic of a double-pipe heat exchanger [4]

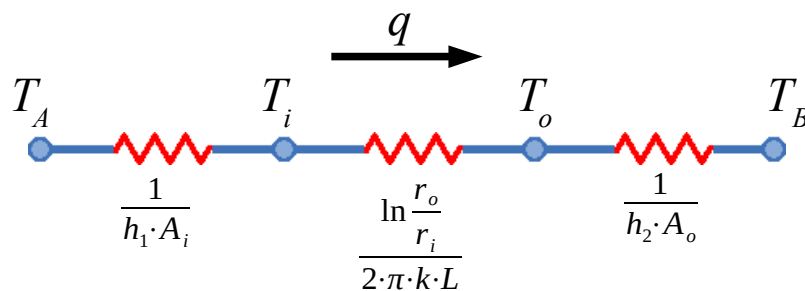


Figure 5: Thermal-resistance network for overall heat transfer for a double-pipe heat exchanger [4]

When one goes about calculating the heat transfer through a tubular wall, the

following calculations apply (eqs. (3) and (4)):

$$Q = k \cdot S \cdot \Delta T_s = \frac{1}{\frac{1}{\alpha_1} \cdot \frac{R_2}{R_1} + \frac{R_2}{\lambda} \cdot \ln \frac{R_2}{R_1} + \frac{1}{\alpha_2}} \cdot 2 \cdot \pi \cdot R_2 \cdot L \cdot \Delta T_s \quad (3)$$

$$k = \left( \frac{1}{\alpha_1} \cdot \frac{R_2}{R_1} + \frac{R_2}{\lambda} \cdot \ln \frac{R_2}{R_1} + \frac{1}{\alpha_2} \right)^{-1} \quad (4)$$

where  $L$  is the length,  $R_1$  is the inner wall radius,  $R_2$  is the outer wall radius,  $\lambda$ ,  $\alpha_1$ ,  $\alpha_2$ ,  $k$  is the heat transfer coefficient, and  $\Delta T_s$  is the mean temperature difference.

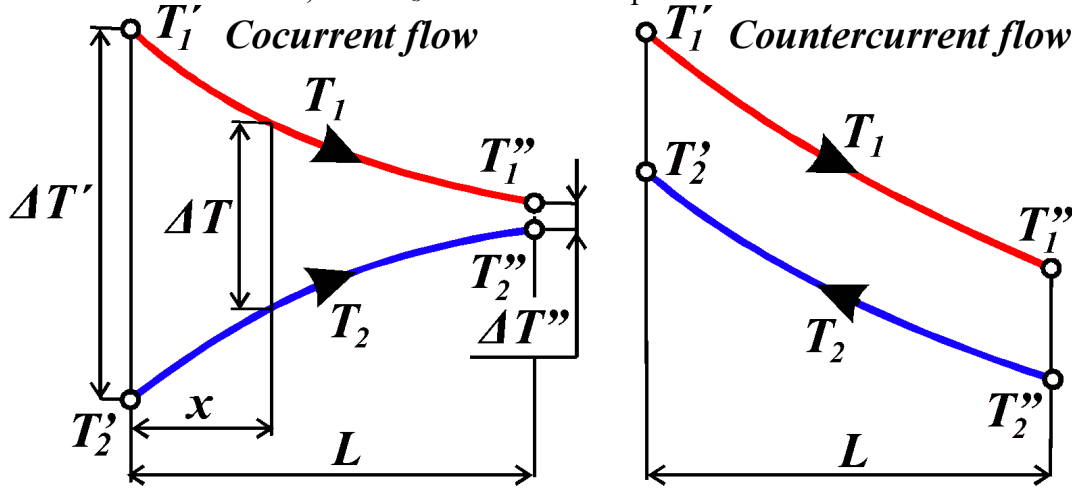


Figure 6: A detailed diagram of the parallel and counter-flow heat exchangers [5]

Figure 6 shows a side-by-side visual comparison of the LMTD diagrams for illustrative purposes. The calculations for the log mean temperature difference are the same for both the parallel and counter-flow heat exchangers, as can be seen in eqs. (5) – (8):

$$\Delta T = \Delta T' \cdot e^{-k \cdot x}, \quad k = ? \quad (5)$$

$$\Delta T'' = \Delta T' \cdot e^{-k \cdot L} \Rightarrow -k \cdot L = \ln \frac{\Delta T''}{\Delta T'} \Rightarrow k = -\frac{1}{L} \cdot \ln \frac{\Delta T''}{\Delta T'} \quad (6)$$

$$\Delta T = \Delta T' \cdot e^{\frac{x}{L} \cdot \ln \frac{\Delta T''}{\Delta T'}} \quad (7)$$

$$\begin{aligned} \Delta T_s &= \frac{1}{L} \int_0^L \Delta T \cdot dx = \frac{\Delta T'}{L} \int_0^L e^{\frac{x}{L} \cdot \ln \frac{\Delta T''}{\Delta T'}} \cdot dx = \frac{\frac{1}{L} \cdot \Delta T' \cdot e^{\frac{x}{L} \cdot \ln \frac{\Delta T''}{\Delta T'}} \Big|_0^L}{\frac{1}{L} \cdot \ln \frac{\Delta T''}{\Delta T'}} = \dots \\ &= \frac{\Delta T' \cdot \left( e^{\ln \frac{\Delta T''}{\Delta T'}} - 1 \right)}{\ln \frac{\Delta T''}{\Delta T'}} = \frac{\Delta T' \cdot \left( \frac{\Delta T''}{\Delta T'} - 1 \right)}{\ln \frac{\Delta T''}{\Delta T'}} = \frac{\Delta T'' - \Delta T'}{\ln \frac{\Delta T''}{\Delta T'}} = \frac{\Delta T' - \Delta T''}{\ln \frac{\Delta T'}{\Delta T''}} \end{aligned} \quad (8)$$

### 1.1.2 Cross-flow heat exchangers

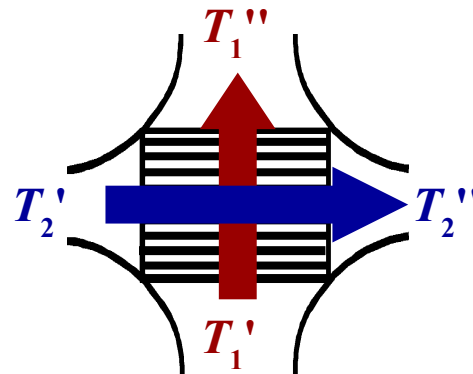


Figure 7: A detailed diagram of the cross-flow heat exchanger [5]

When a heat exchanger is of the cross-flow type, the two fluids in the heat exchanger are perpendicular to each other, as seen in figure 7. One of the fluids flows through a tubular structure, while the other fluid flows around this structure at a 90-degree angle. This type of heat exchanger is most often utilized in situations where one of the fluid undergoes a phase change. An example can be found in a steam-driven power plant, in the condenser. The condenser is comprised of tubes, through which the coolant flows through, thereby absorbing the heat from the steam (which has just left the turbine and entered the condenser), which is flowing around the tubes. The steam is then condensed into liquid water [6].

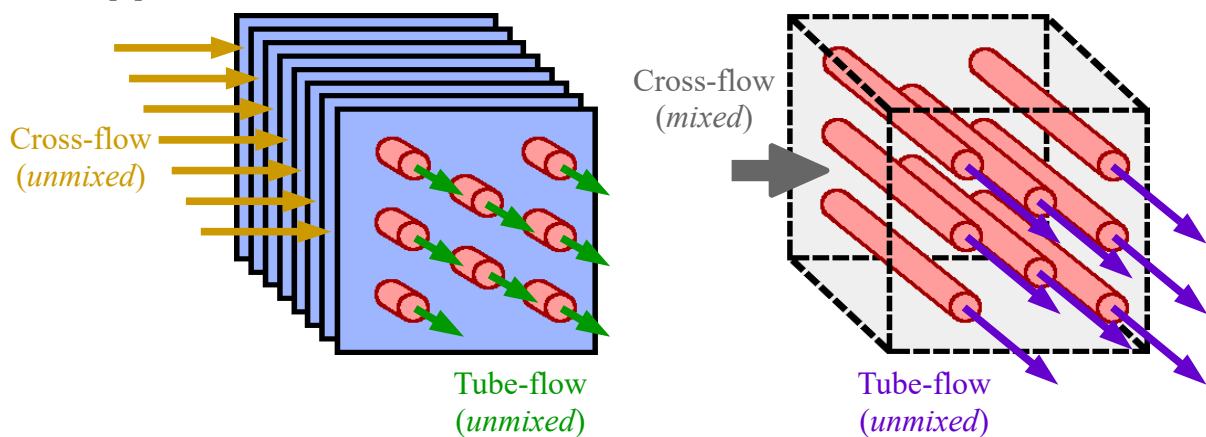


Figure 8: Cross-flow heat exchanger – unmixed and mixed flow [2]

Cross-flow heat exchangers can also be divided into two subgroups – *mixed* and *unmixed flow*, as can be seen in figure 8. Unmixed flow is where neither of the two fluids are mixed, as in the previous example with the steam condenser. Mixed cross-flow heat exchangers are simpler and have one of the fluids, namely that of the fluid flowing through the tubular structure, stay unmixed and the other fluid, also known as the *cross-flow*, become mixed (such as the surrounding air) [2].

These types of heat exchangers, i.e. of the cross-flow type, are most often utilized in cooling applications or in air/gas heating. An example of the mixed type of cross-flow heat exchanger can be seen when it comes to radiators in an apartment, the heated water flows through the tubes of the radiator (unmixed), whereas the air around the radiator is mixed, e.g. with various odors and potential pollutants.

There are some other differences as well when it comes to the mixed and unmixed types of cross-flow heat exchangers. For instance, there can simultaneously be a temperature gradient normal and parallel to the direction of the flow regarding an unmixed flow. By contrast, the fluid temperature normal to the direction of a mixed flow will likely equalize as a consequence of its inherent mixing [4].

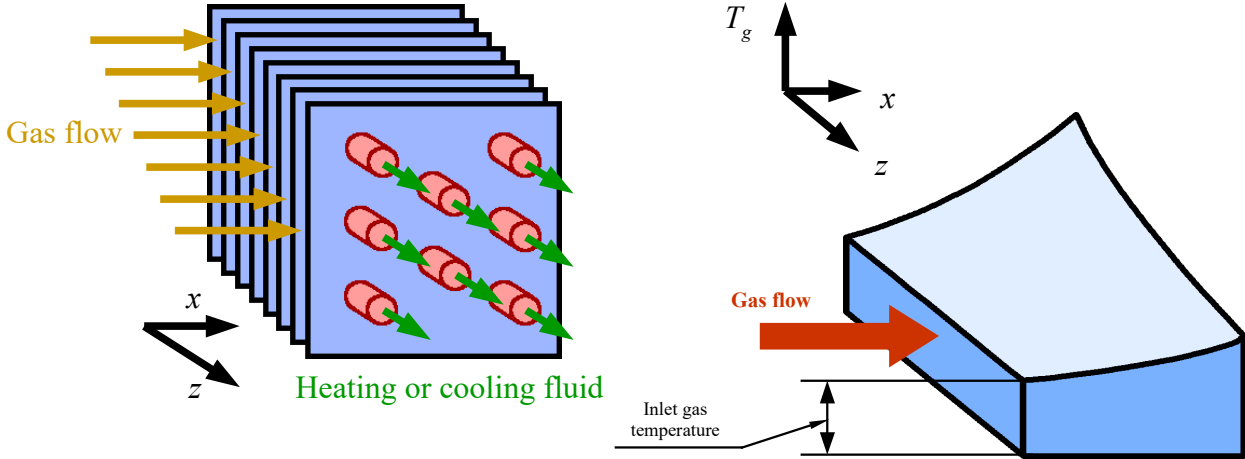


Figure 9: Cross-flow heat exchanger pg 521 [4]

Figure 9 displays a general temperature profile of an unmixed cross-flow heat exchanger. The profile was drawn with the assumption that the gas flowing through the heat exchanger is heated contemporaneously. The total heat transfer inside the heat exchanger is entirely dependent on the temperature difference between the cold and hot fluids, and this in turn is dependent on whether the cross-flow fluid is mixed or unmixed [4].

The log mean temperature difference, which was calculated previously for the parallel and counter-flow heat exchangers, cannot be applied in this case. A similar equation does exist for cross-flow heat exchangers, nevertheless the equation would be considered to be too arduous due to the convoluted flow conditions. There does however exist a simplification (eq. (9)) by way of utilizing a **correction factor  $F$** :

$$\Delta T_{lm} = F \cdot \Delta T_{lm,CF} \quad (9)$$

This correction factor is dependent on not only the inlet and outlet temperatures of both the hot and cold fluids, but also on the geometry of the heat exchanger. Term  $\Delta T_{lm,CF}$  signifies the log mean temperature difference of a counter-flow heat exchanger. The correction factor ranges from  $F = 0.5$  to the limiting  $F = 1$ , whereupon this limit indicates a typical counter-flow heat exchanger. Anything less than the value of 1 indicates a cross-flow heat exchanger. The correction factor can be found in the following diagrams, using two temperature ratios (eqs. (10) – (11)):

$$P = \frac{T_{1,out} - T_{1,in}}{T_{2,in} - T_{1,in}} \quad (10)$$

and

$$R = \frac{T_{2,in} - T_{2,out}}{T_{1,out} - T_{1,in}} = \frac{(\dot{m} \cdot C_p)_{tube\ side}}{(\dot{m} \cdot C_p)_{shell\ side}} \quad (11)$$

The value of  $P$  ranges from 0 to 1, whereas the value of  $R$  ranges from 0 to  $\infty$ . For both of the limiting values of  $R$ , the correction factor is 1 and this indicates a phase change either on one side of the heat exchanger or on the other side [2]. Figures 10 and 11 are

diagrams showing the correction factor for two different types of heat exchangers.

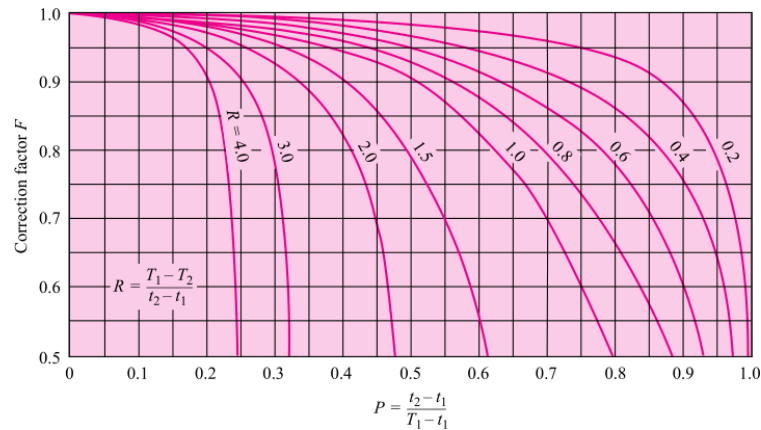


Figure 10: Correction factor for a single-pass cross-flow heat exchanger with both fluids unmixed [4]

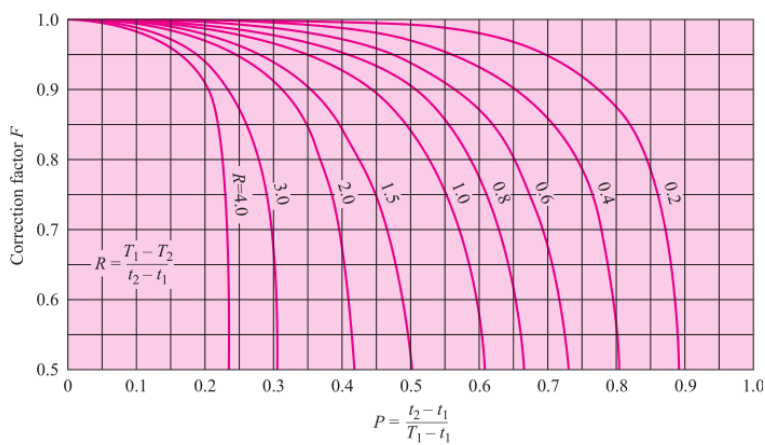


Figure 11: Correction factor for a single-pass cross-flow heat exchanger with one fluid mixed and the other unmixed [4]

### 1.1.3 Shell-and-tube heat exchangers

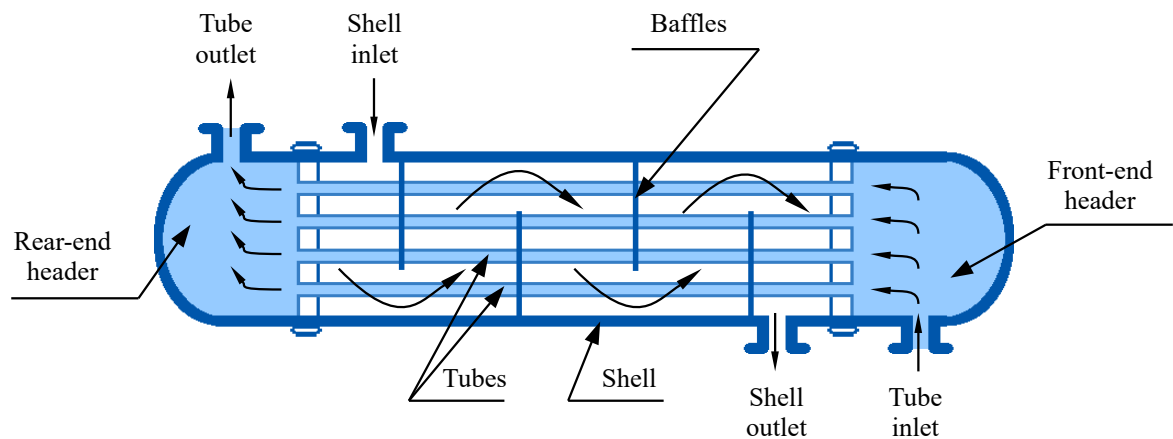


Figure 12: Schematic of a shell-and-tube heat exchanger (one-shell pass and one-tube pass) [2]



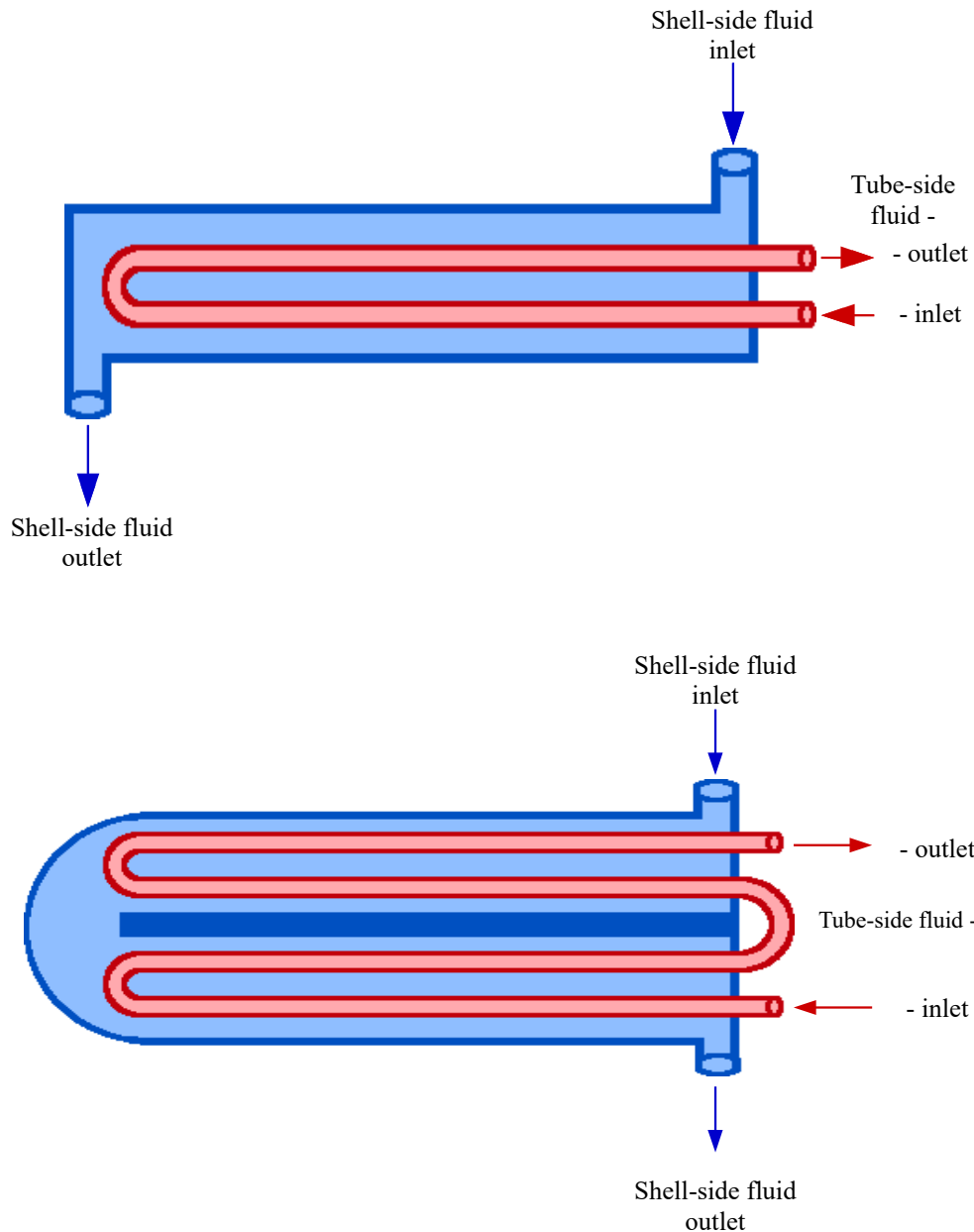


Figure 13: Multi-pass flow arrangements in shell-and-tube heat exchangers [2]

One of the most prevalent kinds of heat exchangers is presented by the shell-and-tube heat exchanger, which is shown in figures 12 and 13. It can be comprised by a large-diameter pipe, the inside of which consists of a few smaller tubes, the number of which can range from around 20 to over around 1000 tubes. There are 2 large flow areas, which are called *headers*, one inside of both ends of the shell each, to which the smaller tubes are open to, the purpose of which is for the accumulation of the fluid prior to and upon exiting the smaller tubes. The axes of the smaller tubes are parallel to the axis of the shell. There are two fluid flows in the shell-and-tube heat exchanger – one flows through inside the shell outside of the tubes, while the other flows through the smaller tubes. Notwithstanding the fact that this type of heat exchanger is fairly commonplace, they're unsuitable for application in the aircraft and automotive industries due to their sizable mass and the amount of space they occupy. [2]

The process of heat transfer between the two fluids is further enhanced by the

placement of artificial obstructions called *baffles*, which also maintain consistent spacing between the tubes. The baffles cause the shell fluid to flow almost perpendicularly to the tube axes. This results in substantial turbulence, along with a rise in value of the heat-transfer coefficients, therein lies the enhancement of the heat transfer. The length of the separation of the baffles from each other is called *baffle pitch* or *baffle spacing*. This spacing has a noticeable impact on the velocity of the shell fluid as it's flowing passed the smaller tubes. The length of the baffle spacing can vary from 20% to 100% the length of the diameter of the inside of the shell. There are a number of different kinds of baffles, such as segmental baffles, disc-and-doughnut baffles, or orifice baffles. Some of these types of baffles can be seen in figure 14. [7]

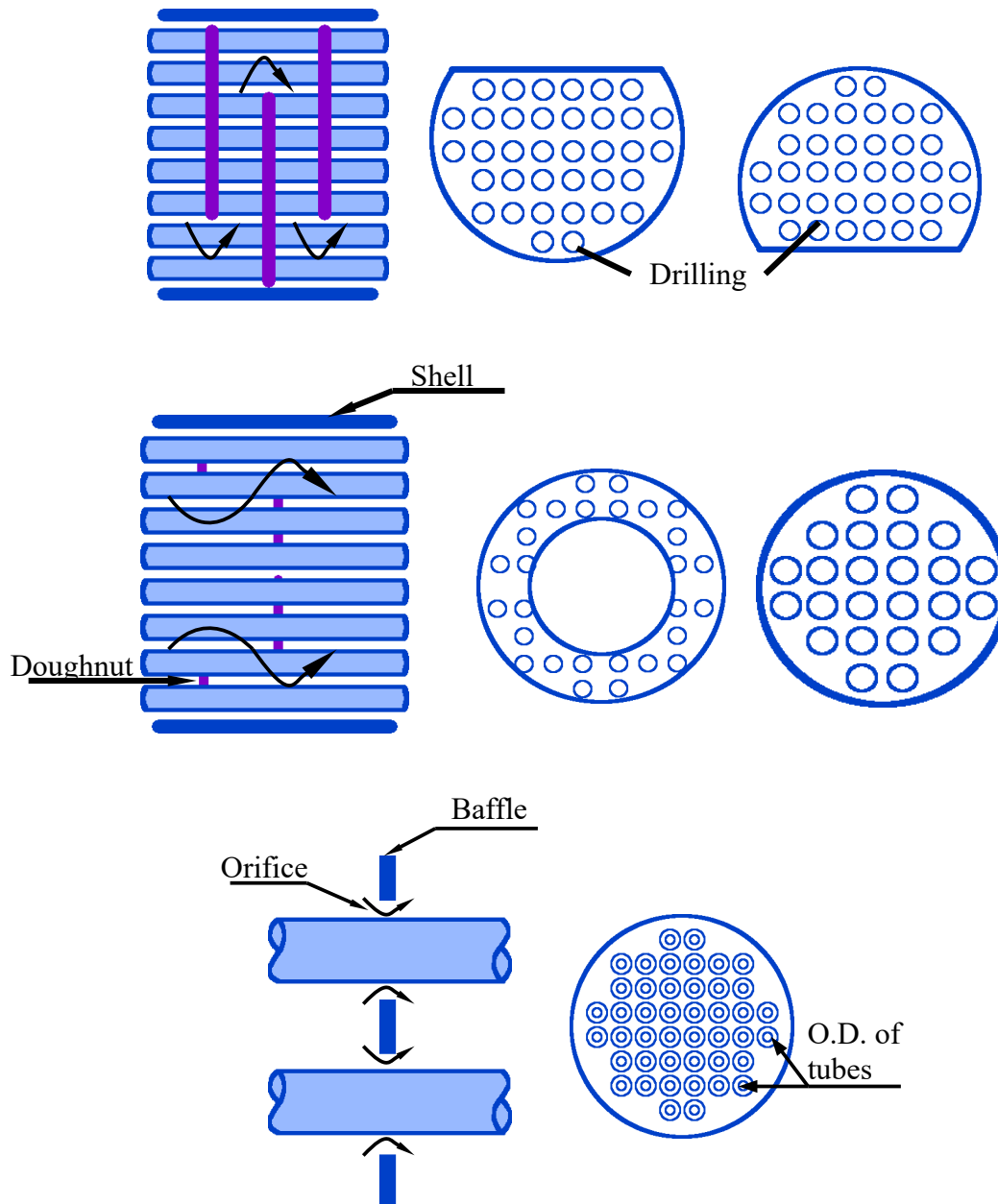


Figure 14: Types of baffles used in shell-and-tube exchangers [7]

One can also organize shell-and-tube heat exchangers into subgroups according to the number of shell and tube passes in the design. When the heat exchanger has all the tubes making only one U-turn within the shell, then it is called a *one-shell-pass and two-*

*tube-passes* heat exchanger. Should it have two passes, then it's known as a *two-shell-passes and four-tube-passes* heat exchanger. As for the cross-flow heat exchanger, figures 15 and 16 are diagrams showing the correction factor for two different types of shell-and-tube heat exchangers. [4]

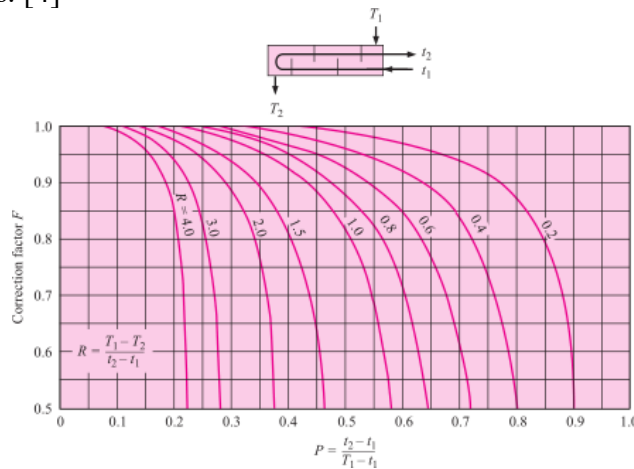


Figure 15: Correction-factor plot for exchanger with one shell pass and two, four, or any multiple of tube passes [4]

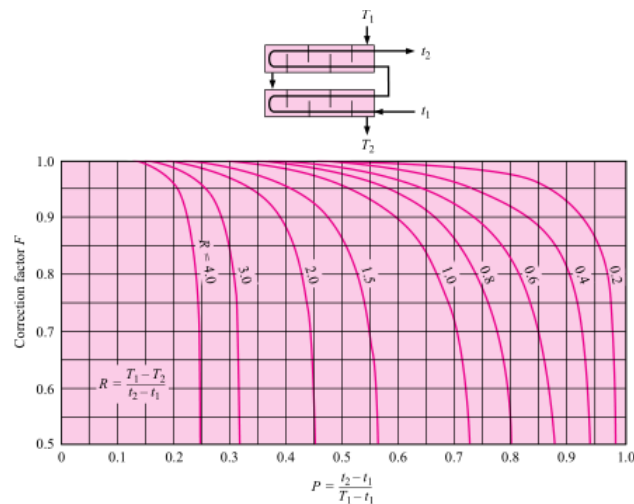


Figure 16: Correction-factor plot for exchanger with two shell passes and four, eight, or any multiple of tube passes [4]

### 1.1.4 Plate heat exchangers

This type of heat exchanger is comprised by a series of thin plates, which are either smooth or corrugated and there's a small space between each plate. These plates have very broad surface areas and encompass narrow fluid passages; these passages alternate between “hot” and “cold” fluids, so that each “cold” fluid is surrounded by two “hot” fluids and vice-versa.

Today's technology, concerning the usage of gaskets and the process of brazing, has advanced far enough so as to make the application of this type of heat exchanger more feasible. Larger heat exchangers of this type are known as the *plate-and-frame* heat exchanger and can be commonly found in HVAC (Heating Ventilation and Air Conditioning) applications. They can be applied either in an open-loop or closed-loop (e.g. refrigeration) setting. The advantage with an open-loop is that this kind of heat exchanger can be easily disassembled, cleaned, and maintained.

It should be noted however, that plate heat exchangers are usually smaller in volume and less expensive than shell-and-tube heat exchangers. The former are also more suited to fluids with lower pressures than that of the latter. Plate heat exchangers also tend to utilize more counter-current flow rather than cross-current flow, this results in higher temperature changes, an increase in efficiency and lower approach temperature differences. Figures 17 and 18 show a detailed glimpse into the parts comprising a gasketed plate-and-frame heat exchanger. Figure 19 shows the various types of plates that can be found in the plate pack of the gasketed plate-and-frame heat exchanger.

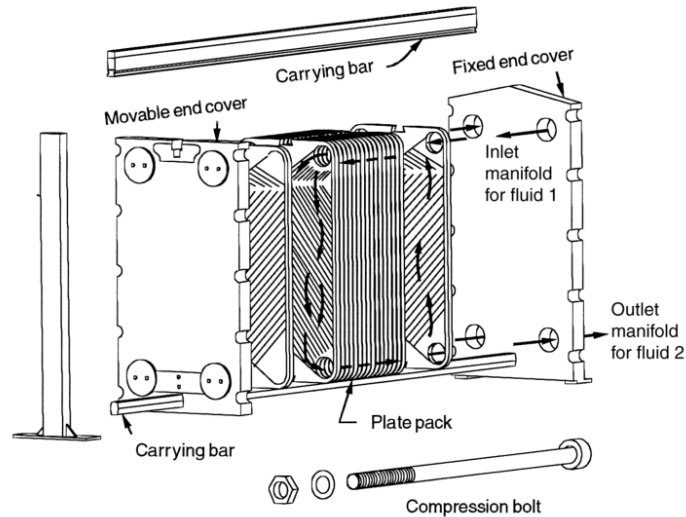


Figure 17: Gasketed plate-and-frame heat exchanger [8]

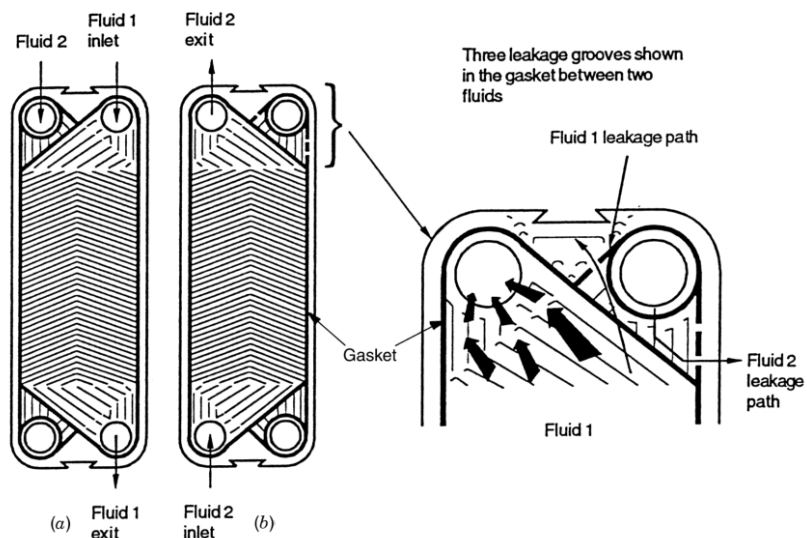
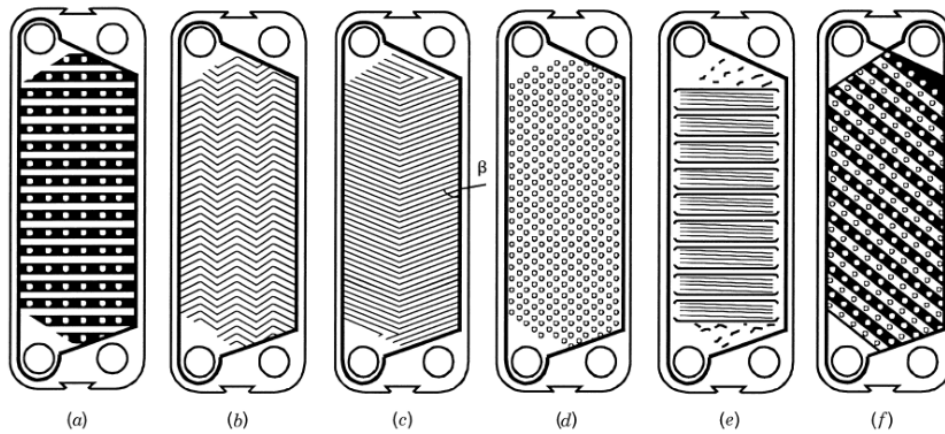


Figure 18: Plates showing gaskets around the ports [8]



**Figure 19: Plate patterns: (a) washboard; (b) zigzag; (c) chevron or herringbone; (d) protrusions and depressions; (e) washboard with secondary corrugations; (f) oblique washboard [8]**

## 2 Entropy and its significance

The definition of entropy is directly related to the Second Law of Thermodynamics, i.e. that any spontaneous process increases the disorder of the universe. One can say that the change of entropy is embodied in all natural affairs as the driving motive. Natural events are irreversible, ergo every single of them alters the universe from its previous state. One can characterize an irreversible process as that being a passage from a less probable to a more probable state of the system, or from a less stable to a more stable state of the system, all the while being of a spontaneous nature, i.e. it starts and proceeds without any external stimuli.

Entropy is a direct measure of each energy configurations probability, it's a measurement of how energy is spread out in the system.

According to Klein [9], the following are some general statements that serve to describe the characteristics of the entropy of a state:

- a) *Entropy is a universal measure of the "disorder" in the mass points of a system.*
- b) *Entropy is a universal measure of the irreversibility of a state and is its criterion as well.*
- c) *Entropy is a universal measure of nature's preference for the state.*
- d) *Entropy is a universal measure of the spontaneity with which a state acts when it is free to change.*
- e) *Entropy of a system can only grow.*
- f) *Entropy asserts the essential one-sidedness of Nature.*
- g) *There exists in Nature a magnitude which always changes in the same sense.*

As mentioned in one of the general definitions of entropy, it can be characterized as a universal measurement of disorder. However, one can ask themselves the question as to what exactly is this disorder? An example can be found in a case where there are two glass cups, one is filled with crushed ice, whereas the other glass is filled with liquid water. At first glance, one can be easily misled into believing that since the glass with the crushed ice appears to be more disordered, that it's the substance with a higher entropy. Nonetheless, it is in fact the substance with a lower level of entropy. This is due to the fact that one requires less information to know about the positions of every molecule in the crushed ice than with the molecules in the liquid water. In the crushed ice, aside from the vibrations of each molecule (as with all solids), the molecules are more or less in the same positions in the lattice structure of the ice, whereas the molecules in the liquid water are free to randomly move past each other, ergo one needs to know the positions of every exact molecule at a specific point in time in the liquid water.

The German theoretical physicist Max Planck discovered that the entropy of a state is entirely dependent on what he termed as the "probability" of the state. The following formula (eq. (12)) was first devised by him.

$$S = k \cdot \log W \quad (12)$$

where  $S$  is entropy [ $\text{J}\cdot\text{K}^{-1}$ ],  $W$  is the probability of a state [-], and  $k$  is the Boltzmann constant, the recommended value of which is approximately  $1.3807 \cdot 10^{-23} \text{ J}\cdot\text{K}^{-1}$ .

One can see how this definition of entropy works in another example, where there

are two containers of the same size and structure. One container has six different objects, while the other container has none. There is only one way one can arrive at this configuration, or only one micro-state. Moving on, the next situation, or macro-state, to arrive at is where there are five different objects in the first container and one object in the second. There are six different configurations, or micro-states in this case, and so more entropy than for the first macro-state. The macro-state with the highest level of entropy, i.e. three objects in the first container and three objects in the second, resulting in a total of twenty micro-states.

This can be seen in the following equation (eq. (13)):

$$W = \binom{n}{m} = \frac{n!}{m! \cdot (n-m)!} \tag{13}$$

where  $W$  is the number of micro-states [-],  $n$  is the number of objects in total (6 in this case) [-], and  $m$  is the number of objects in the second container [-]. The result can be seen in the following diagram (figure 20).

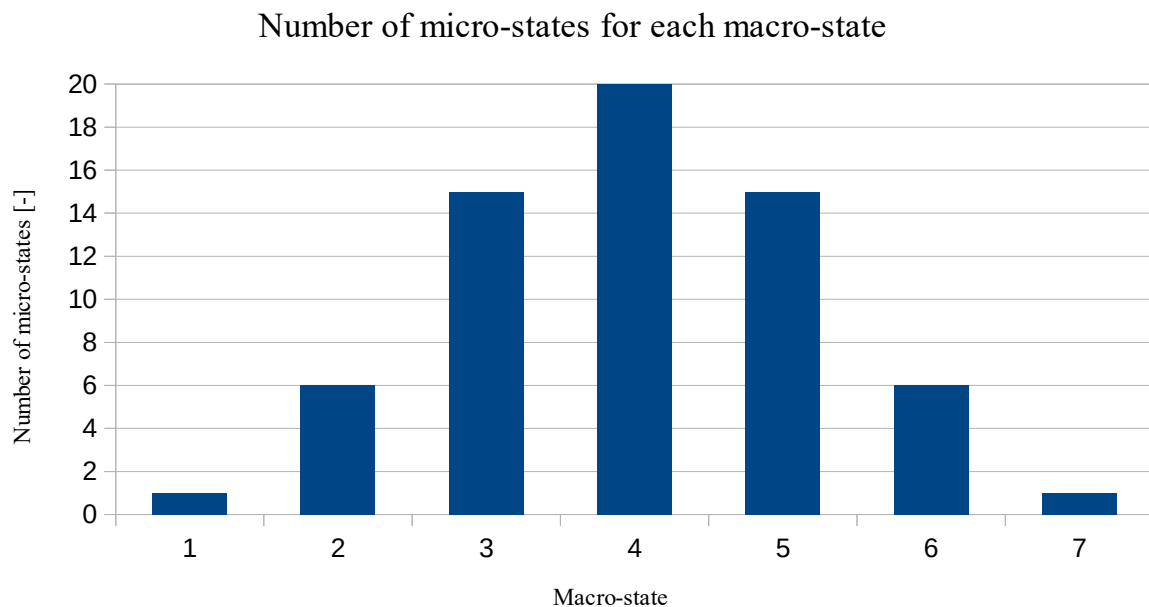


**Figure 20: Number of micro-states for each macro-state**

Naturally, when you have a much larger number of macro-states, the shape of the entropy distribution much less resembles a mountain and starts to resemble more of a plateau. So in the real world, it is statistically more likely for a system to incur higher entropy. This resulted in entropy being labeled as "time's arrow", which means that if energy acquires the opportunity to spread out, it will.

## 2.1 Entropy balance

Harking back to the basic definition of entropy, according to the second law of thermodynamics, entropy can only be created, i.e. it cannot be destroyed. This means that the entropy of a system can either only rise or not change at all, ergo, it can never decrease. This can be easily shown in figure 21:

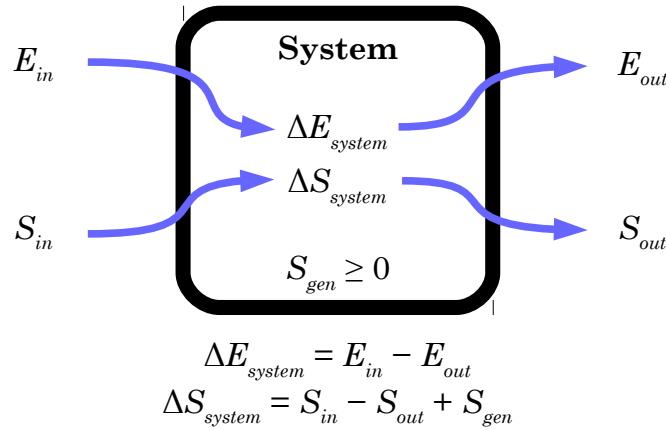


**Figure 21: Energy and entropy balances of a system**

What is shown in figure 21 can also be expressed either as:

$$\left( \begin{array}{c} \text{Total} \\ \text{entropy} \\ \text{entering} \end{array} \right) - \left( \begin{array}{c} \text{Total} \\ \text{entropy} \\ \text{leaving} \end{array} \right) + \left( \begin{array}{c} \text{Total} \\ \text{entropy} \\ \text{generated} \end{array} \right) = \left( \begin{array}{c} \text{Change in the} \\ \text{total entropy} \\ \text{of the system} \end{array} \right)$$

or as equation (14):

$$S_{in} - S_{out} + S_{gen} = \Delta S_{system} \quad (14)$$

which is known as the *entropy balance*. This latter formula, i.e. the *entropy balance* (eq. (14)), can be applied to any system irrespective of any process that it's undergoing. According to corresponding literature [10], there is a fitting description related to the entropy balance, i.e.: *the entropy change of a system during a process is equal to the net entropy transfer through the system boundary and the entropy generated within the system*. In contrast to energy, which can exist in many forms, entropy can only exist in one form. Therefore, it is easy to conclude that the way to determine the entropy change of a system is to evaluate the amount of entropy at the beginning and the conclusion of a process. This can be stated in equation (15):

$$\Delta S_{system} = S_{final} - S_{initial} = S_2 - S_1 \quad (15)$$

It should be stated that the entropy change of a system will be equal to zero, because entropy is a property, the value of which is immutable, unless the state of the system is modified. The latter equation, however, is only applicable to a system, where its properties are uniform. In the opposite case, the way to determine the entropy of the system is by way of integration (eq. (16)):

$$S_{system} = \int s \cdot dm = \int_V s \cdot \rho \cdot dV \quad (16)$$

where  $s$  is the specific entropy of the process [ $\text{kJ} \cdot \text{kg}^{-1}$ ],  $m$  is the mass of the system [ $\text{kg}$ ],  $\rho$  is the density of the system [ $\text{kg} \cdot \text{m}^{-3}$ ], and  $V$  is the volume of the system [ $\text{m}^3$ ].

There are two different ways in how entropy can be transferred to or from a system. One mechanism is by heat transfer and the other is by mass flow. It can be said that it's like energy in this respect, with the difference being that energy can also be transferred by work. Change in entropy occurs as entropy crosses the confines of a system; this change is a measure of the amount of entropy that is obtained or forfeited by the system. It can be concluded that for an adiabatic closed system the entropy transfer is zero, because the only mechanism, with which the entropy transfer of a system is realized, is heat transfer, ergo



the heat transfer to and from an adiabatic closed system is zero.

## 2.2 Entropy generation

It can be said that heat energy is a disorderly form of energy, i.e. it owes its conception to the movement of tiny particles (i.e. the atoms, ions, or molecules) of objects in the universe. At higher temperatures, the molecules in a given object will move faster, thereby bumping into one another and producing heat. When there is a temperature difference between two objects in an isolated system, which are in contact with each other, heat transfer will occur, flowing from the hotter object to the colder object, until a state of equilibrium is reached, which is a consequence of the Zeroeth Law of Thermodynamics. Due to its disordered nature, heat transfer will bring with it an increase in entropy. This means that heat flow to a system will increase the entropy of this specific system, whereas the reverse case would bring about a decrease in entropy. This can be expressed in equation (17) for entropy transfer by heat transfer:

$$S_{heat} = \frac{Q}{T} \quad (17)$$

where  $Q$  is heat transfer [kJ], and  $T$  is the absolute temperature [K]. Here it is evident that the direction of entropy transfer will always be the same as that of the heat transfer, because here the absolute temperature is a constant and since it is expressed in SI units, i.e. Kelvins, it will always be positive.

Nevertheless, there can be a case where the absolute temperature is not constant, then equation (17) can be rewritten as (eq. (18)):

$$S_{heat} = \int_{in}^{out} \frac{dQ}{T} \approx \sum \frac{Q_k}{T_k} \quad (18)$$

where index  $k$  represents the location at the boundary between the two objects, where heat/entropy transfer is taking place.

The other mechanism, by which entropy transfer from one object to another can occur, is by way of mass flow. It is important to note that the energy and entropy composition of a system form a portion relative to the mass, i.e. this percentage of energy and entropy of the system remains unalterable should the size of the mass of the system change. In this same respect, as mass flows to and from a system, the rates of energy and entropy transfer to and from that system are directly proportional to the rate of mass flow. The rate of entropy transfer via mass flow is expressed in equation (19):

$$S_{mass} = m \cdot s \quad (19)$$

here the proportionality of the rate of specific entropy  $s$  [kJ·kg<sup>-1</sup>] compared to the mass of the system  $m$  [kg] can be seen. This means that the amount of entropy of the system  $S_{mass}$  [kJ] is entirely dependent on the amount of mass entering or leaving the system.

However, there could be a case where the properties of the mass can be altered during a process. Again, by way of integration, the previous equation can be rewritten as (eq. (20)):

$$\dot{S}_{mass} = \int_{A_c} s \cdot \rho \cdot V_n \cdot dA_c \quad \text{and} \quad S_{mass} = \int s \cdot dm = \int_{\Delta t} \dot{S}_{mass} \cdot dt \quad (20)$$

where  $A_c$  [m<sup>2</sup>] is the cross-sectional area of the flow and  $V_n$  [m·s<sup>-1</sup>] is the local velocity

normal to  $dA_c$ .

A point of note should also be made about the distinction between energy transfer and entropy transfer. Whereas energy can be transferred by both heat and work, entropy can only be transferred by heat. This means that the entropy transfer rate by way of work amounts to zero.

According to thermodynamic theory [10], *irreversibilities such as friction, mixing, chemical reactions, heat transfer through a finite temperature difference, unrestrained expansion, nonquasi-equilibrium compression, or expansion always cause the entropy of a system to increase, and entropy generation is a measure of the entropy created by such effects during a process*. Nevertheless, since in order for there to be irreversible processes there must be reversible processes. In this latter case, the entropy generation is nonexistent, and so the entropy change of a system undergoing this kind of process amounts to the same value as that of the entropy transfer. One can therefore conclude that the entropy balance relation will correspond with the energy balance relation, i.e. the energy/entropy change of this system will be the same as the energy/entropy transfer during this reversible process.

Ergo it is worthwhile to recap that:

- only in a reversible process does the entropy generation amount to null,
- the entropy transfer by heat is zero for an isolated, adiabatic system,
- the entropy transfer by mass is zero for an isolated, fixed-mass (closed) system.

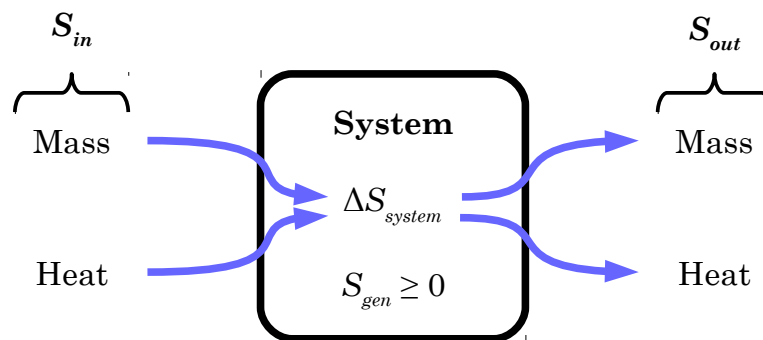


Figure 22: Mechanism of entropy transfer for a general system

When it comes to closed systems (as in figure 22), the entropy change within is solely tied to the entropy that is generated within the confines of the system and to the entropy transfer that comes along with the heat transfer. This can be shown in the following entropy balance equation, with the positive direction of the heat transfer to be that of being *to* the system, as shown in eq. (21):

$$\sum \frac{Q_k}{T_k} + S_{gen} = \Delta S_{system} = S_{out} - S_{in} \quad \left[ \frac{\text{kJ}}{\text{K}} \right] \quad (21)$$

Regarding this latter entropy balance equation, a more precise description can be found in thermodynamic theory [10]: *The entropy change of a closed system during a process is equal to the sum of the net entropy transferred through the system boundary by heat transfer and the entropy generated within the system boundaries*.

We can see that in a case, where there is an adiabatic system, the term  $Q_k/T_k$  will drop out, because  $Q = 0$ , and so the entropy change of this closed system will be equal to the entropy generation within the confines of the system, resulting in the following entropy balance equation (eq. (22)):

$$S_{gen} = \Delta S_{adiab} \quad (22)$$

There is another aspect worthy of consideration, i.e. control volumes, as shown in figure 23. These differ from closed systems in that here there is mass flow across the boundaries of the system, which is another mechanism of entropy exchange. The entropy balance equation (eq. (22)) can be rewritten as equation (23), with the positive direction of heat transfer being to the system:

$$(S_{out} - S_{in})_{CV} = \sum \frac{Q_k}{T_k} + \sum m_{in} \cdot s_{in} - \sum m_{out} \cdot s_{out} + S_{gen} \quad (23)$$

Again, a reference is made to thermodynamic theory [10], for a more sophisticated description of this entropy balance relation: *The rate of entropy change within the control volume during a process is equal to the sum of the rate of entropy transfer through the control volume boundary by heat transfer, the net rate of entropy transfer into the control volume by mass flow, and the rate of entropy generation within the boundaries of the control volume as a result of irreversibilities.*

In the real world, most control volumes operate steadily, which means that there is no change in the entropy of these control volumes. An example of such a control volume is the heat exchanger, which is part of the main topic of this thesis. The entropy balance relation (eq. (23)) can be rewritten for a steady-flow process, by first applying  $dS_{CV}/dt = 0$ , resulting in equation (24):

$$\dot{S}_{gen} = \sum \dot{m}_{out} \cdot s_{out} - \sum \dot{m}_{in} \cdot s_{in} - \sum \frac{\dot{Q}_k}{T_k} \quad (24)$$

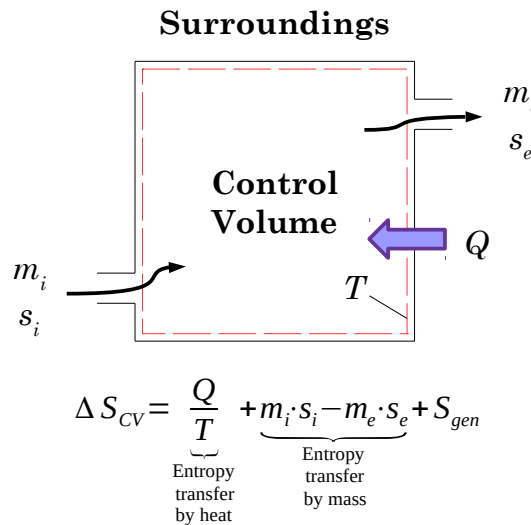


Figure 23: Entropy, heat, and mass transfer for a control volume (CV)

Equation (24) can be further simplified for a single-stream steady-flow apparatus, where there is only one inlet and one exit, resulting in equation (25):

$$\dot{S}_{gen} = \dot{m} \cdot (s_{out} - s_{in}) - \sum \frac{\dot{Q}_k}{T_k} \quad (25)$$

Equation (25) can be further simplified for use in an adiabatic single-stream device (eq. (26)):

$$\dot{S}_{gen} = \dot{m} \cdot (s_{out} - s_{in}) \quad (26)$$

and since  $\dot{S}_{gen} \geq 0$ , this implies that  $s_{out} \geq s_{in}$ , which means that the specific entropy of the

fluid will never decrease as it flows through an adiabatic apparatus. If the flow turns out to be both adiabatic and reversible, then  $s_{out} = s_{in}$ .

## 2.3 Entropy Generation Minimization

According to Bejan [11], “*Entropy-generation minimization (EGM) is the method of modeling and optimization of real devices that owe their thermodynamic imperfection to heat transfer, mass transfer, and fluid flow and other transport processes.*” Bejan also states that, in the realm of engineering, this method can also be called *thermodynamic optimization*. Another term for this can be found under *finite time thermodynamics*. He also makes mention of the usage of this method, that the EGM method involves itself in the areas of fluid mechanics, heat transfer, and thermodynamics.

The goals of optimization may differ significantly depending on the application it's intended for. These can include, among other objectives, the minimization of power input in a refrigeration plant, the maximization of power output in power plants, and in our case the minimization of entropy generation in heat exchangers. These models all tend to include models which utilize rate processes, i.e. fluid flow, mass transfer, and/or heat transfer, fixed volumes of real apparatuses, and fixed speeds or times of actual processes. In order to optimize, one needs to include physical constraints onto the subject of the optimization process; the irreversible operation of said device is dependent on these constraints. The fact is that the heat transfer model, combined with the thermodynamics model, can provide a comprehensive visualization for the end analysis of the irreversible nature of the apparatus. This further can show where and how much entropy is being generated in the device, as well as where and how it flows, and how the thermodynamic performance is affected as a result. [11]

The critical feature that characterizes the EGM method is the minimization of the calculated entropy generation rate. This happens to also differentiate it from exergy analysis. This method first requires the establishment of a way to express  $S_{gen}$ , i.e. entropy generation. To go forward with this process, relations between the heat transfer rates and temperature differences and between mass flow rates and pressure differences need to be set up. There is also a need to define the scope of the thermodynamic nonideality of the system to the physical characteristics thereof; e.g. the dimensions, the configuration, the materials, the shapes, the fixed speeds, and the fixed time intervals of operation. This will invariably involve referencing principles from the realm of fluid mechanics and heat transfer, notwithstanding thermodynamics. In order to actually bring a system, which is subjected to fixed time and fixed size constraints, closer to a situation characterized by minimum entropy generation, one would need to change only one or more of the physical properties of the system.

### 3 Developing the mathematical model

The generation of entropy is significantly intertwined with the two laws of thermodynamics. According to the first law, energy cannot be created or destroyed; it can only be transformed from one form of energy to another form. The second law deals more specifically with entropy in that “*in all energy exchanges, if no energy enters or leaves the system, the potential energy of the state will always be less than that of the initial state.*” This indirectly refers to the fact that losses are inevitable in real cycles, due to irreversibilities and effectiveness. This means that the entropy will increase. Therefore, the mathematical model dealing with the generation of entropy will derive from the second law. [12]

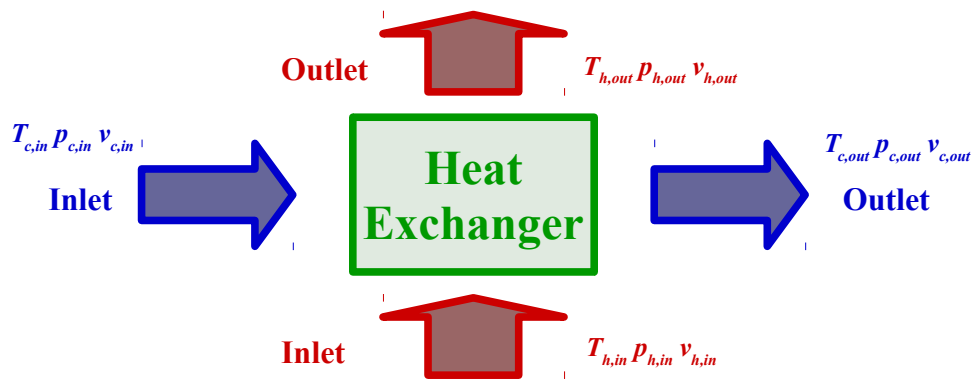


Figure 24: Outlet and inlet points of a heat exchanger

#### 3.1 Effectiveness-NTU Method

The effectiveness-NTU method is used for heat exchangers, where the outlet temperatures of the hot and cold fluids, as well as the heat transfer rate from the hotter to the colder fluid, are unknown. Here the size of the heat exchanger is generally known. An example of a case where this method can be used is for heat exchangers that are currently not being used and are located in storage, and it is desirable to find out if the heat exchanger can be used for a certain application, if its performance will hold up to required specifications. Figure 24 shows in a simple way the inlet and outlet points of a heat exchanger.

The log mean temperature difference method (LMTD) is used in cases where the outlet temperatures of the two mediums are known. However, as mentioned, if the outlet temperatures are unknown, the LMTD is regarded to be unsuitable, as to solve the heat transfer problem, one would have to undertake a certain amount of iterations in order to arrive at the final solution. The effectiveness-NTU method is intended to replace the tediousness of said iterations. It introduces a dimensionless parameter known as the heat transfer effectiveness  $\epsilon$ , which can be expressed as equation (27):

$$\epsilon = \frac{\dot{Q}}{\dot{Q}_{max}} = \frac{\text{Actual heat transfer rate}}{\text{Maximum possible heat transfer rate}} \quad (27)$$

Concerning the parameter  $\dot{Q}$  or actual heat transfer rate, this can be found in an energy balance of either the hotter or colder medium, which is shown in the following (eq. (28)):

$$\dot{Q} = C_c \cdot (T_{c,out} - T_{c,in}) = C_h \cdot (T_{h,in} - T_{h,out}) \quad (28)$$

where  $C_c$  is the heat capacity rate of the colder fluid, and can be found in  $C_c = \dot{m}_c \cdot c_{pc}$ ,

where  $\dot{m}_c$  is the mass transfer rate of the cold fluid, and  $c_{pc}$  is the heat capacity of the cold fluid at a constant pressure. Replacing the index  $c$  with  $h$ , one obtains the same quantities for the hot fluid.

In the  $\varepsilon$ -NTU method, one needs to first identify the maximum temperature difference of a heat exchanger, i.e. the temperature difference between the inlet temperatures of the cold and hot mediums, the formula of which can be found in the following (eq. (29)):

$$\Delta T_{max} = T_{h,in} - T_{c,in} \quad (29)$$

The maximum heat transfer of a heat exchanger can be reached in either of two limiting conditions – either the hot fluid is cooled down to the inlet temperature of the cold fluid, in which case  $C_{min} = C_h$ , or in the case where the cold fluid is warmed up to the inlet temperature of the hot fluid, i.e. here  $C_{min} = C_c$ . An example of this can be seen in figure 25.

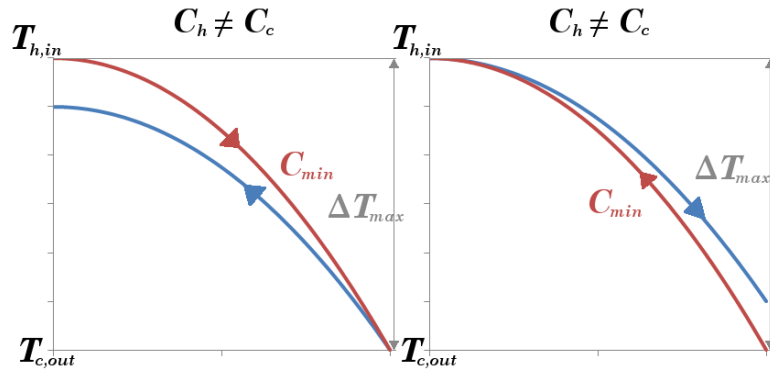


Figure 25: A case where the hot fluid has the minimum heat capacity rate (L) and a case where the cold fluid has the minimum heat capacity rate (R)

Typically these two limits aren't arrived at the same time (i.e.  $C_h = C_c$ ), in which case the logarithmic curves of the two fluids (as in the previous figure) will converge on one another, appearing to combine into one logarithmic curve. Since however the prevailing number of cases with heat exchangers will involve an inequality of  $C_h \neq C_c$ , one of the mediums will have a smaller heat capacity rate, and it will be the one which will experience a bigger temperature change, because the heat transfer rate has to remain the same for both fluids, in lieu of the first law of thermodynamics. This means that this specific fluid will be able to reach the maximum temperature first, thus ceasing the heat transfer between the two fluids in the heat exchanger. This can be seen in the following formula (eq. (30)) for the maximum possible heat transfer rate of a heat exchanger:

$$\dot{Q}_{max} = C_{min} \cdot (T_{h,in} - T_{c,in}) \quad (30)$$

where  $C_{min}$  is either  $C_h$  or  $C_c$ , whichever is less.

In order to calculate  $\dot{Q}$ , we first need to know the effectiveness  $\varepsilon$  of the heat exchanger. This latter parameter depends not only on the flow arrangement of the heat exchanger, but also on the geometry thereof.

The number of transfer units (NTU) is a dimensionless parameter which plays a pivotal role in determining the effectiveness of a heat exchanger. The following relation (eq. (31)) describes the NTU number:

$$NTU = \frac{U \cdot A_s}{C_{min}} \quad (31)$$

where the quantity of  $U$  is the overall heat transfer coefficient, and  $A_s$  is the heat transfer

surface area of the heat exchanger. It can be pointed out that the value of  $A_s$  plays a direct role in the size of the value of NTU, i.e. the larger the value of NTU, the larger the size of the heat exchanger.

It can often be found in literature regarding heat exchangers that there is an additional defined dimensionless quantity known as the capacity ratio  $c$ , which is shown here in equation (32):

$$c = \frac{C_{min}}{C_{max}} \quad (32)$$

Thus the effectiveness of a heat exchanger is directly a function of the NTU number and the capacity ratio  $c$  (eq. (33)):

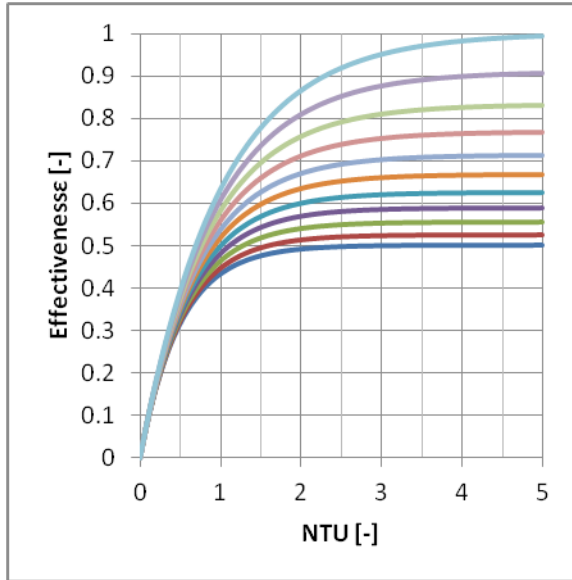
$$\varepsilon = f(NTU, c) \quad (33)$$

Table 1 displays the various heat exchanger types and their respective effectiveness relations:

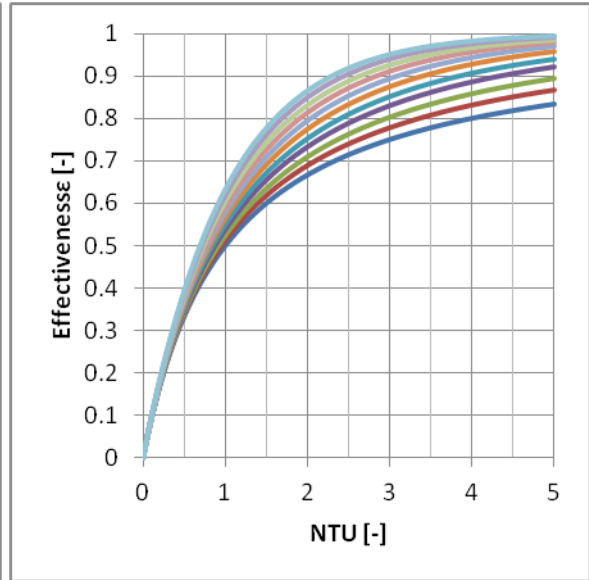
| Heat exchanger type                           | Effectiveness relation   |
|---|--|
| (1) Double pipe:                              |  |
| Parallel-flow                                 | $\varepsilon = \frac{1 - \exp[-NTU \cdot (1 + c)]}{1 + c}$   |
| Counter-flow                                  | $\varepsilon = \frac{1 - \exp[-NTU \cdot (1 - c)]}{1 - c \cdot \exp[-NTU \cdot (1 - c)]}$ (for $c < 1$ )<br>$\varepsilon = \frac{NTU}{1 + NTU}$ (for $c = 1$ )   |
| (2) Shell-and-tube                            |  |
| One-shell pass 2, 4, ... tube passes          | $\varepsilon_1 = 2 \cdot \left( 1 + c + \sqrt{1 + c^2} \cdot \frac{1 + \exp[-NTU_1 \cdot \sqrt{1 + c^2}]}{1 - \exp[-NTU_1 \cdot \sqrt{1 + c^2}]} \right)^{-1}$   |
| $n$ -shell passes $2n, 4n, \dots$ tube passes | $\varepsilon_n = \left[ \left( \frac{1 - \varepsilon_1 \cdot c}{1 - \varepsilon_1} \right)^n - 1 \right] \cdot \left[ \left( \frac{1 - \varepsilon_1 \cdot c}{1 - \varepsilon_1} \right)^2 - c \right]^{-1}$ |
| (3) Cross-flow (single-pass)                  |  |
| Both fluids unmixed                           | $\varepsilon = 1 - \exp\left( \frac{NTU^{0.22}}{c} \cdot [\exp(-c \cdot NTU^{0.78}) - 1] \right)$  |
| $C_{max}$ mixed,<br>$C_{min}$ unmixed         | $\varepsilon = \frac{1}{c} \cdot (1 - \exp(-c [1 - \exp(-NTU)]))$  |
| $C_{min}$ mixed,<br>$C_{max}$ unmixed         | $\varepsilon = 1 - \exp\left( -\frac{1}{c} \cdot [1 - \exp(-c \cdot NTU)] \right)$   |

| Heat exchanger type                  | Effectiveness relation         |
|--------------------------------------|--------------------------------|
| (4) All heat exchangers with $c = 0$ | $\varepsilon = 1 - \exp(-NTU)$ |

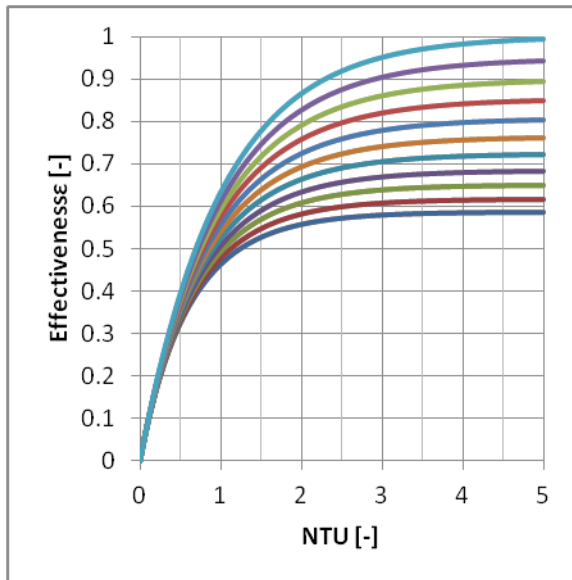
Table 1: Effectiveness relations for heat exchangers [13]



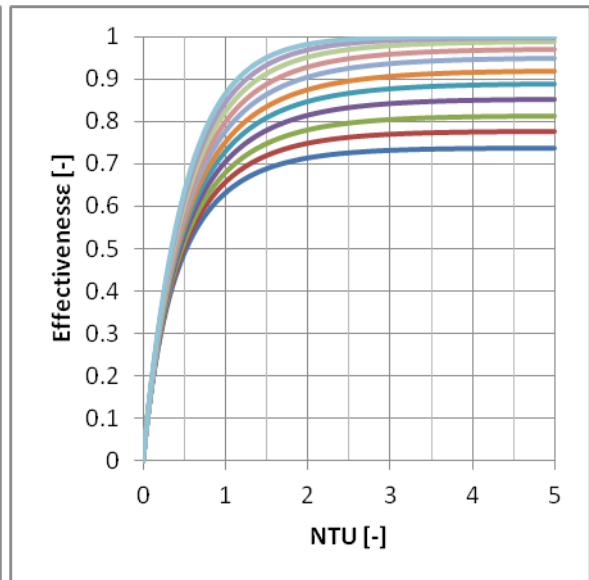
(a) Parallel-flow



(b) Counter-flow



(c) One-shell pass and 2,4,6, ... tube passes



(d) Two-shell passes and 4, 8, 12, ... tube passes



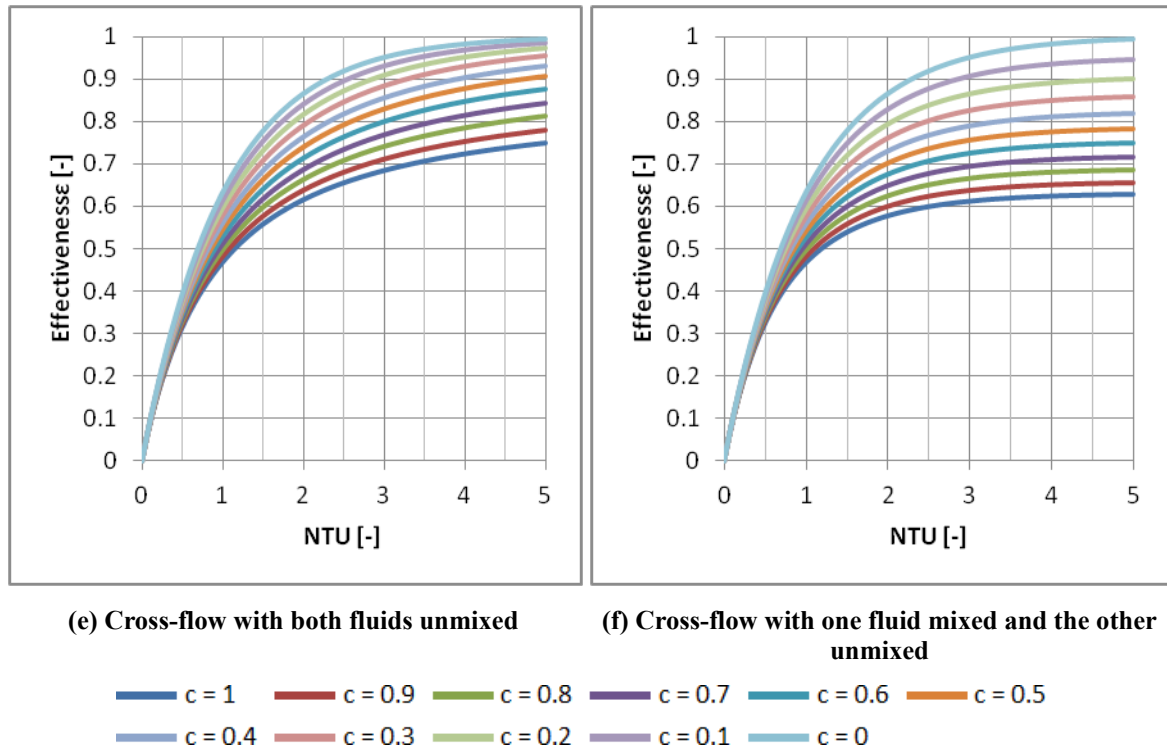


**Figure 26: Effectiveness for heat exchangers**

The following conclusions can be made from observing the behavior of the effectiveness relations for the various heat exchangers:

1. The value of the effectiveness of the heat exchanger ranges from 0 to 1. Its value increases up to an NTU value of 3, after which an increase in NTU results in a slower increase in  $\varepsilon$ , and thus the economical costs may start outweighing the benefits of such a large heat exchanger.
2. The heat exchanger with the highest effectiveness is the counter-flow heat exchanger. The heat exchanger with the lowest effectiveness is the parallel-flow heat exchanger. This applies assuming a given NTU and  $c$  value. This can be seen in figure 27.
3. At an NTU values from 0 to approximately 0.3, the curves of the effectiveness for each heat exchanger are unified, thus signifying the irrelevance of the capacity ratio  $c$  in this range. This can be verified in figure 28.
4. The value of the capacity ratio also ranges from 0 to 1. In the limiting case where  $c = 0$ , this implies that  $C_{max}$  must be reaching values of infinity, which can only happen when there is a phase-change process underway, e.g. the boiling or condensation of the fluid, which means that the effectiveness relation results in case (4), notwithstanding the type of the heat exchanger. This is displayed in figure 29. In the limiting case where  $c = 1$ , the heat capacity rates of both mediums are equal to each other, which mostly happens when the heat exchanger comes into contact with an ambient environment, resulting in large values of  $C_{max}$ .

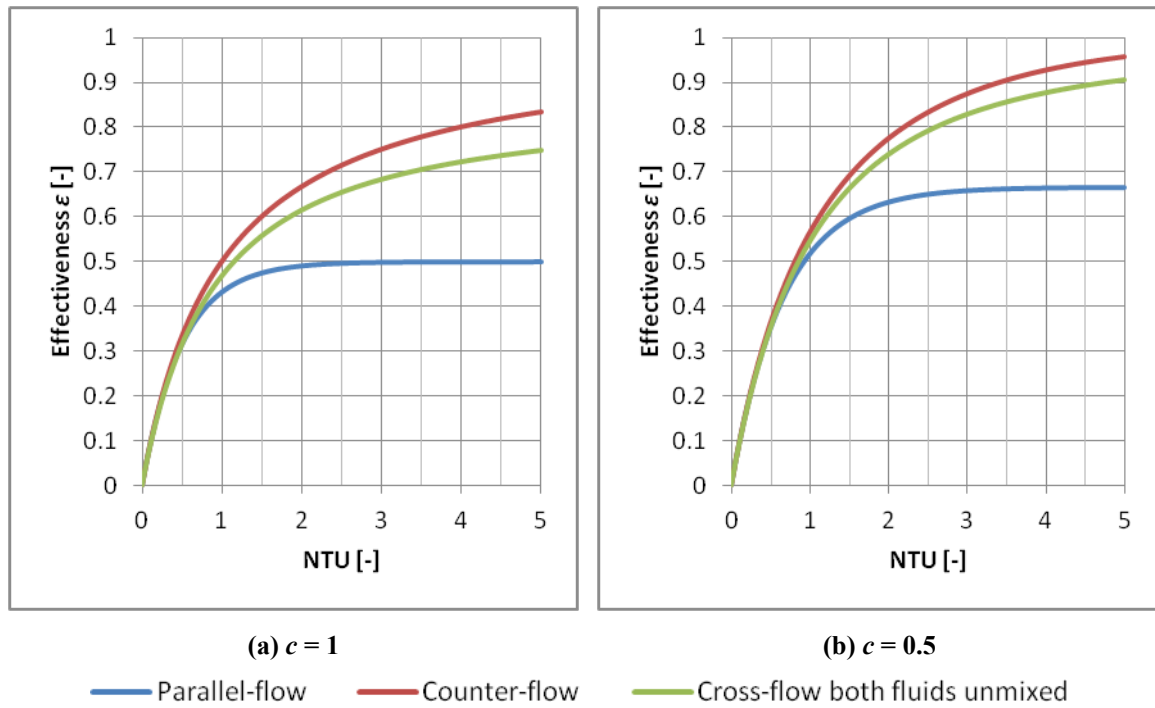


Figure 27: Comparison of the effectiveness of three heat exchangers for two different capacity ratios

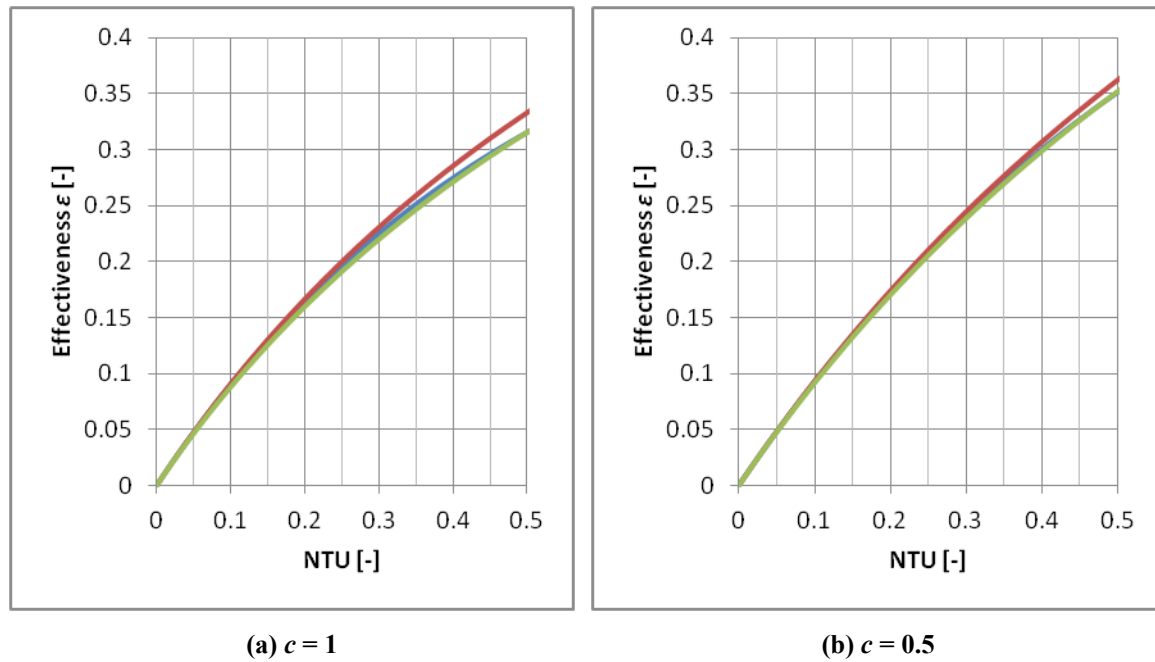


Figure 28: Comparison of the effectiveness of three heat exchangers for two different capacity ratios and small NTU numbers

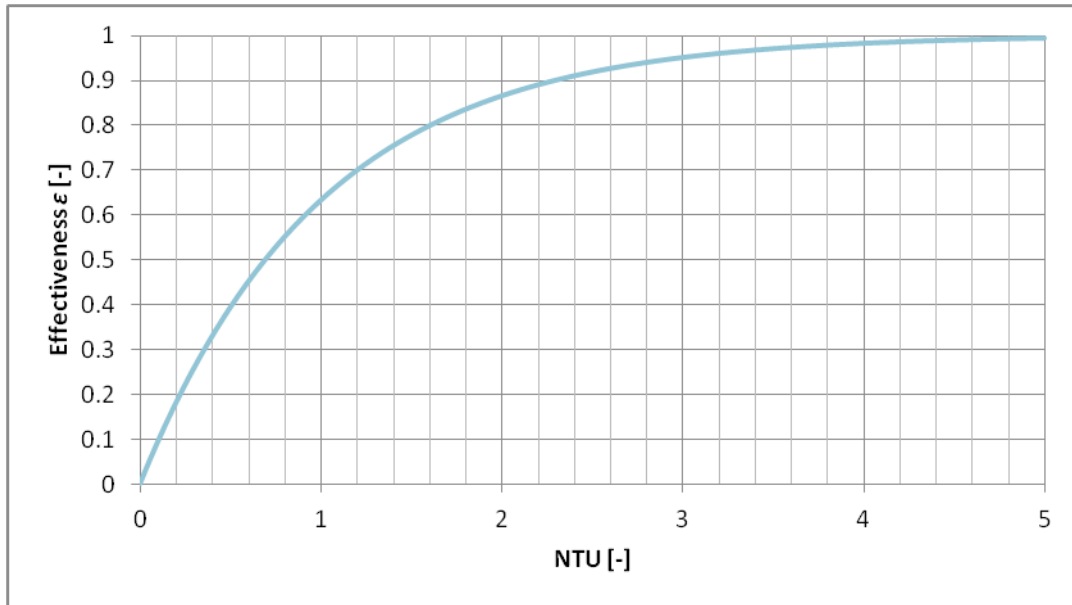


Figure 29: Effectiveness as a relation of NTU for  $c = 0$  for all heat exchangers

The NTU value, or the size of the heat exchanger, can also be determined in reverse when the outlet temperatures are known from the basic definition of  $\epsilon$  and then from table 2.

| Heat exchanger type                           | NTU relation   |
|---|--|
| (1) Double-pipe                               |  |
| Parallel-flow                                 | $NTU = -\frac{\ln[1-\epsilon(1+c)]}{1+c}$  |
| Counter-flow                                  | $NTU = \frac{1}{c-1} \cdot \ln\left(\frac{\epsilon-1}{\epsilon \cdot c-1}\right) \quad (\text{for } c < 1)$ $NTU = \frac{\epsilon}{1-\epsilon} \quad (\text{for } c = 1)$  |
| (2) Shell and tube:                           |  |
| One-shell pass 2, 4, ... tube passes          | $NTU_1 = -\frac{1}{\sqrt{1+c^2}} \cdot \ln\left(\frac{2/\epsilon_1 - 1 - c - \sqrt{1+c^2}}{2/\epsilon_1 - 1 - c + \sqrt{1+c^2}}\right)$  |
| $n$ -shell passes $2n, 4n, \dots$ tube passes | $NTU_n = n \cdot (NTU)_1$ <p>To find the effectiveness of a heat exchanger with one-shell pass use, <math>\epsilon_1 = \frac{F-1}{F-c}</math></p> <p>where <math>F = \left(\frac{\epsilon_n \cdot c - 1}{\epsilon_n - 1}\right)^{1/n}</math></p> |

| Heat exchanger type                   | NTU relation  |
|---------------------------------------|---|
| (3) Cross-flow (single-pass):         |   |
| $C_{max}$ mixed,<br>$C_{min}$ unmixed | $NTU = -\ln\left(1 + \frac{\ln(1 - \varepsilon \cdot c)}{c}\right)$ |
| $C_{min}$ mixed,<br>$C_{max}$ unmixed | $NTU = -\frac{\ln[c \cdot \ln(1 - \varepsilon) + 1]}{c}$            |
| (4) All heat exchangers with $c = 0$  | $NTU = -\ln(1 - \varepsilon)$                                       |

**Table 2: NTU relations for heat exchangers [13]**

When it comes to entropy generation, there are two different types of losses that pertain to a heat exchanger. One type of loss is characterized by a frictional pressure drop in the channels, while the other is the temperature difference in said channels. These losses touch upon the irreversibility aspect, characteristic of real cycles. There are methods that attempt to minimize these losses. One method was brought up by Bejan [11], which involves the use of a parameter known as the entropy generation number  $N_s$ , i.e. equation (34):

$$N_s = \frac{\dot{S}}{C} \quad (34)$$

where  $\dot{S}$  is the quantity representing entropy generation, and  $C$  is a constant, with the same units, therefore the entropy generation number  $N_s$  is a dimensionless number. Should  $N_s$  be a very small number, then that implies that losses of the heat exchanger are also very small, whereas an increase in  $N_s$  implies an increase in the losses.

For the purposes of this investigation, index “1” will be used for the “hot” fluid, and index “2” will be used for the “cold” fluid. The first equation for entropy generation is as follows (eq. (35)):

$$\dot{S}_{gen} = (\dot{m} \cdot c_p)_1 \cdot \ln \frac{T_{1,out}}{T_{1,in}} + (\dot{m} \cdot c_p)_2 \cdot \ln \frac{T_{2,out}}{T_{2,in}} - \dot{m}_1 \cdot R_1 \cdot \ln \frac{P_{1,out}}{P_{1,in}} - \dot{m}_2 \cdot R_2 \cdot \ln \frac{P_{2,out}}{P_{2,in}} \quad (35)$$

The two terms with the temperatures represent the heat transfer irreversibility, whereas the two terms with the pressures are to show the fluid friction. Equation (36) shows the relation between the outlet and inlet pressures.

$$P_{1,out} = P_{1,in} - \Delta P_1, \quad P_{2,out} = P_{2,in} - \Delta P_2 \quad (36)$$

Effectiveness for the following set of equations can be taken from eqs. (28) and (30):

$$\varepsilon = \frac{C_h \cdot (T_{1,in} - T_{1,out})}{C_{min} \cdot (T_{1,in} - T_{2,in})} \quad (37)$$

$$\varepsilon = \frac{C_c \cdot (T_{2,out} - T_{2,in})}{C_{min} \cdot (T_{1,in} - T_{2,in})} \quad (38)$$

For an ideal heat exchanger,  $C^* = C_c/C_h = 1$ , thereby getting equation (39):

$$\varepsilon = \frac{(T_{1,in} - T_{1,out})}{(T_{1,in} - T_{2,in})} = \frac{(T_{2,out} - T_{2,in})}{(T_{1,in} - T_{2,in})} \quad (39)$$

Thus resulting in equations (40) and (41):

$$T_{1,out} = T_{1,in} - \varepsilon \cdot (T_{1,in} - T_{2,in}) \quad (40)$$

$$T_{2,out} = T_{2,in} + \varepsilon \cdot (T_{1,in} - T_{2,in}) \quad (41)$$

The following set of equations is to demonstrate the first simplification of the entropy generation equation. To begin with, the first term on the right-hand side of eq. (35) is taken and worked with:

$$\begin{aligned} (\dot{m} \cdot c_p)_1 \cdot \ln \frac{T_{1,out}}{T_{1,in}} &= (\dot{m} \cdot c_p)_1 \cdot \ln \left( \frac{T_{1,in} - \varepsilon \cdot (T_{1,in} - T_{2,in})}{T_{1,in}} \right) = \dots \\ &= (\dot{m} \cdot c_p)_1 \cdot \ln \left( \frac{T_{1,in} + \varepsilon \cdot (T_{2,in} - T_{1,in})}{T_{1,in}} \right) = \dots \\ &= (\dot{m} \cdot c_p)_1 \cdot \ln \left( \frac{\varepsilon \cdot T_{2,in} + T_{1,in} - \varepsilon \cdot T_{1,in}}{T_{1,in}} \right) = \dots \\ &= (\dot{m} \cdot c_p)_1 \cdot \ln \left( \frac{T_{2,in} - T_{2,in} - \varepsilon \cdot T_{2,in} - T_{1,in} + \varepsilon \cdot T_{1,in}}{T_{1,in}} \right) = \dots \\ &= (\dot{m} \cdot c_p)_1 \cdot \ln \left( \frac{T_{2,in}}{T_{1,in}} - \frac{(1-\varepsilon) \cdot (T_{2,in} - T_{1,in})}{T_{1,in}} \right) = \dots \\ &= (\dot{m} \cdot c_p)_1 \cdot \ln \left( \frac{T_{2,in}}{T_{1,in}} - \frac{(1-\varepsilon) \cdot (T_{2,in} - T_{1,in})}{T_{1,in}} \cdot \frac{T_{2,in}}{T_{2,in}} \right) = \dots \\ &= (\dot{m} \cdot c_p)_1 \cdot \ln \left( \frac{T_{2,in}}{T_{1,in}} \cdot \left( 1 - \frac{(1-\varepsilon) \cdot (T_{2,in} - T_{1,in})}{T_{2,in}} \right) \right) \end{aligned} \quad (42)$$

Next, the second term of eq. (35) is taken and worked with.

$$\begin{aligned} (\dot{m} \cdot c_p)_2 \cdot \ln \frac{T_{2,out}}{T_{2,in}} &= (\dot{m} \cdot c_p)_2 \cdot \ln \left( \frac{T_{2,in} + \varepsilon \cdot (T_{1,in} - T_{2,in})}{T_{2,in}} \right) = \dots \\ &= (\dot{m} \cdot c_p)_2 \cdot \ln \left( \frac{T_{2,in} - \varepsilon \cdot (T_{2,in} - T_{1,in})}{T_{2,in}} \right) = \dots \\ &= (\dot{m} \cdot c_p)_2 \cdot \ln \left( \frac{-\varepsilon \cdot T_{2,in} + T_{2,in} + \varepsilon \cdot T_{1,in}}{T_{2,in}} \right) = \dots \\ &= (\dot{m} \cdot c_p)_2 \cdot \ln \left( \frac{T_{1,in}}{T_{2,in}} + \frac{T_{2,in} - \varepsilon \cdot T_{2,in} - T_{1,in} + \varepsilon \cdot T_{1,in}}{T_{2,in}} \right) = \dots \\ &= (\dot{m} \cdot c_p)_2 \cdot \ln \left( \frac{T_{1,in}}{T_{2,in}} + \frac{(1-\varepsilon) \cdot (T_{2,in} - T_{1,in})}{T_{2,in}} \right) = \dots \end{aligned}$$

$$\begin{aligned} \dots &= (\dot{m} \cdot c_p)_2 \cdot \ln \left( \frac{T_{1,in}}{T_{2,in}} + \frac{(1-\varepsilon) \cdot (T_{2,in} - T_{1,in})}{T_{2,in}} \cdot \frac{T_{1,in}}{T_{1,in}} \right) = \dots \\ &= (\dot{m} \cdot c_p)_2 \cdot \ln \left( \frac{T_{1,in}}{T_{2,in}} \cdot \left( 1 + \frac{(1-\varepsilon) \cdot (T_{2,in} - T_{1,in})}{T_{1,in}} \right) \right) \end{aligned} \quad (43)$$

These are the first two terms for entropy generation due to heat transfer (eqs. (42) and (43)). Now is the time for the two terms for entropy generation due to fluid friction, starting with the third term of the right side of equation (35):

$$\begin{aligned} -\dot{m}_1 \cdot R_1 \cdot \ln \frac{P_{1,out}}{P_{1,in}} &= -\dot{m}_1 \cdot R_1 \cdot \ln \left( \frac{P_{1,in} - \Delta P_1}{P_{1,in}} \right) = \dots \\ &= -\dot{m}_1 \cdot R_1 \cdot \ln \left( \frac{P_{1,in}}{P_{1,in}} - \frac{\Delta P_1}{P_{1,in}} \right) = \dots \\ &= -\dot{m}_1 \cdot R_1 \cdot \ln \left( 1 - \frac{\Delta P_1}{P_{1,in}} \right) \end{aligned} \quad (44)$$

Finally, the last term of eq. (35):

$$\begin{aligned} -\dot{m}_2 \cdot R_2 \cdot \ln \frac{P_{2,out}}{P_{2,in}} &= -\dot{m}_2 \cdot R_2 \cdot \ln \left( \frac{P_{2,in} - \Delta P_2}{P_{2,in}} \right) = \dots \\ &= -\dot{m}_2 \cdot R_2 \cdot \ln \left( \frac{P_{2,in}}{P_{2,in}} - \frac{\Delta P_2}{P_{2,in}} \right) = \dots \\ &= -\dot{m}_2 \cdot R_2 \cdot \ln \left( 1 - \frac{\Delta P_2}{P_{2,in}} \right) \end{aligned} \quad (45)$$

The resulting terms (eqs. (42) – (45)) are put together to make the first form of the equation for the entropy generation number (eq. (46)):

$$\begin{aligned} N_s = \frac{\dot{S}}{C} &= \ln \frac{T_{2,in}}{T_{1,in}} \cdot \left( 1 - (1-\varepsilon) \cdot \frac{T_{2,in} - T_{1,in}}{T_{2,in}} \right) + \ln \frac{T_{1,in}}{T_{2,in}} \cdot \left( 1 + (1-\varepsilon) \cdot \frac{T_{2,in} - T_{1,in}}{T_{1,in}} \right) + \dots \\ &\dots - \left( \frac{R}{c_p} \right)_1 \cdot \ln \left( 1 - \frac{\Delta P_1}{P_{1,in}} \right) - \left( \frac{R}{c_p} \right)_2 \cdot \ln \left( 1 - \frac{\Delta P_2}{P_{2,in}} \right) \end{aligned} \quad (46)$$

Equation (46) can be further simplified as with the following operations. First, the right-hand side of the entropy generation equation is split into four sections; the first two sections each represent entropy generation due to heat transfer. These two sections are rearranged in the following manner:

$$\ln \frac{T_{2,in}}{T_{1,in}} \cdot \left( 1 - (1-\varepsilon) \cdot \frac{T_{2,in} - T_{1,in}}{T_{2,in}} \right) = \ln \frac{T_{2,in}}{T_{1,in}} + \ln \left( 1 - (1-\varepsilon) \cdot \frac{T_{2,in} - T_{1,in}}{T_{2,in}} \right) \quad (47)$$

and

$$\ln \frac{T_{1,in}}{T_{2,in}} \cdot \left( 1 + (1-\varepsilon) \cdot \frac{T_{2,in} - T_{1,in}}{T_{1,in}} \right) = \ln \frac{T_{1,in}}{T_{2,in}} + \ln \left( 1 + (1-\varepsilon) \cdot \frac{T_{2,in} - T_{1,in}}{T_{1,in}} \right) \quad (48)$$

Here the following equation applies:

$$\ln \frac{T_{2,in}}{T_{1,in}} + \ln \frac{T_{1,in}}{T_{2,in}} = \ln \frac{T_{2,in}}{T_{1,in}} \cdot \frac{T_{1,in}}{T_{2,in}} = 0 \quad (49)$$

Applying eq. (49) on eq. (47), we get eq. (50):

$$\ln \left( 1 - (1-\varepsilon) \cdot \frac{T_{2,in} - T_{1,in}}{T_{2,in}} \right) \quad (50)$$

and similarly, applying eq. (49) on eq. (48), we get eq. (51):

$$\ln \left( 1 + (1-\varepsilon) \cdot \frac{T_{2,in} - T_{1,in}}{T_{1,in}} \right) \quad (51)$$

The relation for heat exchanger effectiveness is significantly smaller than unity:

$$(1-\varepsilon) \ll 1 \quad (52)$$

Resulting in the first two sections being as follows, i.e. applying eq. (52) on eq. (50) to get eq. (53) and similarly applying eq. (52) on eq. (51) to get eq. (54):

$$\ln \left( 1 - (1-\varepsilon) \cdot \frac{T_{2,in} - T_{1,in}}{T_{2,in}} \right) \simeq - (1-\varepsilon) \cdot \frac{T_{2,in} - T_{1,in}}{T_{2,in}} \quad (53)$$

$$\ln \left( 1 + (1-\varepsilon) \cdot \frac{T_{2,in} - T_{1,in}}{T_{1,in}} \right) \simeq (1-\varepsilon) \cdot \frac{T_{2,in} - T_{1,in}}{T_{1,in}} \quad (54)$$

The first two sections (eqs. (53) and (54)) are put together, in order to end up with equation (55):

$$\begin{aligned} & - (1-\varepsilon) \cdot \frac{T_{2,in} - T_{1,in}}{T_{2,in}} + (1-\varepsilon) \cdot \frac{T_{2,in} - T_{1,in}}{T_{1,in}} = \dots \\ & \dots = (1-\varepsilon) \cdot (T_{2,in} - T_{1,in}) \cdot \left( -\frac{1}{T_{2,in}} + \frac{1}{T_{1,in}} \right) = \dots \\ & \dots = (1-\varepsilon) \cdot (T_{2,in} - T_{1,in}) \cdot \left( -\frac{T_{1,in}}{T_{2,in} \cdot T_{1,in}} + \frac{T_{2,in}}{T_{1,in} \cdot T_{2,in}} \right) = \dots \\ & \dots = (1-\varepsilon) \cdot (T_{2,in} - T_{1,in}) \cdot \left( \frac{T_{2,in} - T_{1,in}}{T_{2,in} \cdot T_{1,in}} \right) = \dots \\ & \dots = (1-\varepsilon) \cdot \frac{(T_{2,in} - T_{1,in})^2}{T_{2,in} \cdot T_{1,in}} \quad (55) \end{aligned}$$

Now that one side of the right-hand side of the simplified equation for the entropy generation number (eq. (46)) has been achieved, the part of eq. (46) with the pressure terms

will be further simplified, as per the following procedures:

$$-\frac{R}{c_p} \cdot \ln\left(1 - \frac{\Delta P_1}{P_{1,in}}\right) - \frac{R}{c_p} \cdot \ln\left(1 - \frac{\Delta P_2}{P_{2,in}}\right) = -\frac{R}{c_p} \cdot \left( \ln\left(1 - \frac{\Delta P_1}{P_{1,in}}\right) + \ln\left(1 - \frac{\Delta P_2}{P_{2,in}}\right) \right) \quad (56)$$

where for an ideal heat exchanger,  $\frac{R}{c_p} = \left(\frac{R}{c_p}\right)_1 = \left(\frac{R}{c_p}\right)_2$ .

The pressure term is considerably smaller than unity (eq. (57)):

$$\left(\frac{\Delta P}{P_{in}}\right)_{1,2} \ll 1 \quad (57)$$

Which results in the following operations (eq. (58)):

$$\begin{aligned} \Rightarrow -\frac{R}{c_p} \cdot \left( -\frac{\Delta P_1}{P_{1,in}} - \frac{\Delta P_2}{P_{2,in}} \right) &= \dots \\ \dots &= \frac{R}{c_p} \cdot \left( \frac{\Delta P_1}{P_{1,in}} + \frac{\Delta P_2}{P_{2,in}} \right) \end{aligned} \quad (58)$$

Now that we have the pressure terms of equation (46), the entire simplified equation for the entropy generation number is as follows (eq. (59)):

$$N_s = (1 - \varepsilon) \cdot \frac{(T_{2,in} - T_{1,in})^2}{T_{2,in} \cdot T_{1,in}} + \frac{R}{c_p} \cdot \left( \frac{\Delta P_1}{P_{1,in}} + \frac{\Delta P_2}{P_{2,in}} \right) \quad (59)$$

In order to apply equation (59) for all of the heat exchangers, the effectiveness  $\varepsilon$  is substituted with the equations from table 1, so as to get eqs. (60) – (63), listed in table 3.

| Heat Exchanger Type |         | Entropy Generation Equation  |
|---------------------|---------|--|
| Double pipe:        |         |  |
| Parallel-flow       |         | $N_s = \left( 1 - \frac{1 - \exp[-NTU \cdot (1+c)]}{1+c} \right) \cdot \frac{(T_{2,in} - T_{1,in})^2}{T_{2,in} \cdot T_{1,in}} + \dots$ $\dots + \frac{R}{c_p} \cdot \left( \frac{\Delta P_1}{P_{1,in}} + \frac{\Delta P_2}{P_{2,in}} \right) \quad (60)$                              |
| Counter-flow        | $c < 1$ | $N_s = \left( 1 - \frac{1 - \exp[-NTU \cdot (1-c)]}{1-c \cdot \exp[-NTU \cdot (1-c)]} \right) \cdot \frac{(T_{2,in} - T_{1,in})^2}{T_{2,in} \cdot T_{1,in}} + \dots$ $\dots + \frac{R}{c_p} \cdot \left( \frac{\Delta P_1}{P_{1,in}} + \frac{\Delta P_2}{P_{2,in}} \right) \quad (61)$ |



| Heat Exchanger Type      |         | Entropy Generation Equation   |
|--------------------------|---------|---|
|                          | $c = 1$ | $N_s = \left( 1 - \frac{NTU}{1 + NTU} \right) \cdot \frac{(T_{2,in} - T_{1,in})^2}{T_{2,in} \cdot T_{1,in}} + \dots$ $\dots + \frac{R}{c_p} \cdot \left( \frac{\Delta P_1}{P_{1,in}} + \frac{\Delta P_2}{P_{2,in}} \right) \quad (62)$  |
| Cross-flow (single-pass) |         |   |
| Both fluids unmixed      |         | $N_s = \left( \exp \left( \frac{NTU^{0.22}}{c} \cdot [\exp(-c \cdot NTU^{0.78}) - 1] \right) \right) \dots$ $\dots \cdot \frac{(T_{2,in} - T_{1,in})^2}{T_{2,in} \cdot T_{1,in}} + \frac{R}{c_p} \cdot \left( \frac{\Delta P_1}{P_{1,in}} + \frac{\Delta P_2}{P_{2,in}} \right) \quad (63)$ |

**Table 3: Modified entropy generation equations**

It should be noted that one of the intended goals of the minimization of the entropy generation number is to curtail losses in heat transfer. This means that it would be best to rewrite the entropy generation equations using eqs. (64) – (68) for any heat exchanger design.

$$\Delta T^* = \frac{|T_{2,in} - T_{1,in}|}{\sqrt{T_{1,in} \cdot T_{2,in}}} \quad (64)$$

$$\left( \frac{\Delta P_1}{P_{1,in}} + \frac{\Delta P_2}{P_{2,in}} \right) = \left( \frac{\Delta P}{P_{in}} \right)_{1,2} = f \cdot \frac{4 \cdot L}{D} \cdot \frac{G^2}{2 \cdot \rho \cdot P} \quad (65)$$

$$NTU = \frac{4 \cdot L}{D} \cdot St \quad (66)$$

$$G^* = \frac{G}{\sqrt{2 \cdot \rho \cdot P}} \quad (67)$$

$$St = \frac{Nu}{Re \cdot Pr} \quad (68)$$

The equations for entropy generation ((69) – (72)) can now be rewritten as listed in table 4.

| Heat Exchanger Type      |         | Entropy Generation Equation   |
|--------------------------|---------|---|
| Double pipe:             |         |   |
| Parallel-flow            |         | $N_s = \left( 1 - \frac{1 - \exp\left[-\frac{4 \cdot L}{D} \cdot \text{St} \cdot (1+c)\right]}{1+c} \right) \cdot (\Delta T^*)^2 + \dots \quad (69)$ $\dots + \frac{R}{c_p} \cdot f \cdot \left(\frac{4 \cdot L}{D}\right) \cdot (G^*)^2$   |
| Counter-flow             | $c < 1$ | $N_s = \left( 1 - \frac{1 - \exp\left[-\frac{4 \cdot L}{D} \cdot \text{St} \cdot (1-c)\right]}{1-c \cdot \exp\left[-\frac{4 \cdot L}{D} \cdot \text{St} \cdot (1-c)\right]} \right) \cdot (\Delta T^*)^2 + \dots \quad (70)$ $\dots + \frac{R}{c_p} \cdot f \cdot \left(\frac{4 \cdot L}{D}\right) \cdot (G^*)^2$                                       |
|                          | $c = 1$ | $N_s = \left( 1 - \frac{\frac{4 \cdot L}{D} \cdot \text{St}}{1 + \frac{4 \cdot L}{D} \cdot \text{St}} \right) \cdot (\Delta T^*)^2 + \frac{R}{c_p} \cdot f \cdot \left(\frac{4 \cdot L}{D}\right) \cdot (G^*)^2 \quad (71)$   |
| Cross-flow (single-pass) |         |   |
| Both fluids unmixed      |         | $N_s = \left( \exp\left[ \frac{\left(\frac{4 \cdot L}{D} \cdot \text{St}\right)^{0.22}}{c} \cdot \left[ \exp\left(-c \cdot \left(\frac{4 \cdot L}{D} \cdot \text{St}\right)^{0.78}\right) - 1 \right] \right] \right) \cdot \dots \quad (72)$ $\dots \cdot (\Delta T^*)^2 + \frac{R}{c_p} \cdot f \cdot \left(\frac{4 \cdot L}{D}\right) \cdot (G^*)^2$ |

**Table 4: Modified entropy generation equations**

### 3.2 Sensitivity analysis of the mathematical model

In order to figure out which parameter of the mathematical model is going to have the greatest influence and effect on the entropy generation number, a sensitivity analysis needs to be done. This is done by first differentiating the equation for the entropy generation number into first order, second order, and third order derivatives. It is also important to have a NOP (Normal Operating Point), which serves as a reference point, i.e. the initial values of the parameters of the model. Thereupon a relative sensitivity analysis is performed, to see which parameter has the greatest influence on the generation of entropy.

An example of how to derive the equation is shown in the following set of equations, by first taking a modified version of eq. (35):

$$C_{min} \cdot \left( \ln \left( \frac{T_{1,out}}{T_{1,in}} \right) + \left( \frac{R}{c_p} \right)_1 \cdot \ln \left( \frac{P_{1,in}}{P_{1,out}} \right) \right) + C_{max} \cdot \left( \ln \left( \frac{P_{2,in}}{P_{2,out}} \right) \cdot \left( \frac{R}{c_p} \right)_2 + \ln \left( \frac{T_{2,out}}{T_{2,in}} \right) \right) \quad (73)$$

For this example, equation (73) is differentiated by the parameter of  $T_{1,out}$ :

$$\begin{aligned} \frac{\partial \dot{S}}{\partial T_{1,out}} &= C_{min} \cdot \left( \frac{\partial}{\partial T_{1,out}} \left( \ln \left( \frac{T_{1,out}}{T_{1,in}} \right) \right) + \frac{\partial}{\partial T_{1,out}} \left( \left( \frac{R}{c_p} \right)_1 \cdot \ln \left( \frac{P_{1,in}}{P_{1,out}} \right) \right) \right) + \dots \\ &\dots + \frac{\partial}{\partial T_{1,out}} \left( C_{max} \cdot \left( \ln \left( \frac{P_{2,in}}{P_{2,out}} \right) \cdot \left( \frac{R}{c_p} \right)_2 + \ln \left( \frac{T_{2,out}}{T_{2,in}} \right) \right) \right) = \dots \\ &\dots = \left( \frac{T_{1,in}}{T_{1,out}} \cdot \frac{\partial}{\partial T_{1,out}} \left( \frac{T_{1,out}}{T_{1,in}} \right) + 0 \right) \cdot C_{min} + 0 = \frac{1}{T_{1,in}} \cdot \frac{\partial}{\partial T_{1,out}} (T_{1,out}) \cdot T_{1,in} \cdot C_{min} = \\ &\dots = \frac{\partial \dot{S}}{\partial T_{1,out}} = \frac{C_{min}}{T_{1,out}} \\ &\boxed{\frac{\partial \dot{S}}{\partial T_{1,out}} = \frac{(\dot{m} \cdot c_p)_1}{T_{1,out}}} \quad (74) \end{aligned}$$

The derivatives (eqs. (75) – (110)) have been arranged into table 5 for clarity:

| Order | Derivative   |
|-------|--|
| 1     | $\frac{\partial \dot{S}}{\partial T_{1,out}} = \frac{(\dot{m} \cdot c_p)_1}{T_{1,out}} \quad (75)$ |
| 1     | $\frac{\partial \dot{S}}{\partial T_{1,in}} = -\frac{(\dot{m} \cdot c_p)_1}{T_{1,in}} \quad (76)$  |
| 1     | $\frac{\partial \dot{S}}{\partial T_{2,out}} = \frac{(\dot{m} \cdot c_p)_2}{T_{2,out}} \quad (77)$ |

| Order | Derivative  |
|-------|---|
| 1     | $\frac{\partial \dot{S}}{\partial T_{2,in}} = -\frac{(\dot{m} \cdot c_p)_2}{T_{2,in}} \quad (78)$   |
| 1     | $\frac{\partial \dot{S}}{\partial P_{1,out}} = -\frac{\dot{m}_1 \cdot R_1}{P_{1,out}} \quad (79)$   |
| 1     | $\frac{\partial \dot{S}}{\partial P_{1,in}} = \frac{\dot{m}_1 \cdot R_1}{P_{1,in}} \quad (80)$  |
| 1     | $\frac{\partial \dot{S}}{\partial P_{2,out}} = -\frac{\dot{m}_2 \cdot R_2}{P_{2,out}} \quad (81)$   |
| 1     | $\frac{\partial \dot{S}}{\partial P_{2,in}} = \frac{\dot{m}_2 \cdot R_2}{P_{2,in}} \quad (82)$  |
| 1     | $\frac{\partial \dot{S}}{\partial C_{min}} = \left(\frac{R}{c_p}\right)_1 \cdot \ln\left(\frac{P_{1,in}}{P_{1,out}}\right) + \ln\left(\frac{T_{1,out}}{T_{1,in}}\right) \quad (83)$ |
| 1     | $\frac{\partial \dot{S}}{\partial C_{max}} = \left(\frac{R}{c_p}\right)_2 \cdot \ln\left(\frac{P_{2,in}}{P_{2,out}}\right) + \ln\left(\frac{T_{2,out}}{T_{2,in}}\right) \quad (84)$ |
| 1     | $\frac{\partial \dot{S}}{\partial \left(\frac{R}{c_p}\right)_1} = (\dot{m} \cdot c_p)_1 \cdot \ln\left(\frac{P_{1,in}}{P_{1,out}}\right) \quad (85)$                                |
| 1     | $\frac{\partial \dot{S}}{\partial \left(\frac{R}{c_p}\right)_2} = (\dot{m} \cdot c_p)_2 \cdot \ln\left(\frac{P_{2,in}}{P_{2,out}}\right) \quad (86)$                                |
| 2     | $\frac{\partial^2 \dot{S}}{\partial T_{1,out}^2} = -\frac{(\dot{m} \cdot c_p)_1}{T_{1,out}^2} \quad (87)$   |
| 2     | $\frac{\partial^2 \dot{S}}{\partial T_{1,out} \partial C_{min}} = \frac{1}{T_{1,out}} \quad (88)$   |
| 2     | $\frac{\partial^2 \dot{S}}{\partial T_{1,in}^2} = \frac{(\dot{m} \cdot c_p)_1}{T_{1,in}^2} \quad (89)$  |
| 2     | $\frac{\partial^2 \dot{S}}{\partial T_{1,in} \partial C_{min}} = -\frac{1}{T_{1,in}} \quad (90)$  |
| 2     | $\frac{\partial^2 \dot{S}}{\partial T_{2,out}^2} = -\frac{(\dot{m} \cdot c_p)_2}{T_{2,out}^2} \quad (91)$   |

| Order | Derivative   |
|-------|--|
| 2     | $\frac{\partial^2 \dot{S}}{\partial T_{2,out} \partial C_{max}} = \frac{1}{T_{2,out}} \quad (92)$  |
| 2     | $\frac{\partial^2 \dot{S}}{\partial T_{2,in}^2} = \frac{(\dot{m} \cdot c_p)_2}{T_{2,in}^2} \quad (93)$   |
| 2     | $\frac{\partial^2 \dot{S}}{\partial T_{2,in} \partial C_{max}} = -\frac{1}{T_{2,in}} \quad (94)$   |
| 2     | $\frac{\partial^2 \dot{S}}{\partial P_{1,out}^2} = \frac{\dot{m}_1 \cdot R_1}{P_{1,out}^2} \quad (95)$   |
| 2     | $\frac{\partial^2 \dot{S}}{\partial P_{1,out} \partial C_{min}} = -\frac{1}{P_{1,out}} \cdot \left( \frac{R}{c_p} \right)_1 \quad (96)$        |
| 2     | $\frac{\partial^2 \dot{S}}{\partial P_{1,out} \partial \left( \frac{R}{c_p} \right)_1} = -\frac{(\dot{m} \cdot c_p)_1}{P_{1,out}} \quad (97)$  |
| 2     | $\frac{\partial^2 \dot{S}}{\partial P_{1,in}^2} = -\frac{\dot{m}_1 \cdot R_1}{P_{1,in}^2} \quad (98)$  |
| 2     | $\frac{\partial^2 \dot{S}}{\partial P_{1,in} \partial C_{min}} = \frac{1}{P_{1,in}} \cdot \left( \frac{R}{c_p} \right)_1 \quad (99)$           |
| 2     | $\frac{\partial^2 \dot{S}}{\partial P_{1,in} \partial \left( \frac{R}{c_p} \right)_1} = \frac{(\dot{m} \cdot c_p)_1}{P_{1,in}} \quad (100)$    |
| 2     | $\frac{\partial^2 \dot{S}}{\partial P_{2,out}^2} = \frac{\dot{m}_2 \cdot R_2}{P_{2,out}^2} \quad (101)$  |
| 2     | $\frac{\partial^2 \dot{S}}{\partial P_{2,out} \partial C_{max}} = -\frac{1}{P_{2,out}} \cdot \left( \frac{R}{c_p} \right)_2 \quad (102)$       |
| 2     | $\frac{\partial^2 \dot{S}}{\partial P_{2,out} \partial \left( \frac{R}{c_p} \right)_2} = -\frac{(\dot{m} \cdot c_p)_2}{P_{2,out}} \quad (103)$ |
| 2     | $\frac{\partial^2 \dot{S}}{\partial P_{2,in}^2} = -\frac{\dot{m}_2 \cdot R_2}{P_{2,in}^2} \quad (104)$   |

| Order | Derivative  |
|-------|---|
| 2     | $\frac{\partial^2 \dot{S}}{\partial P_{2,in} \partial C_{max}} = \frac{1}{P_{2,in}} \cdot \left( \frac{R}{c_p} \right)_2 \quad (105)$       |
| 2     | $\frac{\partial^2 \dot{S}}{\partial P_{2,in} \partial \left( \frac{R}{c_p} \right)_2} = \frac{(\dot{m} \cdot c_p)_2}{P_{2,in}} \quad (106)$ |
| 3     | $\frac{\partial^3 \dot{S}}{\partial P_{1,out} \partial C_{min} \partial \left( \frac{R}{c_p} \right)_1} = -\frac{1}{P_{1,out}} \quad (107)$ |
| 3     | $\frac{\partial^3 \dot{S}}{\partial P_{1,in} \partial C_{min} \partial \left( \frac{R}{c_p} \right)_1} = \frac{1}{P_{1,in}} \quad (108)$    |
| 3     | $\frac{\partial^3 \dot{S}}{\partial P_{2,out} \partial C_{max} \partial \left( \frac{R}{c_p} \right)_2} = -\frac{1}{P_{2,out}} \quad (109)$ |
| 3     | $\frac{\partial^3 \dot{S}}{\partial P_{2,in} \partial C_{max} \partial \left( \frac{R}{c_p} \right)_2} = \frac{1}{P_{2,in}} \quad (110)$    |

**Table 5: Table of derivatives for the sensitivity analysis**

It should be noted for the sake of clarity that partial derivatives are continuous, i.e. it doesn't matter in which order the partial differentiations are formed, e.g.  $\frac{\partial^2 f}{\partial x \cdot \partial y} = \frac{\partial^2 f}{\partial y \cdot \partial x}$ . Ergo, no additional second-order or third-order derivatives are necessary.

The next part that is needed for the sensitivity analysis is to have the initial values for the parameters, i.e. the Normal Operating Point (NOP). These are placed in table 6. For the purposes of analysis, the values were arbitrarily selected based on experimental values found in literature [14], which deals with a similar topic.

| Parameter  | Value  | Unit |
|------------|--------|------|
| $T_{1out}$ | 430.15 | K    |
| $T_{1in}$  | 450.15 | K    |
| $P_{1out}$ | 800    | kPa  |
| $P_{1in}$  | 500    | kPa  |

| Parameter  | Value  | Unit     |
|------------|--------|----------|
| $T_{2out}$ | 440.15 | K        |
| $T_{2in}$  | 415.15 | K        |
| $P_{2out}$ | 300    | kPa      |
| $P_{2in}$  | 200    | kPa      |
| $R_1$      | 461.5  | J/(kg·K) |
| $m_1$      | 0.4    | kg/s     |
| $c_{p1}$   | 2500   | J/(kg·K) |
| $C_{min}$  | 1000   | J/(s·K)  |
| $R_2$      | 461.5  | J/(kg·K) |
| $m_2$      | 0.4    | kg/s     |
| $c_{p2}$   | 4200   | J/(kg·K) |
| $C_{max}$  | 1680   | J/(s·K)  |

**Table 6: Normal Operating Point (NOP)**

To figure out which parameter, when subjected to a change in value, will have the greatest effect on the change in value of the entropy generation number, one simply inserts the values of the NOP into any of the derivatives listed previously, and then multiplying the result by the normal value of the parameter and at the same time dividing it by the normal value of the function (i.e. the value of the entropy generation function with all of the values of the NOP inserted). This is known as a *relative-sensitivity analysis*. The basic structure of how to work with the relative-sensitivity analysis can be seen in the following equation (111), taken from Smith et al. [15]:

$$\overline{S}_\alpha^F = \left. \frac{\partial F}{\partial \alpha} \right|_{\text{NOP}} \cdot \frac{\alpha_0}{F_0} \approx \frac{\% \text{ change in } F}{\% \text{ change in } \alpha} = \frac{\frac{\Delta F}{F}}{\frac{\Delta \alpha}{\alpha}} \quad (111)$$

An example of how this works is in the following set of equations (Eqs. (112) and (113)).

The value of the entropy generation function with all of the values of the NOP inserted:

$$\begin{aligned} \dot{S}_0 = & 1000 \cdot \left( \ln \left( \frac{430.15}{450.15} \right) + \left( \frac{461.5}{2500} \right) \cdot \ln \left( \frac{800}{500} \right) \right) + \dots \\ & \dots + 1680 \cdot \left( \ln \left( \frac{440.15}{415.15} \right) + \left( \frac{461.5}{4200} \right) \cdot \ln \left( \frac{200}{300} \right) \right) = \dots \\ & \dots = 64.7060732 \quad [-] \end{aligned} \quad (112)$$

The value of the first listed derivative using the relative-sensitivity analysis:

$$\begin{aligned} \bar{S}_{T_{1,out}}^{\dot{S}} &= \left. \frac{\partial \dot{S}}{\partial T_{1,out}} \right|_{\text{NOP}} \cdot \frac{T_{1,out0}}{\dot{S}_0} = \frac{(\dot{m} \cdot c_p)_1 \cdot T_{1,out}}{T_{1,out} \cdot \dot{S}_0} = \dots \\ &\dots = \frac{0.4 \cdot 2500}{430.15} \cdot \frac{430.15}{64.7060732} = 15.4544999 \quad [-] \end{aligned} \quad (113)$$

Figure 30 illustrates the relative sensitivity of each derivative in a simplified format.

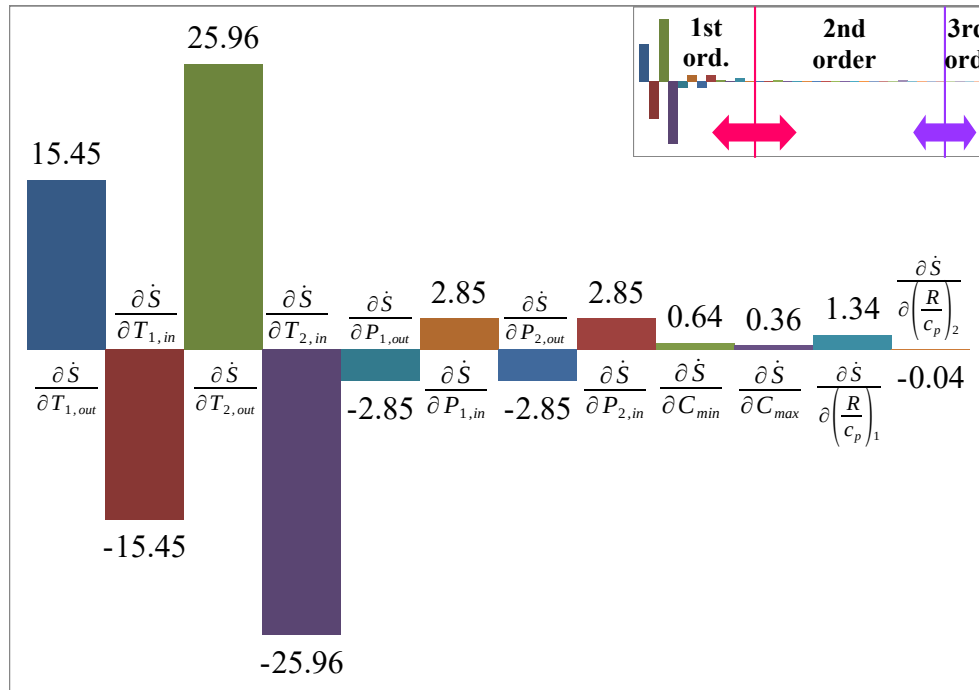


Figure 30: Relative-sensitivity analysis for the entropy generation function

It appears that the second-order and third-order derivatives seem to have the lowest influence on the value of the entropy generation function, therefore their visualization is relegated to the top-right corner. The greatest influence on the change in the entropy generation value is from the inlet and outlet temperatures of the second fluid, i.e.  $T_{2out}$  and  $T_{2in}$ . This appears to be what also occurred in the work of Koorts [14], where the greatest average change in entropy generation came from a 30K temperature change in the steam inlet temperature (103.6%) and in the steam outlet temperature (72.83%). In the case of this thesis, the change in entropy generation stemming from a change in temperature of the second fluid of either the outlet or inlet is the same ( $\pm 25,96$  [-]), the congruence of which can be observed in figure (30). This congruity can also be observed for  $T_{1in}$ ,  $T_{1out}$ ,  $P_{1in}$ ,  $P_{1out}$ ,  $P_{2in}$ , and  $P_{2out}$ .



### 3.3 Graphs and results

The results of the mathematical model in this thesis can be seen in figures 31 – 40 as trends between the optimum flow path length  $((4L/D)_{opt})$  and the dimensionless mass velocity  $(G^*)$  for the three basic types of heat exchangers analyzed here, i.e. the parallel-flow heat exchanger, the counter-flow heat exchanger, and the cross-flow heat exchanger. For each of the heat exchangers, a variant with  $c = 0.595238095238095$  was developed and a variant with  $c = 1$  was developed. The value of  $c = 0.595238095238095$  was chosen because it was used in the analysis by Ogulata et al. [16]. The results were first validated with the cross-flow heat exchanger, because it was the same type of heat exchanger that was used by the Ogulata et al. [16].

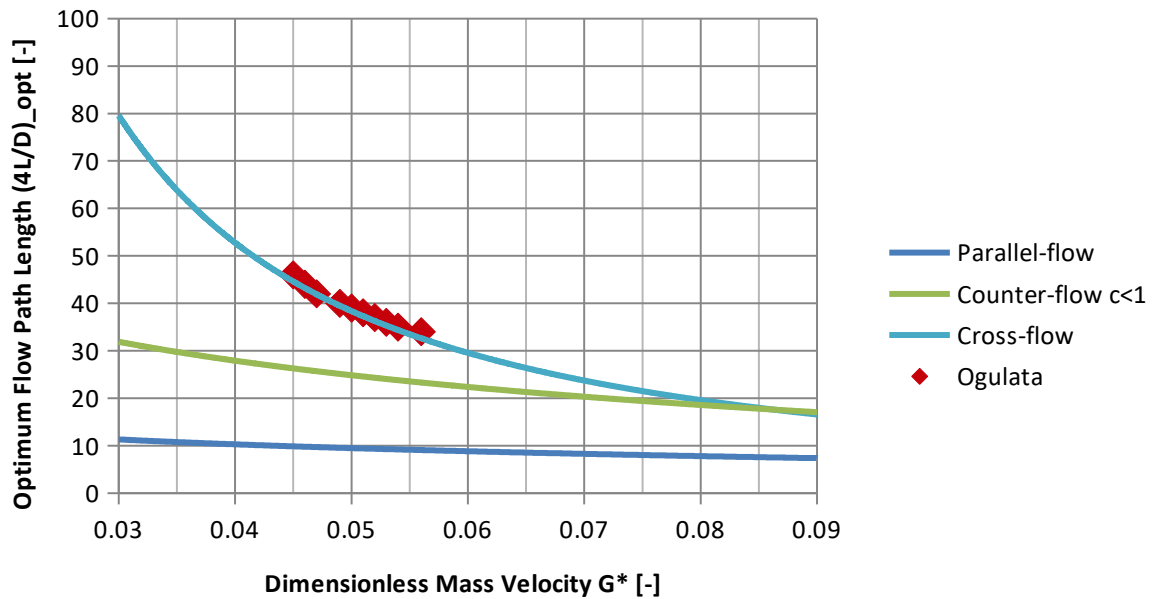


Figure 31: Variation between the optimum flow path length and the dimensionless mass velocity for all of the heat exchangers with  $c = 0.595238095238095$

Figure 31 for  $c < 1$  displays the trendlines of how the optimum flow path length depends on the dimensionless mass velocity for all three of the examined heat exchangers. It is evident that the Cross-flow heat exchanger here closely follows that of the experimental data from Ogulata et al. [16]. The values for the dimensionless mass velocity on the horizontal axis were chosen to correspond with that of the literature with the experimental data. Here the parallel-flow heat exchanger appears to have the lowest values for the optimum flow path, while the cross-flow heat exchanger has the widest range.

In figure 32, one can observe again that the cross-flow heat exchanger follows the experimental data closely. What is interesting is due to the mathematical nature of the equations for entropy generation (eqs. (69) – (72)), the functions could not be plotted for the whole range that is shown on the horizontal axis (which is again the same range as that used in Ogulata et al. [16]). For a given NOP, the parallel-flow heat exchanger has a range of 7 to approximately 32 for the optimum flow path length, which is the shortest range, as shown in the graph. What is more important to see is that it appears here that the counter-flow heat exchanger appears to be the best.

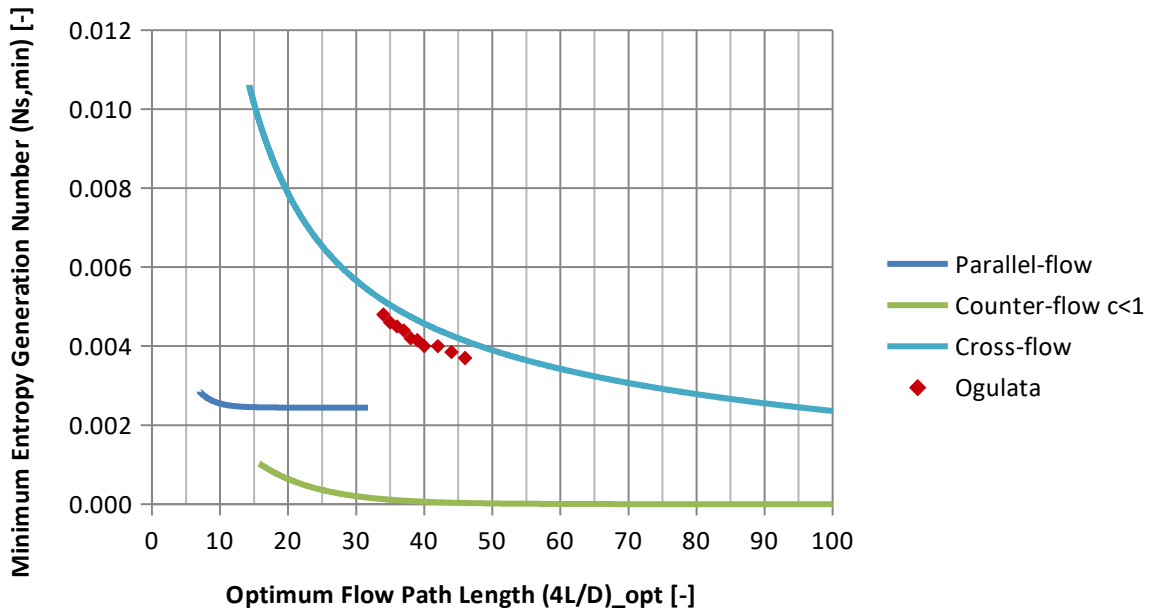


Figure 32: Variation between the minimum entropy generation number and the optimum flow path length for all of the heat exchangers with  $c = 0.595238095238095$

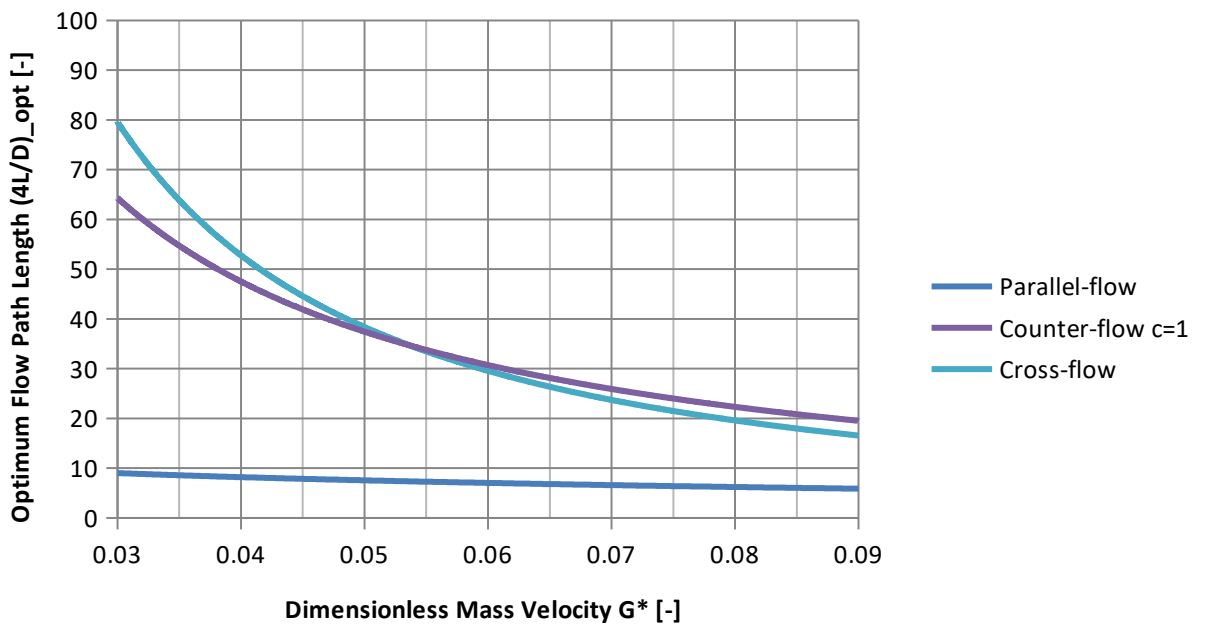


Figure 33: Variation between the optimum flow path length and the dimensionless mass velocity for all of the heat exchangers with  $c = 1$

Figure 33 shows the dependence of the optimum flow path length on the dimensionless mass velocity for heat exchangers with  $c = 1$ . Here the plot is similar to figure 31, except that the counter-flow heat exchanger appears to more closely follow the cross-flow heat exchanger, intersecting once at about point  $[0.053, 36]$ .

The similarities do not end with figure 34, which shows stark resemblance to figure 32, except that here the cross-flow heat exchanger appears to give higher entropy generation values.

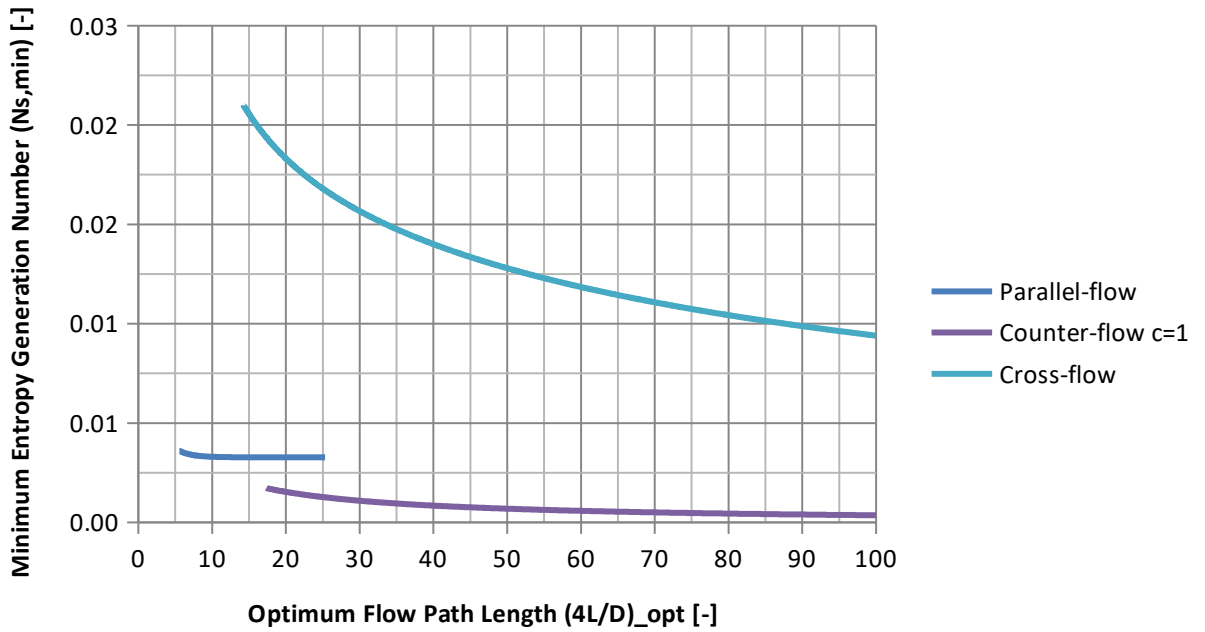


Figure 34: Variation between the minimum entropy generation number and the optimum flow path length for all of the heat exchangers with  $c = 1$

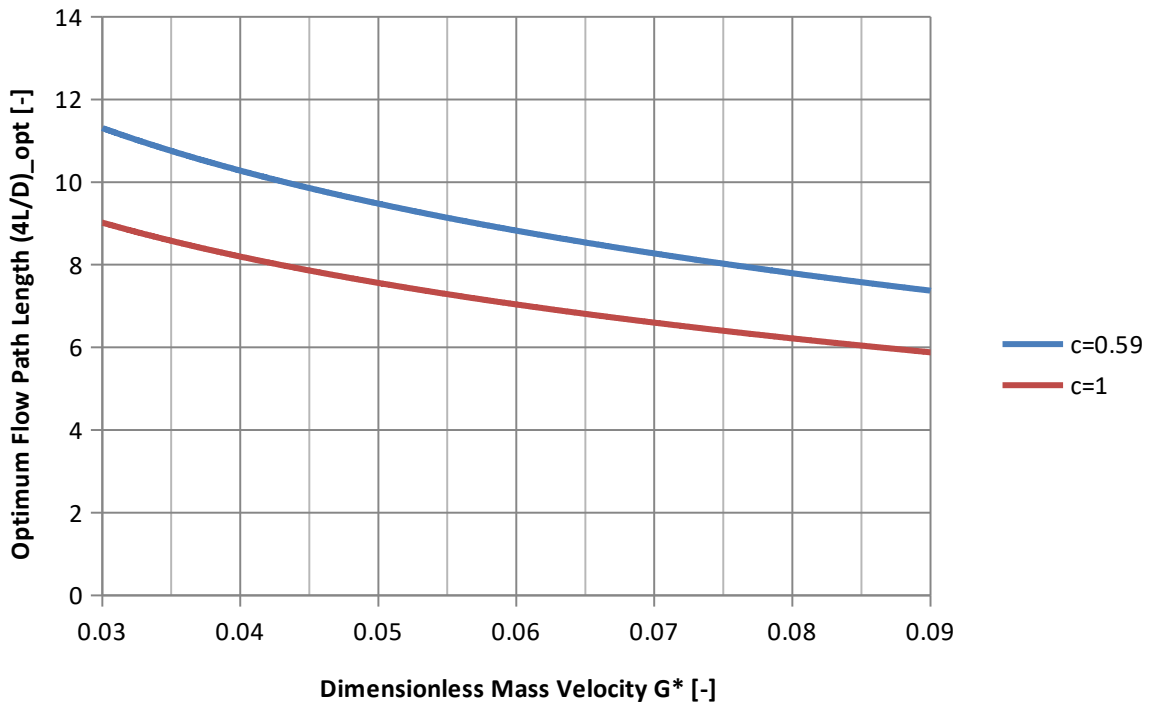


Figure 35: Optimum flow path comparison of parallel-flow heat exchangers

In figures 35 and 36 we can see plots comparing the heat capacity ratios for the parallel-flow heat exchanger. A smaller heat capacity ratio ( $c < 1$ ) gives larger values for the optimum flow path, while at the same time providing smaller values for the entropy generation number.

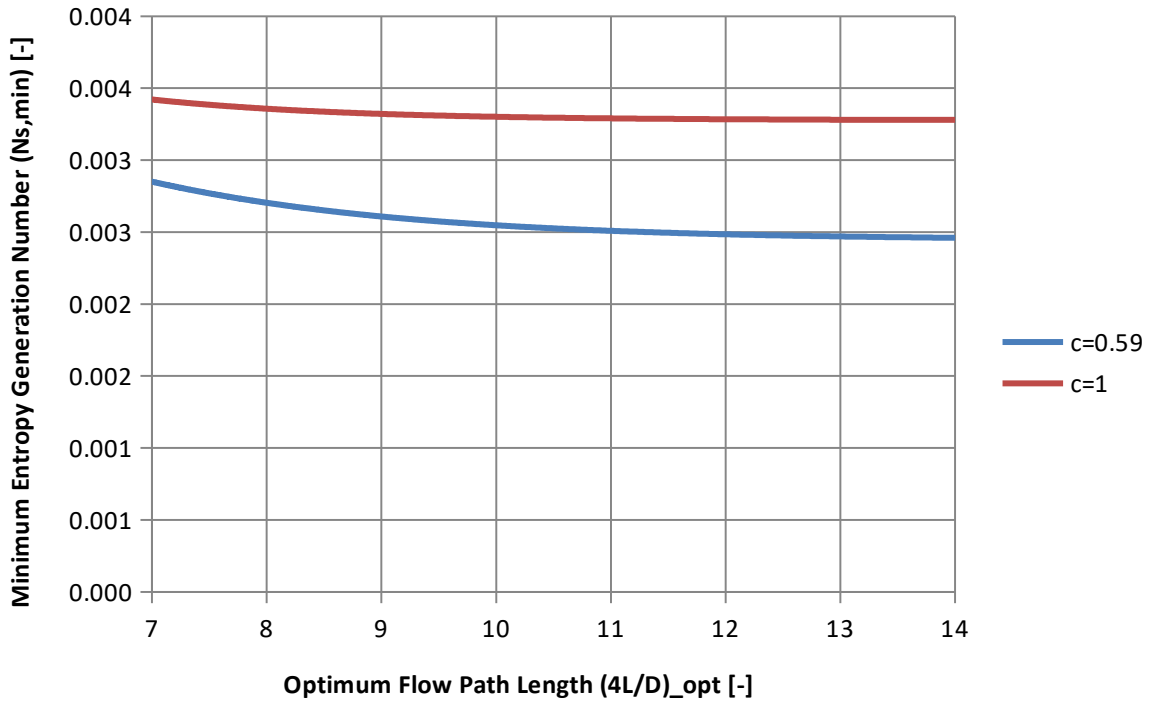


Figure 36: Minimum entropy generation number comparison of parallel-flow heat exchangers

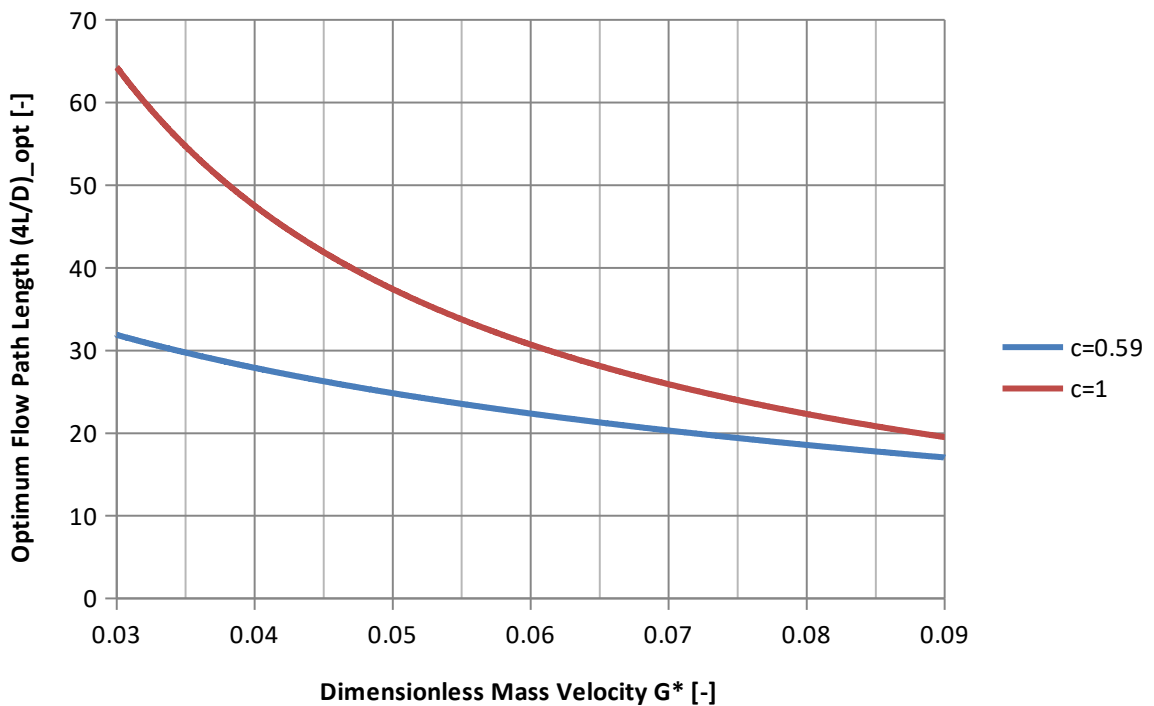


Figure 37: Optimum flow path comparison of counter-flow heat exchangers

In figure 37 we can see a different scenario, where the smaller heat capacity ratio ( $c < 1$ ) gives smaller values for the optimum flow path length. Figure 38 shows a gap between the two functions for the counter-flow heat exchanger. The two equations (eqs. (70) and (71)) are entirely different from one another and this differences appears to

present itself in this plot. It is also apt to mention that the balanced counter-flow heat exchanger ( $c = 0$ ) has higher values for the entropy generation number.

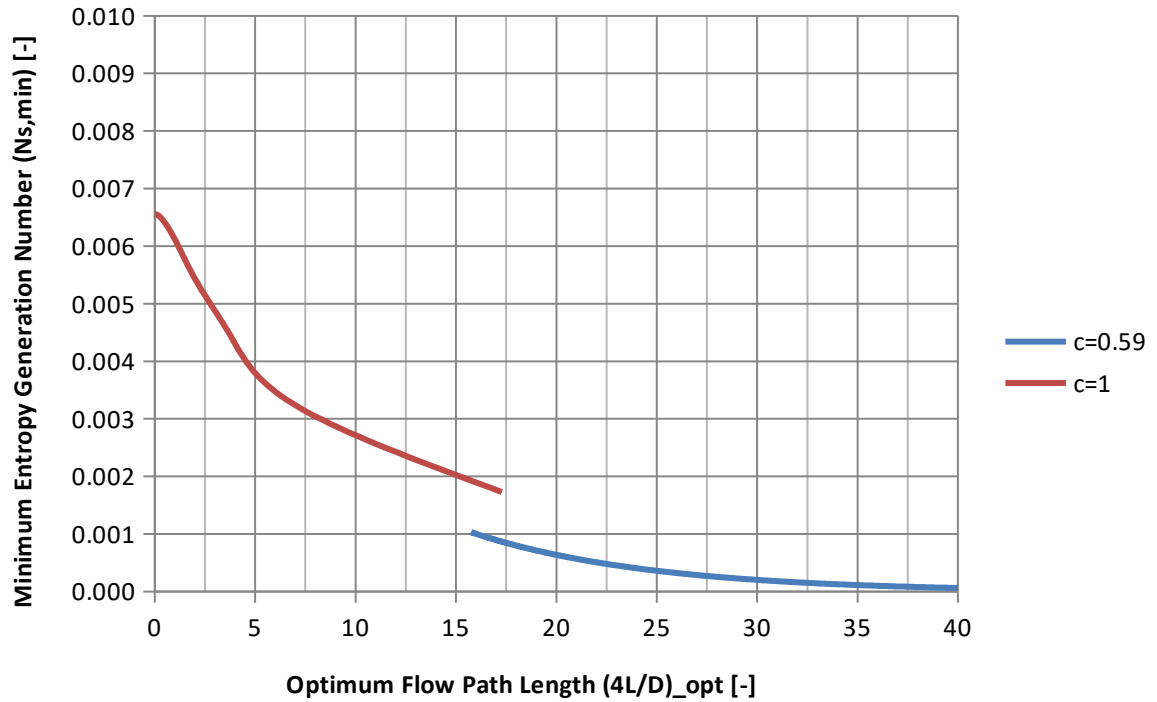


Figure 38: Minimum entropy generation number comparison of counter-flow heat exchangers

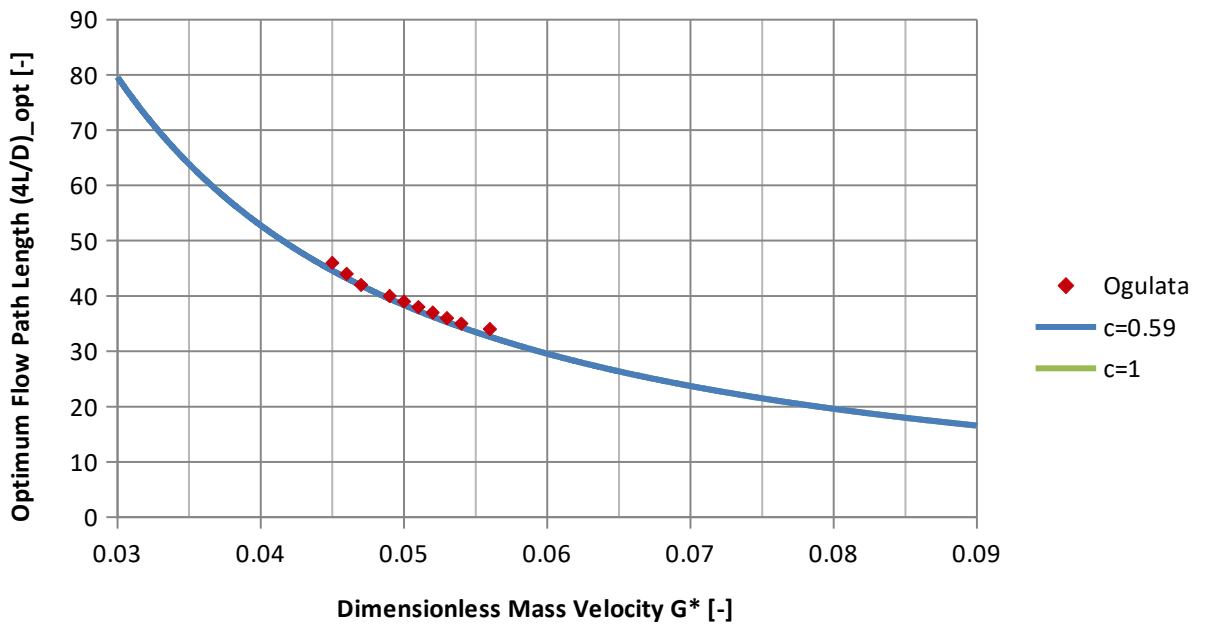
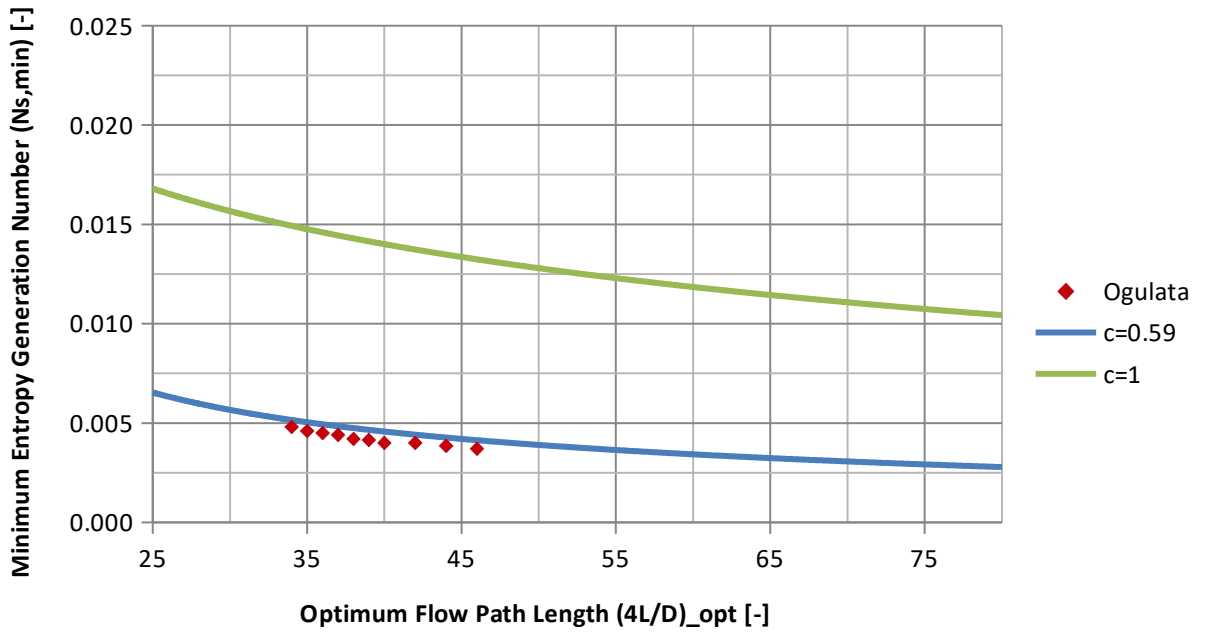


Figure 39: Optimum flow path comparison of cross-flow heat exchangers

Here in figure 39, irrespective of the heat capacity ratio, the results are identical and closely correspond with the experimental data.



**Figure 40: Minimum entropy generation number comparison of cross-flow heat exchangers**

It is here in figure 40 that the heat capacity ratio plays a role. The cross-flow heat exchanger with a smaller heat capacity ratio ( $c < 1$ ) closely corresponds to the experimental data and produces smaller values for the entropy generation number.

The theoretical results for the optimum flow path of the cross-flow heat exchanger averaged around 2% and did not exceed 3%. The theoretical results for the minimum entropy generation number of the cross-flow heat exchanger averaged around 11% and did not exceed 14%. It could be reasoned regarding the larger error values of the minimum entropy generation number that the authors of Ogulata et al. [16] did not make precise measurements in their laboratory conditions, or it could have been fluctuations in temperature, volume flow rate, the air pressure of the surrounding area, etc.

It has been established that the irreversibility of any heat exchanger is a result of the losses generated by the frictional pressure drop and the heat transfer process. What this means is that in analyzing the effectiveness of a heat exchanger, one can take into account the construction dimensions of the heat exchanger, i.e. the variation of the optimum flow path length with the dimensionless mass velocity. It can be said that the size of the optimum flow path decreases as the dimensionless mass velocity increases. There are pros and cons to having to both ends of the plots with the variation between the optimum flow path length and the dimensionless mass velocity for each heat exchanger. Having a larger optimum flow path length, thereby having a smaller dimensionless mass velocity, results in a smaller entropy generation number because there is a lower pressure drop in the pipes, however it also results in larger heat exchanger dimensions (a larger  $L$  or a smaller  $D$  in  $(4L/D)_{opt}$ ) for a specified temperature difference, along with more frictional irreversibility. A smaller optimum flow path length results in a smaller heat exchanger, in conjunction with an increase in heat transfer irreversibility.

Generally it can be said that an increase in optimum flow path length results in a decrease of the minimum entropy generation number. According to theory [16], the minimum entropy generation number can vary from 0 to infinity; therefore none of the heat exchangers appear to be violating this condition. An entropy generation number of  $N_{s,min} = 0$  means that the irreversibility losses from the heat exchanger are almost null. For the same interval of the dimensionless mass velocity (0.03 to 0.09), each heat exchanger had a different interval of operational optimum flow path length. Within these intervals of the optimum flow path length, it appears indeed that the minimum entropy generation number ranged from 0 to a max of 0.021. The cross-flow heat exchanger appeared to yield the worst results, whereas the counter-flow heat exchanger seemed to fare the best, i.e. at a value of  $c = 0.595238095238095$ . Regarding the heat exchangers at  $c = 1$ , the parallel-flow heat exchanger seemed to provide the lowest entropy generation number. What is also interesting to note is that there are different ranges of the optimum flow path length for the entropy generation number of the counter-flow heat exchanger, which appears to be highly dependent on the  $c$  value.

It can be concluded that an increase in the dimensions of a heat exchanger will typically lead to a reduction in the minimum entropy generation number, thereby resulting in less losses due to heat transfer and frictional irreversibilities and thus engendering a more effective heat exchanger.

## 4 Guidelines for an optimized design of a heat exchanger

### 4.1 Empirical equations

In order to proceed further, it was necessary to find an alternate way of writing the equations for the entropy generation number, and from it, the equations for the optimum flow path  $(4L/D)_{opt}$ . The existing equations (eqs. (69) – (72)) are unsuitable for the implementation of design constraints. The new equations for the entropy generation minimization number are determined empirically using exponential trendlines from the effectiveness-NTU charts, and so are therefore a useful approximation.

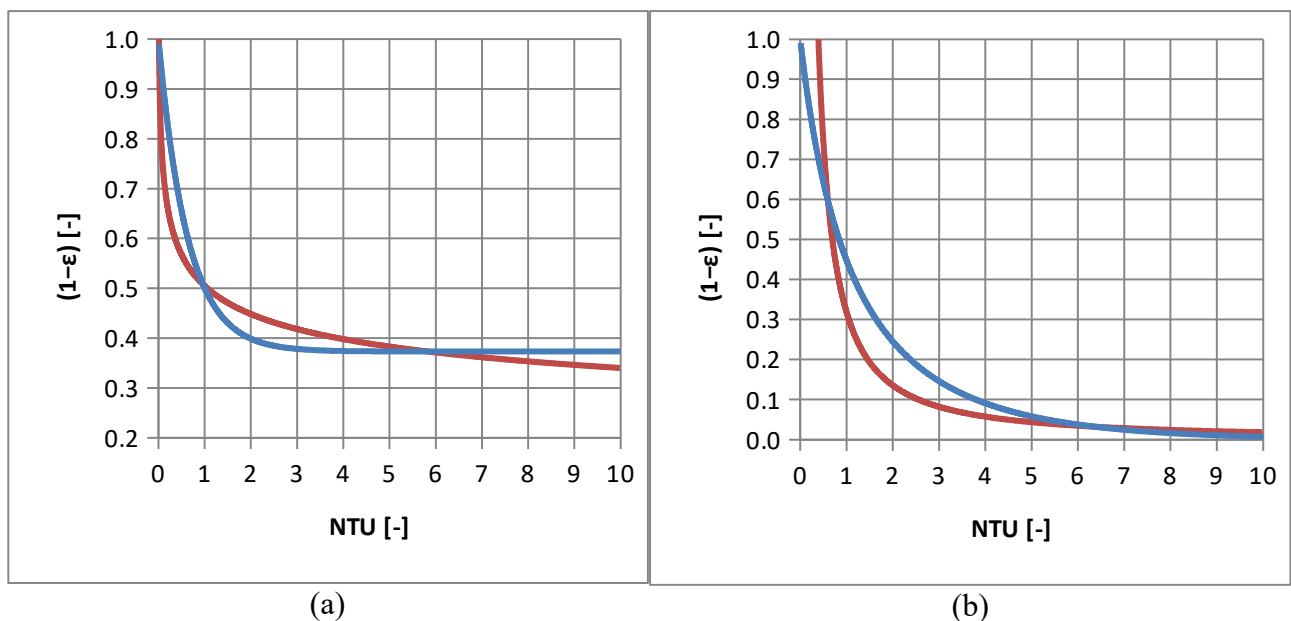
The equations stem from a basic approximation equation (eq. (114)):

$$(1-\varepsilon) = X \cdot NTU^{-Y} \tag{114}$$

where the  $X$  and the  $Y$  are according to the following table (Tab. (7)). Eq. (114) refers to the basic trendline for each of the 6 equations for the 3 heat exchangers.

|                                 |                         | $X$    | $Y$   |
|---------------------------------|-------------------------|--------|-------|
| <b>Parallel-flow</b>            | $c = 0.595238095238095$ | 0.5055 | 0.172 |
|                                 | $c = 1$                 | 0.5945 | 0.101 |
| <b>Counter flow</b>             | $c = 0.595238095238095$ | 0.3226 | 1.243 |
|                                 | $c = 1$                 | 0.4209 | 0.592 |
| <b>Cross-flow (single-pass)</b> | $c = 0.595238095238095$ | 0.3735 | 0.69  |
|                                 | $c = 1$                 | 0.4768 | 0.388 |

Table 7:  $X$  and  $Y$  coefficients of the empirically-derived equations





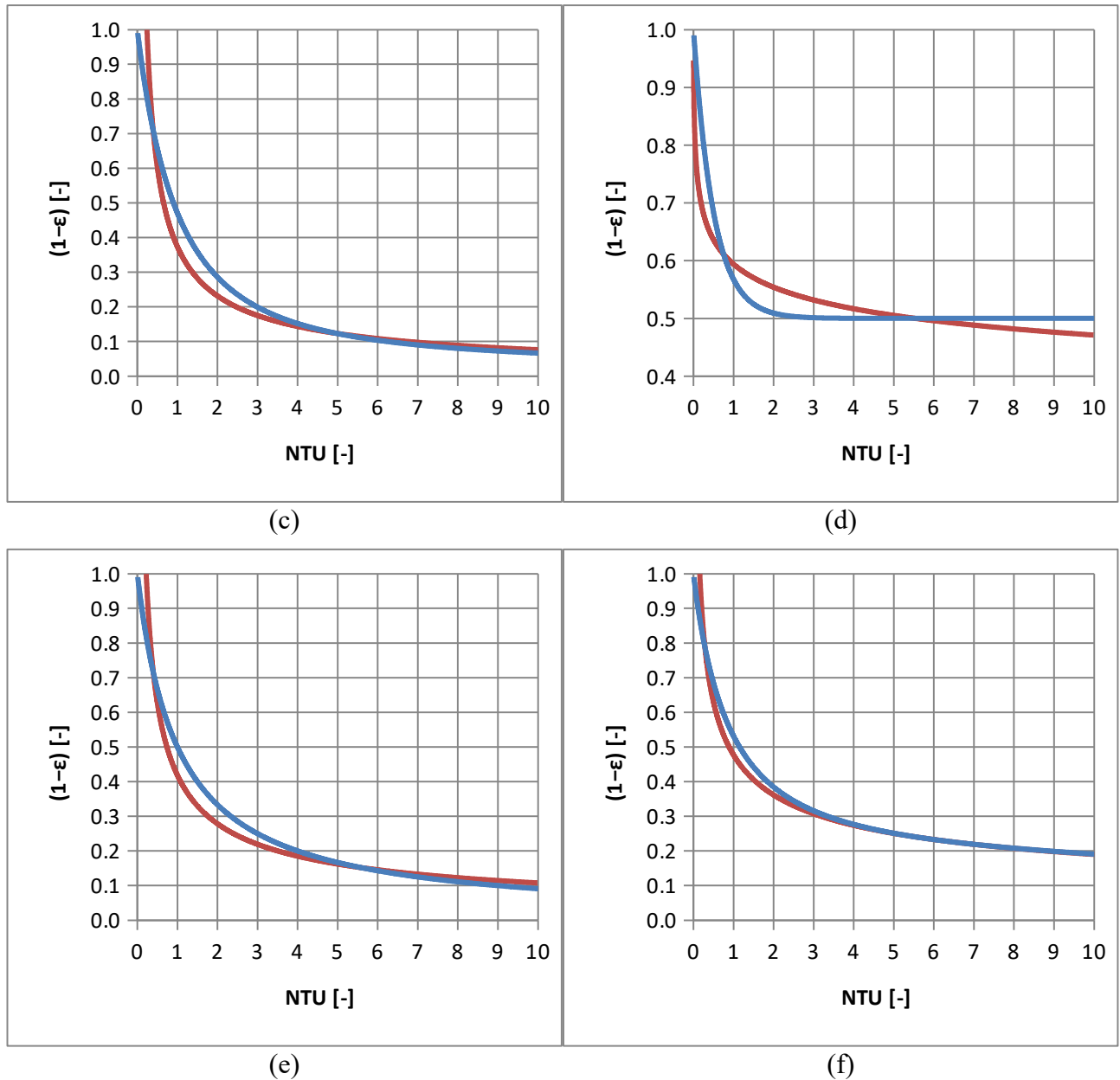


**Figure 41: Plots of the comparison between the original  $\epsilon$ -NTU relation (blue) and the empirically-derived approximations (red)**

In Figure 41, (a) and (d) are for parallel-flow, (b) and (e) for counter-flow, (c) and (f) for cross-flow, (a), (b), and (c) for  $c = 0.595238095238095$ , (d), (e), and (f) for  $c = 1$ . The blue lines indicate the original  $\epsilon$ -NTU relation, whereas the new, empirically-derived approximations are in red. It appears that the empirically-derived approximations come fairly close to representing the real  $\epsilon$ -NTU relations, with the only significant increase in inaccuracy being in that of the counter-flow heat exchanger, with a maximum inaccuracy of 45.07% at an NTU value of 2.37 ( $c < 1$  variant). For the rest of the 5 trends, the maximum inaccuracies stay under 20%.

Substituting Eq. (114) into Eq. (59), one will arrive at the following template equation for the minimum entropy generation number (eq. (115)):

$$N_s = \frac{X \cdot (\Delta T^*)^2}{\left(\frac{4 \cdot L}{D}\right)^Y \cdot St^Y} + \frac{R}{c_p} \cdot f \cdot \left(\frac{4 \cdot L}{D}\right) \cdot G^{*2} \quad (115)$$

again, the  $X$  and  $Y$  coefficients are as previous. The resulting equations (eqs. (116) – (121)) for the entropy generation number are listed in table 8.

|                          |                         | Entropy Generation Equation   |       |
|--------------------------|-------------------------|---|-------|
| Parallel-flow            | $c = 0.595238095238095$ | $N_s = \frac{0.5055 \cdot (\Delta T^*)^2}{\left(\frac{4 \cdot L}{D}\right)^{0.172} \cdot St^{0.172}} + \frac{R}{c_p} \cdot f \cdot \left(\frac{4 \cdot L}{D}\right) \cdot G^{*2}$ | (116) |
|                          | $c = 1$                 | $N_s = \frac{0.5945 \cdot (\Delta T^*)^2}{\left(\frac{4 \cdot L}{D}\right)^{0.101} \cdot St^{0.101}} + \frac{R}{c_p} \cdot f \cdot \left(\frac{4 \cdot L}{D}\right) \cdot G^{*2}$ | (117) |
| Counter flow             | $c = 0.595238095238095$ | $N_s = \frac{0.3226 \cdot (\Delta T^*)^2}{\left(\frac{4 \cdot L}{D}\right)^{1.243} \cdot St^{1.243}} + \frac{R}{c_p} \cdot f \cdot \left(\frac{4 \cdot L}{D}\right) \cdot G^{*2}$ | (118) |
|                          | $c = 1$                 | $N_s = \frac{0.4209 \cdot (\Delta T^*)^2}{\left(\frac{4 \cdot L}{D}\right)^{0.592} \cdot St^{0.592}} + \frac{R}{c_p} \cdot f \cdot \left(\frac{4 \cdot L}{D}\right) \cdot G^{*2}$ | (119) |
| Cross-flow (single-pass) | $c = 0.595238095238095$ | $N_s = \frac{0.3735 \cdot (\Delta T^*)^2}{\left(\frac{4 \cdot L}{D}\right)^{0.69} \cdot St^{0.69}} + \frac{R}{c_p} \cdot f \cdot \left(\frac{4 \cdot L}{D}\right) \cdot G^{*2}$   | (120) |
|                          | $c = 1$                 | $N_s = \frac{0.4768 \cdot (\Delta T^*)^2}{\left(\frac{4 \cdot L}{D}\right)^{0.388} \cdot St^{0.388}} + \frac{R}{c_p} \cdot f \cdot \left(\frac{4 \cdot L}{D}\right) \cdot G^{*2}$ | (121) |

**Table 8: Entropy generation equations for the empirically-derived equations**

The equations for the optimum flow path (a.k.a. in some sources *slenderness ratio*), which is crucial for the optimization of the heat exchanger, are listed in table 9. The equations (eqs. (122) – (127)) were achieved by first differentiating the entropy generation equation by the optimum flow path, and then solving the resulting equation for the optimum flow path.

|               |                         | Optimum flow path  |       |
|---------------|-------------------------|--|-------|
| Parallel-flow | $c = 0.595238095238095$ | $\left(\frac{4 \cdot L}{D}\right)_{opt} = \left(0.086946 \cdot \frac{(\Delta T^*)^2 \cdot c_p}{St^{43/250} \cdot R \cdot f \cdot G^{*2}}\right)^{250/293}$ | (122) |

|                                 |                         | Optimum flow path  |       |
|---------------------------------|-------------------------|--|-------|
|                                 | $c = 1$                 | $\left(\frac{4 \cdot L}{D}\right)_{opt} = \left(0.0600445 \cdot \frac{(\Delta T^*)^2 \cdot c_p}{St^{101/1000} \cdot R \cdot f \cdot G^{*2}}\right)^{1000/1101}$  | (123) |
| <b>Counter flow</b>             | $c = 0.595238095238095$ | $\left(\frac{4 \cdot L}{D}\right)_{opt} = \left(0.4009918 \cdot \frac{(\Delta T^*)^2 \cdot c_p}{St^{1243/1000} \cdot R \cdot f \cdot G^{*2}}\right)^{1000/2243}$ | (124) |
|                                 | $c = 1$                 | $\left(\frac{4 \cdot L}{D}\right)_{opt} = \left(0.2491728 \cdot \frac{(\Delta T^*)^2 \cdot c_p}{St^{74/125} \cdot R \cdot f \cdot G^{*2}}\right)^{125/199}$      | (125) |
| <b>Cross-flow (single-pass)</b> | $c = 0.595238095238095$ | $\left(\frac{4 \cdot L}{D}\right)_{opt} = \left(0.257715 \cdot \frac{(\Delta T^*)^2 \cdot c_p}{St^{69/100} \cdot R \cdot f \cdot G^{*2}}\right)^{100/169}$       | (126) |
|                                 | $c = 1$                 | $\left(\frac{4 \cdot L}{D}\right)_{opt} = \left(0.1849984 \cdot \frac{(\Delta T^*)^2 \cdot c_p}{St^{97/250} \cdot R \cdot f \cdot G^{*2}}\right)^{250/347}$      | (127) |

**Table 9: Optimum flow path equations for the empirically-derived equations**

## 4.2 Design constraints

According to Bejan [17], there are three dimensionless unknown variables for one side of the heat exchanger, they are the flow path ( $4L/D$ ), dimensionless mass velocity  $G^*$ , and the Stanton number  $St$  (which is dependent on the Reynolds number  $Re$ ). For a given minimum entropy generation number  $N_{s,min}$ , there are only two degrees of freedom as per the empirically derived equations (eqs. (116) – (121)), i.e. the slenderness ratio ( $4L/D$ ) and the dimensionless mass velocity  $G^*$ . Should the case arise that there is a given dimensionless mass ratio (along with a Stanton number) instead of the minimum entropy generation number, then again there are two degrees of freedom, i.e. the slenderness ratio and the minimum entropy generation number.

There are two basic examples of design constraints, which Bejan [17] labels as "frequent":

- **Heat Transfer Area**
- **Heat Exchanger Volume**

Nevertheless, when it comes to real-life situations, there isn't always necessarily two degrees of freedom when designing a heat exchanger, as there could be additional design constraints that could apply to the given situation.

Discussing the latter example first, heat exchanger volume dimensioning is crucial when space is constricted or it's economically beneficial for the heat exchanger to occupy as small a volume as possible. For the case regarding the three dimensionless unknown variables, the volume constraint  $V$  can be formulated as (eq. (128)):

$$V \cdot \frac{8 \cdot \rho \cdot P}{\mu \cdot \dot{m}} = \frac{\text{Re} \cdot \left( \frac{4 \cdot L}{D} \right)}{G} \quad (128)$$

### 4.2.1 Heat transfer area design constraint

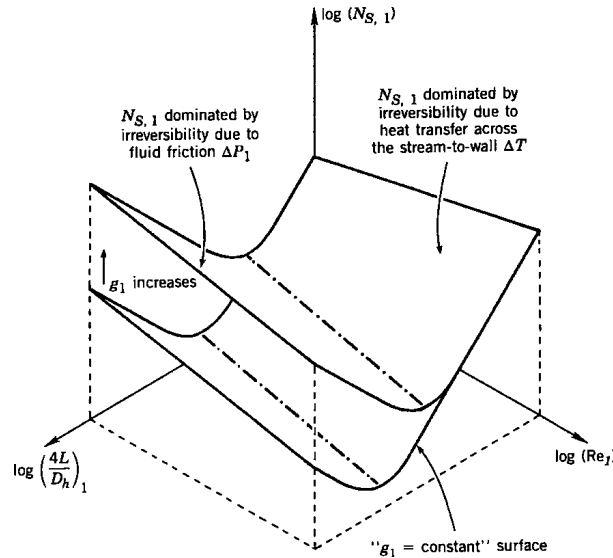


Figure 42: Number of entropy generation units per side, as a function of  $(L/r_h)$ ,  $g$ , and  $N_{Re}$  [17]

The other notable design constraint that can come into play when optimizing a heat exchanger is the heat transfer area. Dimensioning according to this constraint is mostly based on financial reasons. This being because with the rise in size of the heat transfer area comes an increase in the cost and weight of the heat exchanger. In practical situations, the size of the heat transfer area may already be predetermined by the client, or the goal may be to design a heat exchanger with as small a heat transfer area as possible. There is a certain point of fact about the heat transfer area, in that once the size of the heat transfer area is determined for one side of the heat exchange; the other side has basically the same size. Therefore, should a value for the size of the heat transfer area be specified, then it serves as a constraint for both sides of the heat exchanger.

In accordance with utilizing the dimensionless unknown variables, as per equation (128), the heat transfer area  $A$  can be written as (eq. (129)):

$$A \cdot \frac{\sqrt{2 \cdot \rho \cdot P}}{\dot{m}} = \frac{\left( \frac{4 \cdot L}{D} \right)}{G} \quad (129)$$

### 4.2.2 Practical application of the heat transfer area design constraint

The  $N_s$  method developed by Bejan [17] can be implemented in a practical application where there is a fixed number of entropy generation units for each side, and where the goal is to either minimize or keep it constant at a level specified beforehand. The two constraints in this case are eqs. (115) and (129). As mentioned previously, there are three dimensionless unknowns –  $(4L/D)$ ,  $G$ , and  $St$ . Since the entropy generation number

$N_s$  is not strongly tied to the Stanton number  $St$ , the latter can be regarded as an independent parameter, i.e. a constant. This means that eqs. (115) and (129) can be combined in order to cancel out  $G$ , which has as a result equation (130):

$$\frac{A \cdot \sqrt{2 \cdot \rho \cdot P}}{\dot{m}} = \sqrt{\frac{\left(\frac{R}{c_p}\right) \cdot f \cdot \left(\frac{4 \cdot L}{D}\right)^{3+Y} \cdot St^Y}{N_s \cdot \left(\frac{4 \cdot L}{D}\right)^Y \cdot St^Y - X \cdot (\Delta T^*)^2}} \quad (130)$$

where the heat transfer area  $A$  is now a function of the slenderness ratio ( $4L/D$ ).

In order to find when the heat transfer area will reach its minimum, it is necessary to first differentiate equation (130) according to ( $4L/D$ ) and then to solve the resulting equation for ( $4L/D$ ), resulting in equation (131):

$$\left(\frac{4 \cdot L}{D}\right)_{opt} = 3^{-1/Y} \cdot \left(\frac{St^{-Y} \cdot X \cdot (\Delta T^*)^2 \cdot (Y+3)}{N_s}\right)^{1/Y} \quad (131)$$

The optimum flow paths for each of the types of the examined heat exchangers are listed as eqs. (132) – (137) in table 10.

|                          |                         | Optimum flow path   |       |
|--------------------------|-------------------------|---|-------|
| Parallel-flow            | $c = 0.595238095238095$ | $\left(\frac{4 \cdot L}{D}\right)_{opt} = 3^{-1/0.172} \cdot \left(\frac{1.603446 \cdot St^{-0.172} \cdot (\Delta T^*)^2}{N_s}\right)^{1/0.172}$  | (132) |
|                          | $c = 1$                 | $\left(\frac{4 \cdot L}{D}\right)_{opt} = 3^{-1/0.101} \cdot \left(\frac{1.8435445 \cdot St^{-0.101} \cdot (\Delta T^*)^2}{N_s}\right)^{1/0.101}$ | (133) |
| Counter flow             | $c = 0.595238095238095$ | $\left(\frac{4 \cdot L}{D}\right)_{opt} = 3^{-1/1.243} \cdot \left(\frac{1.3687918 \cdot St^{-1.243} \cdot (\Delta T^*)^2}{N_s}\right)^{1/1.243}$ | (134) |
|                          | $c = 1$                 | $\left(\frac{4 \cdot L}{D}\right)_{opt} = 3^{-1/0.592} \cdot \left(\frac{1.5118728 \cdot St^{-0.592} \cdot (\Delta T^*)^2}{N_s}\right)^{1/0.592}$ | (135) |
| Cross-flow (single-pass) | $c = 0.595238095238095$ | $\left(\frac{4 \cdot L}{D}\right)_{opt} = 3^{-1/0.69} \cdot \left(\frac{1.378215 \cdot St^{-0.69} \cdot (\Delta T^*)^2}{N_s}\right)^{1/0.69}$     | (136) |
|                          | $c = 1$                 | $\left(\frac{4 \cdot L}{D}\right)_{opt} = 3^{-1/0.388} \cdot \left(\frac{1.6153984 \cdot St^{-0.388} \cdot (\Delta T^*)^2}{N_s}\right)^{1/0.388}$ | (137) |

**Table 10: Optimum flow path equations for the empirically-derived equations**

Inserting eq. (131) back into (130), the result eq. (138):

$$\frac{A \cdot \sqrt{2 \cdot \rho \cdot P}}{\dot{m}} = \sqrt{\frac{\left(\frac{R}{c_p}\right) \cdot f \cdot (Y+3)^{\frac{3+Y}{Y}} \cdot (X \cdot (\Delta T^*)^2)^{\frac{3}{Y}}}{3^{\frac{3}{Y}} \cdot Y \cdot St^3 \cdot N_s^{\frac{Y+3}{Y}}}} \quad (138)$$

Table 11 lists the equations for the minimum area for the different types of heat exchangers (eqs. (139) – (144)).

|                                 |                         | Minimum heat transfer area  |       |
|---------------------------------|-------------------------|---|-------|
| <b>Parallel-flow</b>            | $c = 0.595238095238095$ | $\frac{A \cdot \sqrt{2 \cdot \rho \cdot P}}{\dot{m}} = \sqrt{\frac{0.000331476 \cdot \left(\frac{R}{c_p}\right) \cdot f \cdot (\Delta T^*)^{34.88372093}}{\text{St}^3 \cdot N_s^{18.44186047}}}$          | (139) |
|                                 | $c = 1$                 | $\frac{A \cdot \sqrt{2 \cdot \rho \cdot P}}{\dot{m}} = \sqrt{\frac{1.60681 \cdot 10^{-5} \cdot \left(\frac{R}{c_p}\right) \cdot f \cdot (\Delta T^*)^{59.40594059}}{\text{St}^3 \cdot N_s^{30.7029703}}}$ | (140) |
| <b>Counter flow</b>             | $c = 0.595238095238095$ | $\frac{A \cdot \sqrt{2 \cdot \rho \cdot P}}{\dot{m}} = \sqrt{\frac{0.513706086 \cdot \left(\frac{R}{c_p}\right) \cdot f \cdot (\Delta T^*)^{4.827031376}}{\text{St}^3 \cdot N_s^{3.413515688}}}$          | (141) |
|                                 | $c = 1$                 | $\frac{A \cdot \sqrt{2 \cdot \rho \cdot P}}{\dot{m}} = \sqrt{\frac{0.188311179 \cdot \left(\frac{R}{c_p}\right) \cdot f \cdot (\Delta T^*)^{10.13513514}}{\text{St}^3 \cdot N_s^{6.067567568}}}$          | (142) |
| <b>Cross-flow (single-pass)</b> | $c = 0.595238095238095$ | $\frac{A \cdot \sqrt{2 \cdot \rho \cdot P}}{\dot{m}} = \sqrt{\frac{0.181745223 \cdot \left(\frac{R}{c_p}\right) \cdot f \cdot (\Delta T^*)^{8.695652174}}{\text{St}^3 \cdot N_s^{5.347826087}}}$          | (143) |
|                                 | $c = 1$                 | $\frac{A \cdot \sqrt{2 \cdot \rho \cdot P}}{\dot{m}} = \sqrt{\frac{0.072851662 \cdot \left(\frac{R}{c_p}\right) \cdot f \cdot (\Delta T^*)^{15.46391753}}{\text{St}^3 \cdot N_s^{8.731958763}}}$          | (144) |

**Table 11: Minimum heat transfer area equations for the empirically-derived equations**

The optimum dimensionless mass velocity can be calculated from eqs. (115) and (131):

$$G^* = \frac{N_s^{\frac{Y+2}{Y}} \cdot \text{St}^2}{(\Delta T^*)^2} \cdot \sqrt{\frac{3^{\frac{1}{Y}} \cdot Y}{X^{\frac{1}{Y}} \cdot (Y+3)^{\frac{1+Y}{Y}} \cdot \left(\frac{R}{c_p}\right) \cdot f}} \quad (145)$$

The equations for the optimum dimensionless mass velocity (eqs. (146) – (151)) are listed in table 12.

|                                     |                         | <b>Optimum dimensionless mass velocity</b>  |       |
|-------------------------------------|-------------------------|---|-------|
| <b>Parallel-flow</b>                | $c = 0.595238095238095$ | $G^* = \frac{N_s^{12.62790698} \cdot St^2}{(\Delta T^*)^2} \cdot \sqrt{\frac{2.070044418}{\left(\frac{R}{c_p}\right) \cdot f}}$ | (146) |
|                                     | $c = 1$                 | $G^* = \frac{N_s^{20.8019802} \cdot St^2}{(\Delta T^*)^2} \cdot \sqrt{\frac{4.041648251}{\left(\frac{R}{c_p}\right) \cdot f}}$  | (147) |
| <b>Counter flow</b>                 | $c = 0.595238095238095$ | $G^* = \frac{N_s^{2.609010459} \cdot St^2}{(\Delta T^*)^2} \cdot \sqrt{\frac{0.550757594}{\left(\frac{R}{c_p}\right) \cdot f}}$ | (148) |
|                                     | $c = 1$                 | $G^* = \frac{N_s^{4.378378378} \cdot St^2}{(\Delta T^*)^2} \cdot \sqrt{\frac{0.52444291}{\left(\frac{R}{c_p}\right) \cdot f}}$  | (149) |
| <b>Cross-flow<br/>(single-pass)</b> | $c = 0.595238095238095$ | $G^* = \frac{N_s^{3.898550725} \cdot St^2}{(\Delta T^*)^2} \cdot \sqrt{\frac{0.577290151}{\left(\frac{R}{c_p}\right) \cdot f}}$ | (150) |
|                                     | $c = 1$                 | $G^* = \frac{N_s^{6.154639175} \cdot St^2}{(\Delta T^*)^2} \cdot \sqrt{\frac{0.564649648}{\left(\frac{R}{c_p}\right) \cdot f}}$ | (151) |

**Table 12: Optimum dimensionless mass velocity equations for the empirically-derived equations**

The number of entropy generation units  $N_s$  is central in calculating the  $(4L/D)_{opt}$  and  $G^*_{opt}$ . Both  $A_{opt}$  and  $(4L/D)_{opt}$  will tend to decrease with a decrease in the Re number. The Re number can only be reduced only by minimizing the hydraulic diameter, which is not always possible in the practical sphere. Figure 43 demonstrates how important the slenderness ratio or flow path length  $(4L/D)$  is when it comes to entropy generation.

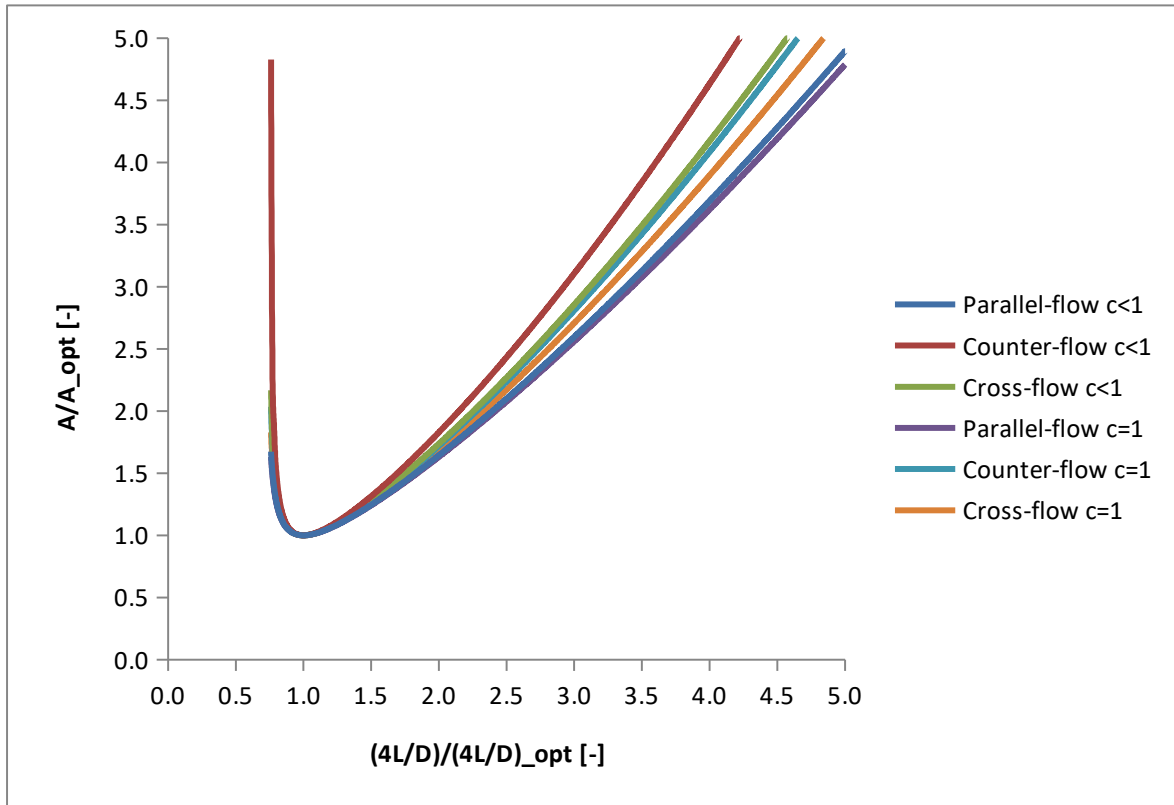


**Figure 43: Dependence of the heat transfer area on  $(4L/D)$  for a given  $Re$  and fixed  $N_s$  for the various types of heat exchangers**

The area to the right of point (1,1), i.e. where  $(4L/D) > (4L/D)_{opt}$ , the specified entropy generation stems primarily from frictional losses owing to the difference in the inlet and outlet pressures, not to mention a larger heat transfer area than necessary. To the left of point (1,1), i.e. where  $(4L/D) < (4L/D)_{opt}$ , there is a decrease in the dimensionless mass velocity, engendering entropy generation due to heat transfer, which results in a more rapid increase in the heat transfer area.

## 5 Conclusion

This master's thesis begins with an elaboration on the topic of heat exchangers in general. The importance of heat exchangers to daily life and the broad industry is expounded upon. More importantly, the various types of heat exchangers are introduced, based on the setup and fluid flow. The three heat exchangers chosen for analysis are the parallel-flow, counter-flow, and the cross-flow (with both fluids unmixed) heat exchangers.

In order to analyze how to figure out the efficiency of each heat exchanger, it was necessary to introduce the sometimes complicated topic of entropy, most notably the generation of entropy during the operation of a heat exchanger. An attempt is made at developing a simplified understanding of entropy and the entropy balance of an isolated system, how entropy is generated, etc. To clinch the topic of entropy, the basics of entropy generation minimization are introduced.

The third part of the thesis concerns the evolution of the mathematical model, based on the concept of entropy generation minimization. The effectiveness-NTU method ( $\epsilon$ -NTU), as an alternative to the logarithmic mean temperature difference method (LMTD),



is introduced as a way to measure the generation of entropy. The mathematical model is developed based on the types of heat exchangers in this thesis and also on whether it's a balanced ( $c = 1$ ) or unbalanced ( $c = 0.595238095238095$ ) heat exchanger. The value for the unbalanced heat exchanger was used so as to be able to compare the results with experimental data from scientific literature. Notwithstanding, a sensitivity analysis of the mathematical model was done in order to find out which parameter will have the greatest impact on the change in the entropy generation number.

Regarding the results, it can be concluded that an increase in the dimensions of a heat exchanger will typically lead to a reduction in the minimum entropy generation number, thereby resulting in less losses due to heat transfer and frictional irreversibilities, resulting in a more effective heat exchanger. A heat capacity ratio of less than 1 seems to be more efficient than a balanced heat exchanger (where  $c = 1$ ). It is apparent that out of the three examined types of heat exchangers that the counter-flow heat exchanger has the smallest minimum entropy generation numbers.

Lastly, when it comes to designing a heat exchanger, the topic of design constraints comes to mind. There are two notable ways of how the design of a heat exchanger can be limited – by the available heat transfer area and the heat exchanger volume. This thesis only concerns itself with the former. Due to mathematical limitations, the original equations for the entropy generation number needed to be altered slightly to include empirically-derived relations, which appear to have an insignificant impact on the accuracy of the results. Nonetheless, the resulting equations show that for each heat exchanger there is an optimal heat transfer area for a given optimum flow path (slenderness ratio), or dimensioning of the tubes of the heat exchanger.

## References

- [1] **QUORA**: *Why is a counter flow heat exchanger better than a parallel flow heat exchanger?* [online] [cit. 16. May. 2018], URL: <https://www.quora.com/Why-is-a-counter-flow-heat-exchanger-better-than-a-parallel-flow-heat-exchanger>
- [2] **CENGEL, Y. A.**: *HEAT TRANSFER – A Practical Approach*, McGraw-Hill (Tx); 2<sup>nd</sup> edition (November 1, 2002), ISBN-13: 978-0072458930, pgs. 668, 669, 683, 670
- [3] **ENGINEERS EDGE, LLC**: *Parallel and Counter Flow Designs* [online] [cit. 16. May. 2018], URL: [http://www.engineersedge.com/heat\\_transfer/parallel\\_counter\\_flow\\_designs.htm](http://www.engineersedge.com/heat_transfer/parallel_counter_flow_designs.htm)
- [4] **HOLMAN, J. P.**: *Heat Transfer*, McGraw-Hill Education; 10<sup>th</sup> edition (January 13, 2009), ISBN-13: 978-0073529363, pgs. 522, 528, 531, 534, 535, 536
- [5] **LINHART, J.**: *Přenos tepla a hmoty – Přednášky*, Západočeská univerzita v Plzni
- [6] **ENGINEERS EDGE, LLC**: *Cross Flow Type Heat Exchanger* [online] [cit. 16. May. 2018], URL: [http://www.engineersedge.com/heat\\_exchanger/cross\\_flow.htm](http://www.engineersedge.com/heat_exchanger/cross_flow.htm)
- [7] **JANNA, WILLIAM S.**: *Engineering Heat Transfer*, CRC Press; 3<sup>rd</sup> edition (January 14, 2009), ISBN-13: 978-1420072020, pg. 476
- [8] **SUBBARAO, P. M. V.**: *Classification of Heat Exchangers*; [online] [cit. 16. May. 2018], pgs. 22-23, URL: <http://web.iitd.ac.in/~pmvs/courses/mel709/classification-hx.pdf>
- [9] **KLEIN, J. F.**: *Physical Significance of Entropy or of the Second Law*, D. Van Nostrand Company (1910), ISBN: 1517334993, pg. 41
- [10] **CENGEL, Y. A.**: *Introduction to Thermodynamics and Heat Transfer*, McGraw-Hill Higher Education; 2<sup>nd</sup> edition (February 1, 2009), ISBN-13: 978-0071287739, pgs. 341-346
- [11] **BEJAN, A.**: *Advanced Engineering Thermodynamics*, Wiley; 3<sup>rd</sup> edition (August 18, 2006), ISBN-13: 978-0471677635 pg. 134, 138
- [12] **FARABEE, M. J.**: *Laws of Thermodynamics* [online] [cit. 16. May. 2018], URL: <https://www2.estrellamountain.edu/faculty/farabee/biobk/BioBookEner1.html>
- [13] **CENGEL, Y. A., GHAJAR, A. J.**: *Heat and Mass Transfer – Fundamentals & Applications*, McGraw-Hill Education; 5<sup>th</sup> edition (April 4, 2014), ISBN-13: 978-0073398181, pgs. 677, 678, 680
- [14] **KOORTS, J. M.**: *Entropy Minimisation and Structural Design for Industrial Heat Exchanger Optimisation*, University of Pretoria (June 24, 2014), pg. 63
- [15] **SMITH, E. D., SZIDAROVSKY, F., KARNAVAS, W. J., BAHILL, A. T.**: *Sensitivity Analysis, a Powerful System Validation Technique*, The Open Cybernetics and Systemics Journal, 2008, 2, 39-56
- [16] **OGULATA, R. T., DOBA, F., YILMAZ, T.**: *Second-Law and Experimental Analysis of a Cross-Flow Heat Exchanger*, Heat Transfer Engineering, Volume 24, 2003 – Issue 4 (30 Nov 2010)
- [17] **BEJAN, A.**: *The Concept of Irreversibility in Heat Exchanger Design: Counterflow Heat Exchangers for Gas-to-Gas Applications*, Journal of Heat Transfer, Volume 99 (August 1977). DOI: 10.1115/1.3450705

## A Charts

### Parallel-flow heat exchanger, $c = 0.595238095238095$

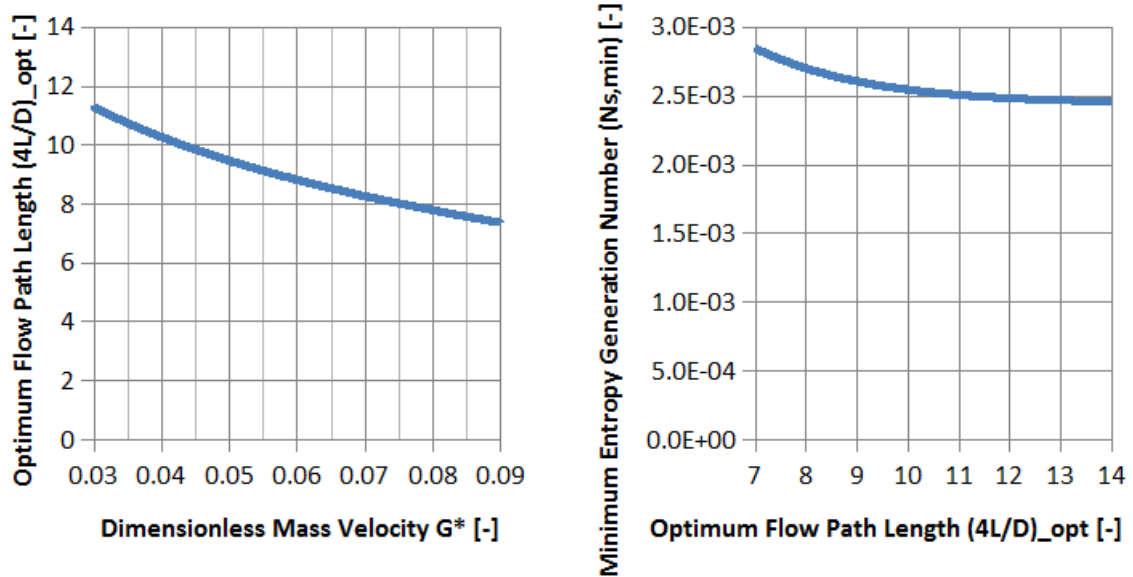


Figure 44: Variation between the optimum flow path length and the dimensionless mass velocity (L) and variation between the minimum entropy generation number and the optimum flow path length (R) for a parallel-flow heat exchanger ( $c = 0.595238095238095$ )

### Parallel-flow heat exchanger, $c = 1$

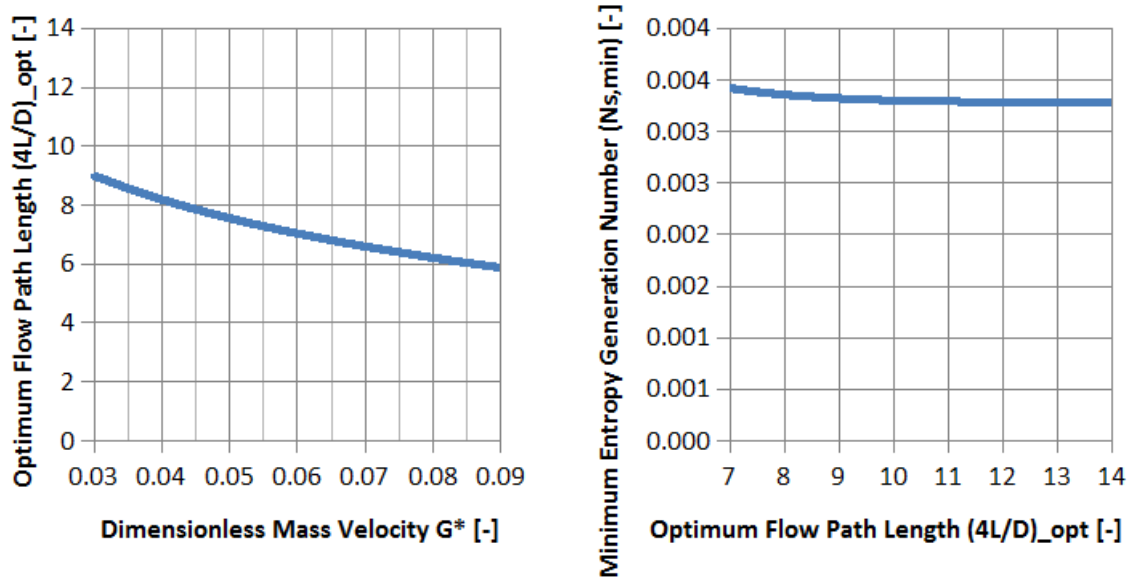
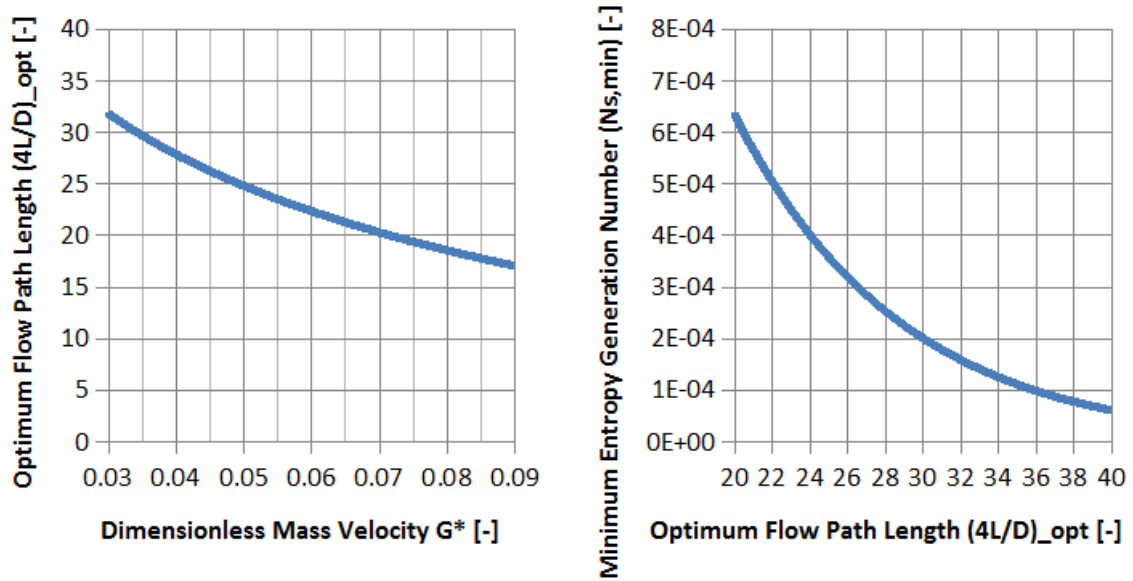


Figure 45: Variation between the optimum flow path length and the dimensionless mass velocity (L) and variation between the minimum entropy generation number and the optimum flow path length (R) for a parallel-flow heat exchanger ( $c = 1$ )

**Counter-flow heat exchanger,  $c = 0.595238095238095$**



**Figure 46: Variation between the optimum flow path length and the dimensionless mass velocity (L) and variation between the minimum entropy generation number and the optimum flow path length (R) for a counter-flow heat exchanger ( $c = 0.595238095238095$ )**

**Counter-flow heat exchanger,  $c = 1$**

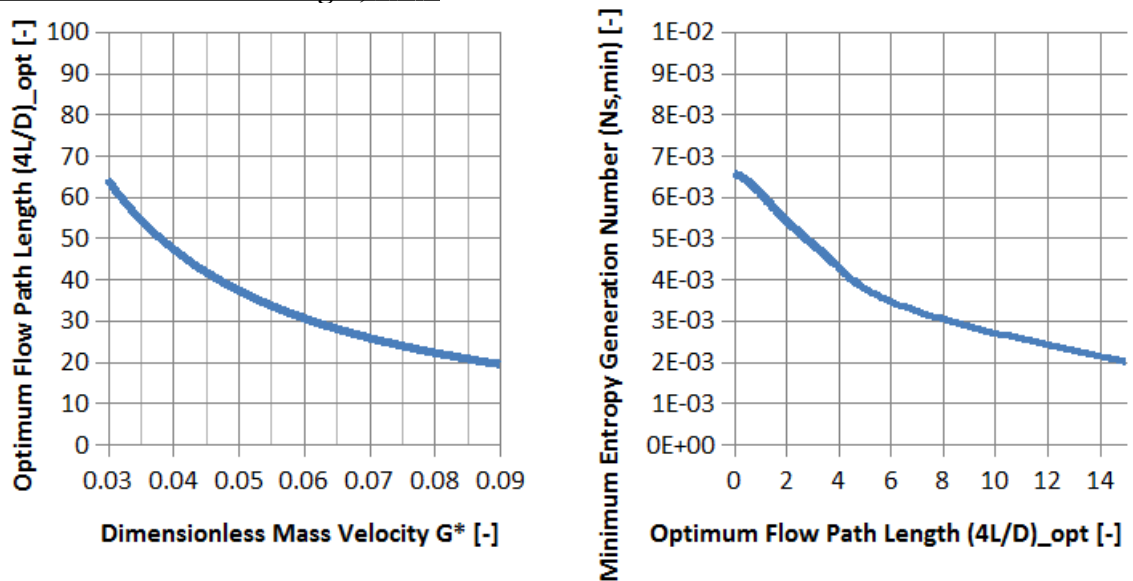


**Figure 47: Variation between the optimum flow path length and the dimensionless mass velocity (L) and variation between the minimum entropy generation number and the optimum flow path length (R) for a counter-flow heat exchanger ( $c = 1$ )**

**Cross-flow heat exchanger,  $c = 0.595238095238095$**

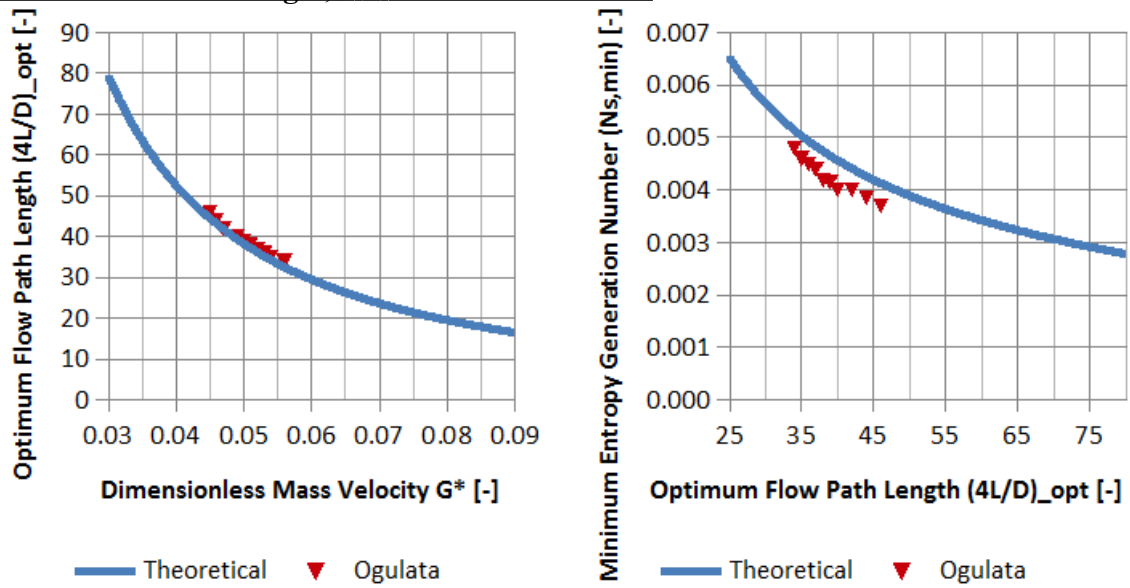


Figure 48: Variation between the optimum flow path length and the dimensionless mass velocity (L) and variation between the minimum entropy generation number and the optimum flow path length (R) for a cross-flow heat exchanger ( $c = 0.595238095238095$ )

**Cross-flow heat exchanger,  $c = 1$**

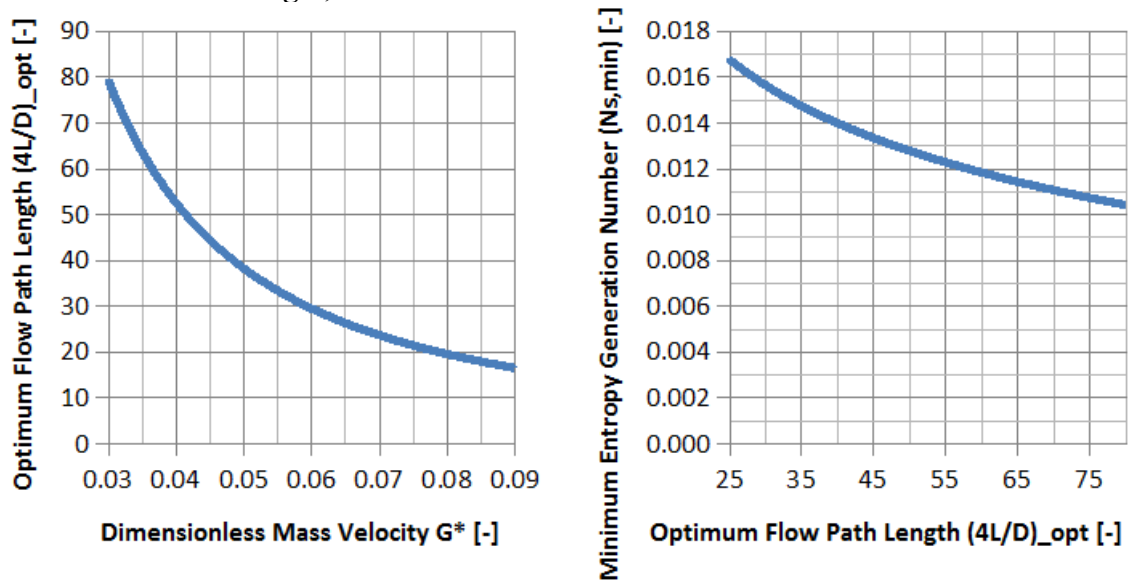


Figure 49: Variation between the optimum flow path length and the dimensionless mass velocity (L) and variation between the minimum entropy generation number and the optimum flow path length (R) for a cross-flow heat exchanger ( $c = 1$ )

## A.1 Effectiveness-NTU charts

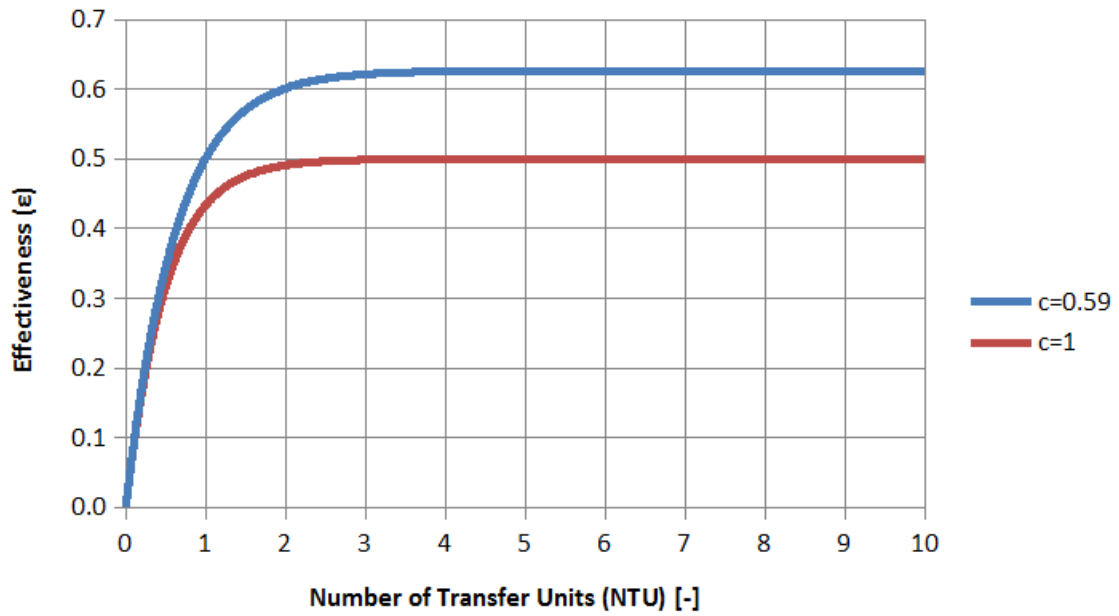


Figure 50: Variation between the effectiveness and the number of transfer units for a parallel-flow heat exchanger

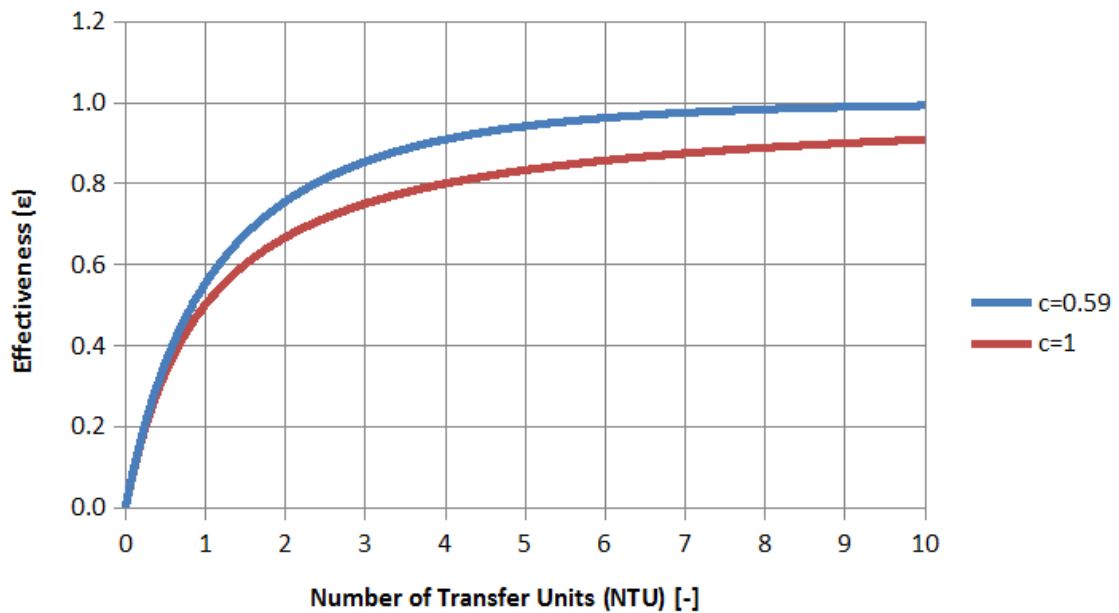


Figure 51: Variation between the effectiveness and the number of transfer units for a counter-flow heat exchanger

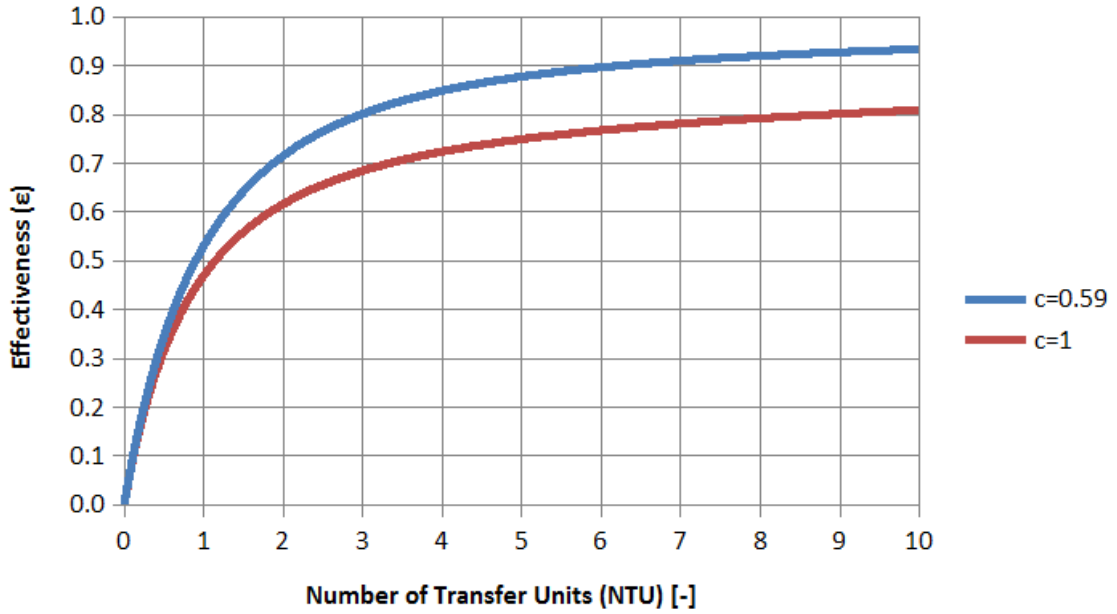


Figure 52: Variation between the effectiveness and the number of transfer units for a cross-flow heat exchanger

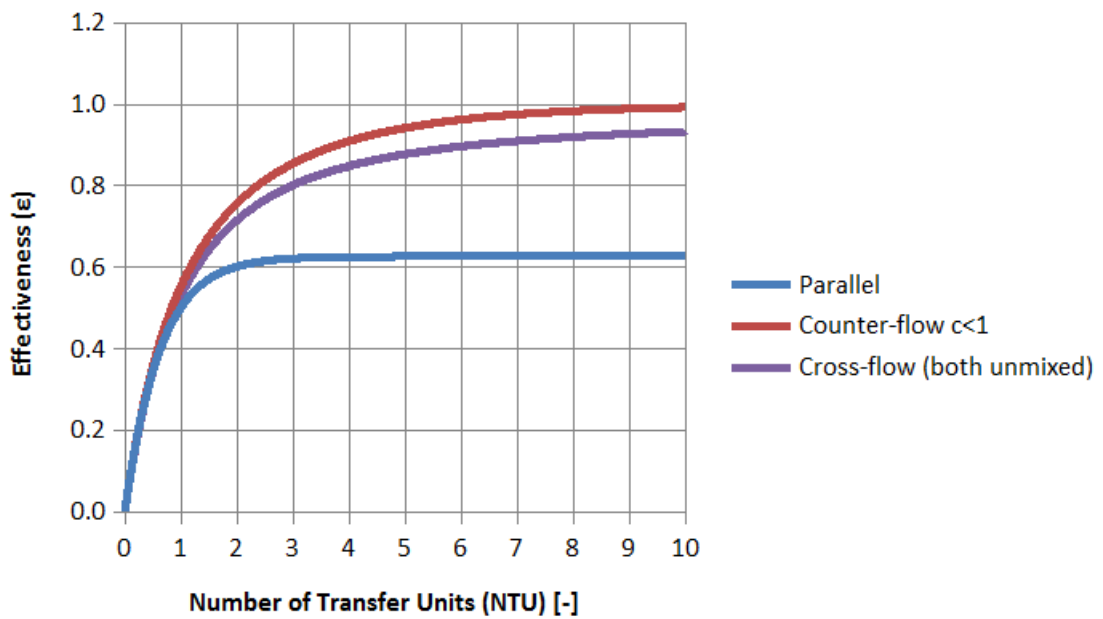


Figure 53: Variation between the effectiveness and the number of transfer units for all of the heat exchangers with  $c = 0.595238095238095$

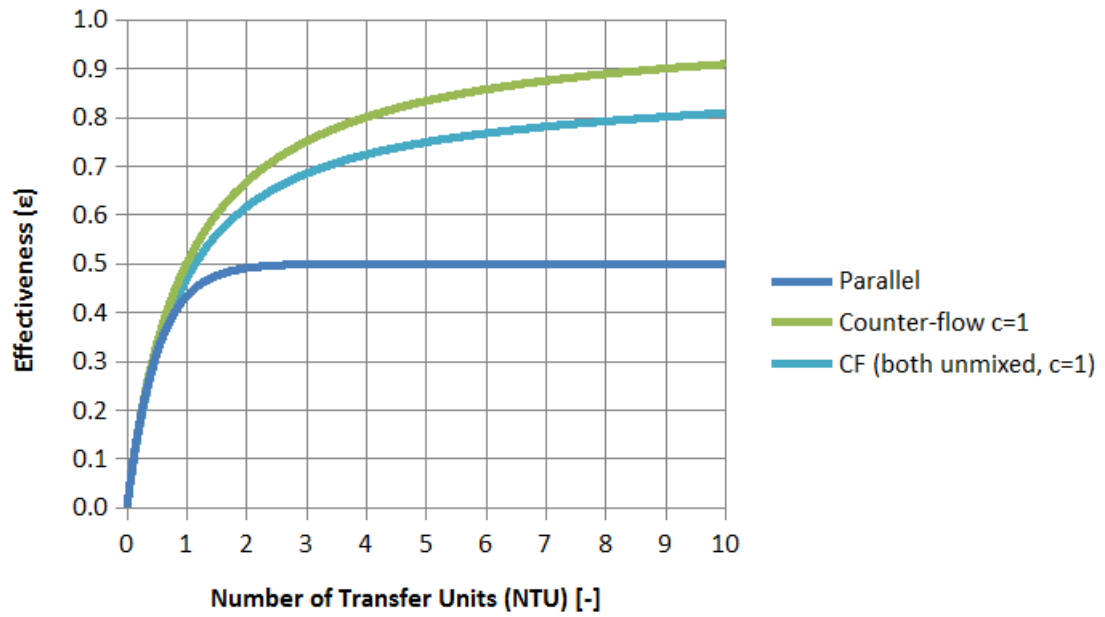


Figure 54: Variation between the effectiveness and the number of transfer units for all of the heat exchangers with  $c = 1$



## B Equations for the optimum flow path

The equations for  $(4L/D)_{opt}$  for section [3.3 Graphs and results] are listed here.

### Parallel-flow heat exchanger:

$$\left(\frac{4 \cdot L}{D}\right)_{opt} = \frac{\ln\left(\frac{f \cdot (G^*)^2 \cdot R}{St \cdot (\Delta T^*)^2 \cdot c_p}\right)}{(c+1) \cdot St}$$

### Counter-flow heat exchanger ( $c < 1$ ):

$$\left(\frac{4 \cdot L}{D}\right)_{opt} = \ln \frac{\left(\frac{(c-1) \cdot \Delta T^* \cdot \sqrt{c_p \cdot St} \cdot \sqrt{c^2 \cdot c_p \cdot St \cdot (\Delta T^*)^2 + 4 \cdot c \cdot f \cdot (G^*)^2 \cdot R - 2 \cdot c \cdot c_p \cdot St \cdot (\Delta T^*)^2} + c_p \cdot St \cdot (\Delta T^*)^2 + c^2 \cdot c_p \cdot St \cdot (\Delta T^*)^2 + 2 \cdot c \cdot f \cdot (G^*)^2 \cdot R - 2 \cdot c \cdot c_p \cdot St \cdot (\Delta T^*)^2 + c_p \cdot St \cdot (\Delta T^*)^2\right)}{2 \cdot c^2 \cdot f \cdot (G^*)^2 \cdot R}}{(c-1) \cdot St}$$

### Counter-flow heat exchanger ( $c = 1$ ):

$$\left(\frac{4 \cdot L}{D}\right)_{opt} = \frac{(\Delta T^*)^2 \cdot \sqrt{St^3 \cdot f \cdot c_p \cdot R - St \cdot f \cdot R \cdot (G^*)^2}}{St^2 \cdot f \cdot R \cdot (G^*)^2}$$

### Cross-flow heat exchanger:

$$\left(\frac{4 \cdot L}{D}\right)_{opt} = \left(0.1908 \cdot \frac{(\Delta T^*)^2 \cdot c_p}{St^{0.4} \cdot R \cdot f \cdot G^{*2}}\right)^{1/1.4}$$